

ECMWF forecast report No. 0.

J.-F. Geleyn, C. Girard,
H. Sävijärvi and J.A. Woods

Research Department

December 1979

This paper has not been published and should be regarded as an Internal Report from ECMWF.
Permission to quote from it should be obtained from the ECMWF.



European Centre for Medium-Range Weather Forecasts
Europäisches Zentrum für mittelfristige Wettervorhersage
Centre européen pour les prévisions météorologiques à moyen

1. INTRODUCTION

This is the fourth report on the performance of the ECMWF operational model. The previous reports were published internally as Technical Memoranda No. 9 and No. 10, 1979 and No. 11, 1980. Starting with the month of January 1980, a new external publication series entitled ECMWF Forecast Report will begin and this report's structure is intended to be as close as possible to the final structure with Sections

2. SYNOPTIC EVALUATION
3. VERIFICATION STATISTICS
4. SYSTEMATIC ERRORS
5. SPECIAL TOPICS
6. GENERAL REMARKS

The month of December includes 22 forecast cases. For the first time since the implementation of the present forecast model, a modification was introduced that could have affected the performance of the model: the non-linear horizontal diffusion scheme was replaced by a linear version. The change occurred at the end of November and was made essentially to improve the efficiency of the model, without expected noticeable effect on model performance.

2. SYNOPTIC EVALUATION OF DECEMBER FORECASTS

The first week of December 1979 was characterized by mostly zonal flow over Northern Europe. A major depression moving from south eastern Greenland towards and across Northern Scandinavia was tracked too far to the south in the later stages of the forecasts from late November. By the 9th of the month, the 500 mb field showed the establishment of an omega block with a split in the jet over north western Europe. The block did not persist, and the period from

13 to 20 showed small scale troughs moving rapidly eastwards across central Europe. The forecasts in general successfully described the broad scale features of the flow, although there were phase and amplitude errors especially in the later stages of some forecasts.

A major change in weather type occurred between the 18 and 20 of the month, and the D+5 to D+8 forecasts successfully indicated this development of a long wave ridge over the mid-Atlantic, resulting in an undulating upper-level flow over Europe in succeeding days, but with reduced amplitude in the earlier forecasts.

A high amplitude 500 mb trough from Novaya Zemlya through the Baltic over Europe and to north western Africa on the 21st was associated with an intense surface low over Algeria moving quickly north. This development was well predicted in the forecasts from Sunday the 16th and later.

The forecasts from the second half of the month are in general better than those from the first half. The evolution during the last 5 days was particularly well forecast, e.g. the 1000 mb forecasts for the 27th, which show individual details accurately to D+4 and the broad-scale pattern still giving useful guidance in days D+7 to D+10. A systematic feature in these however is the erroneous displacement and breakdown of the high over south-eastern Europe and Russia.

3. VERIFICATION STATISTICS

3.1 Hemispheric scores

The RMS errors incurred by the ECMWF operational model during the month of December 1979 (ensemble mean of 22 forecasts) over the northern hemisphere (20.0 - 82.5 °N) are given in Fig. 3.1 for the height (m) field and in

Fig. 3.2 for the temperature ($^{\circ}\text{C}/10$) fields. Anomaly correlation (%) for the same two variables are also given (Figs. 3.3 and 3.4). The top diagram in each of the figures give the total, vertically averaged (between 200 - 1000 mb for height and 200 - 850 mb for temperature) scores as a function of the forecast length (days). Together with the RMS errors, the persistence error and climatological variance (norm) are shown. For anomaly correlations, the 0.6 level taken to represent an estimate of the predictability limit is shown as a dotted line. The remaining diagrams show vertical cross-sections with pressure (mb) as the vertical coordinate of the same scores whereby the fields are also Fourier analysed and averaged over spectral bands: total (all wavenumbers), zonal (mean, wavenumber 0), wavenumber bands 4-9 and 1-3. For quick reference some of the scores are reproduced in digital form in Table 1: for heights, vertically averaged, 500 and 1000 mb values; for temperatures, vertically averaged, 500 and 850 mb values; for both, every 12 hours up to day 7.

The pattern shown in the spectral decomposition of these scores and their vertical structure are fairly typical for atmospheric models. Fig. 3.1 shows that the largest contribution to the RMS height errors is coming from the long waves (1-3) with the medium waves (4-9) contributing slightly less. The errors tend to be minimum around 850 mb and maximum near 300 mb with a realistic maximum at 1000 mb. Errors in the zonal part are relatively more important near the surface. The vertical structure of the RMS temperature errors (Fig.3.2) is very much the opposite of the one for RMS height errors with a maximum at 850 mb, a minimum near 300 mb and a relative maximum above. Height correlations (Fig. 3.3) are larger for the long waves and generally increase from the surface upwards. Temperature correlations (Fig. 3.4) are also larger for the long waves. In the first half of the

forecast period, their vertical structure show minima at both 300 and 850 mb with maxima at 200 and around 700 mb. In the second half of the forecast period, their structure changes considerably and in a different manner for long and medium waves..

Both scores (RMS errors when weighted by persistence and anomaly correlations) agree in showing a decrease in model predictability for December in comparison with November although December scores remain better than for both September and October.

FORECAST LENGTH (HRS)		12	24	36	48	60	72	84	96	108	120	132	144	156	168	
HEIGHTS	1000-200 Persistence	44	73	93	107	118	126	132	135	139	141	145	148	152	154	
	1000-200	21	28	36	45	54	62	73	83	93	102	110	116	123	127	
	500	20	27	36	45	54	63	74	84	96	105	113	119	126	130	
	1000	19	26	33	40	47	53	60	67	74	80	85	88	92	95	
	1000-200	98	97	95	92	89	85	80	73	66	60	54	49	43	39	
	Anom. Corr. (%)															
	Stand. Dev. (M)															
	500	99	97	95	93	89	85	80	73	66	60	54	48	42	38	
	1000	97	95	92	88	84	79	73	65	57	50	44	39	34	29	
	TEMPERATURES	850-200 Persistence	23	34	40	44	48	50	52	52	53	54	54	55	56	57
850-200		13	17	21	24	27	30	32	36	39	42	44	46	47	48	
500		12	15	18	21	24	28	30	34	37	40	42	45	46	47	
850		16	21	26	29	33	36	40	43	47	51	53	55	56	58	
850-200		97	92	88	85	81	76	72	66	61	54	49	45	41	37	
Anom. Corr. (%)																
Stand. Dev. (C/10)																
500		96	93	90	86	82	77	73	66	60	52	47	41	38	35	
850		94	91	87	84	80	76	72	67	61	55	44	46	42	38	

Table 1. Standard deviation of the persistence and forecast errors (Stand.Dev.) and anomaly correlation coefficients (Anom.Corr.) for heights and temperatures over the northern hemisphere (82.5 to 20.0 N) vertically averaged and at various pressure levels for the month of December 1979 (22 cases)

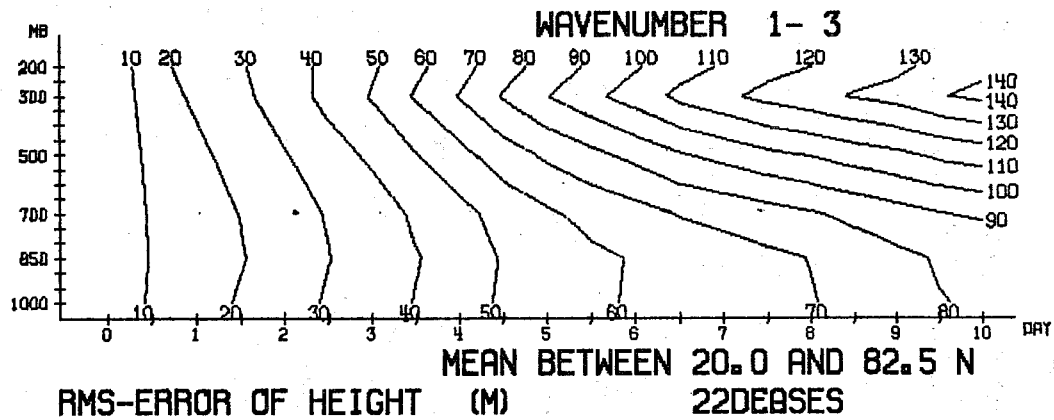
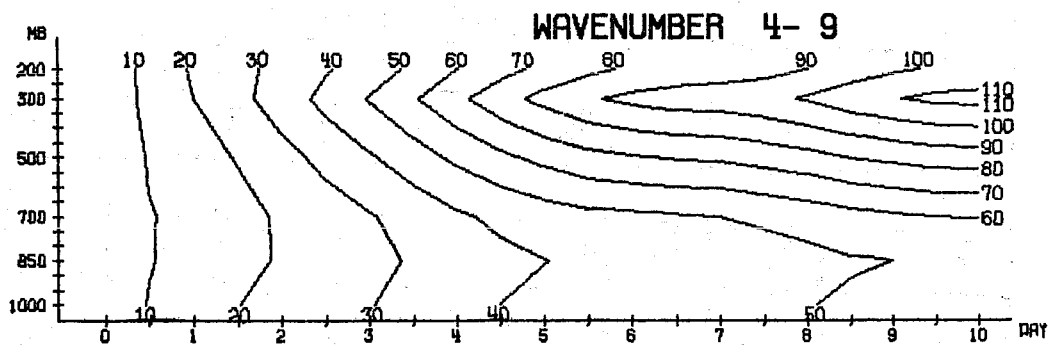
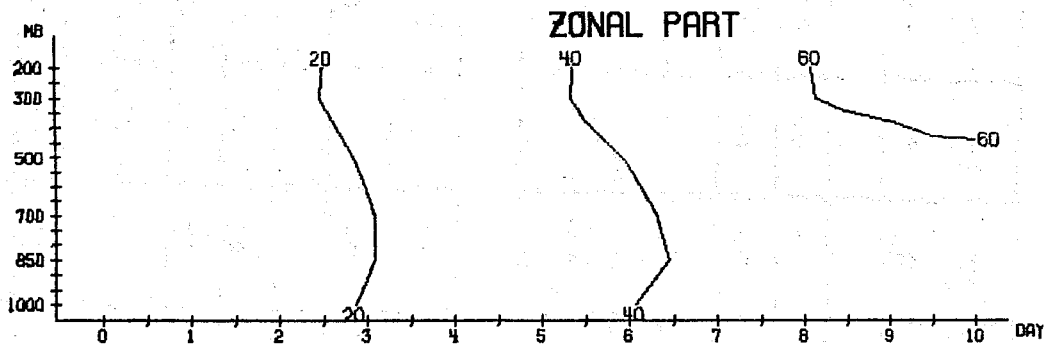
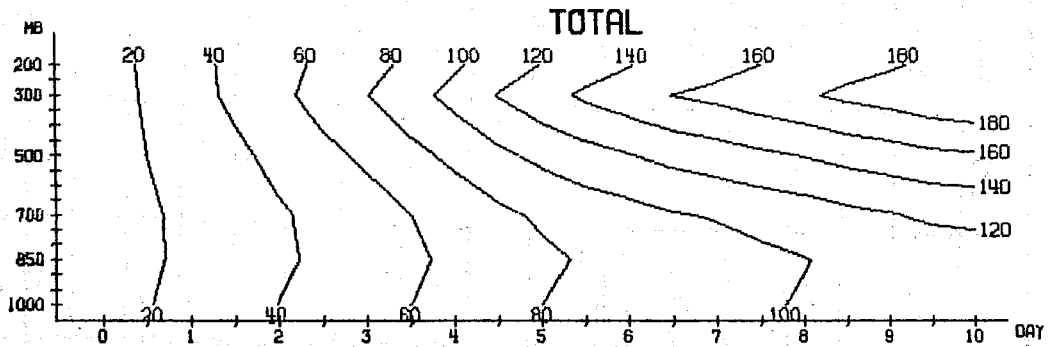
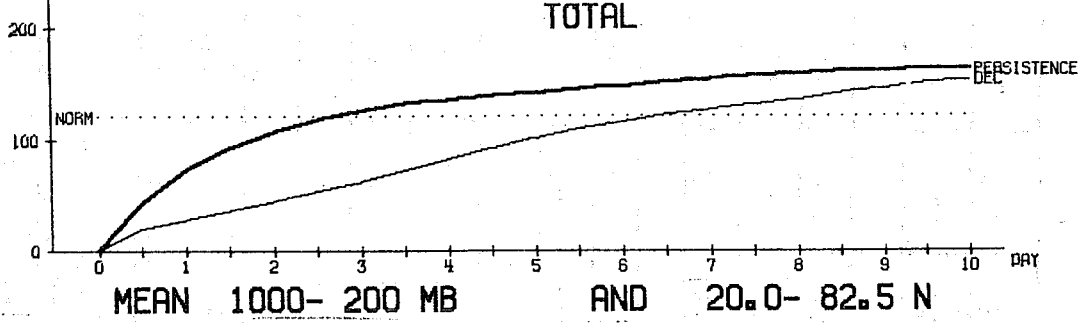


FIG. 3.1

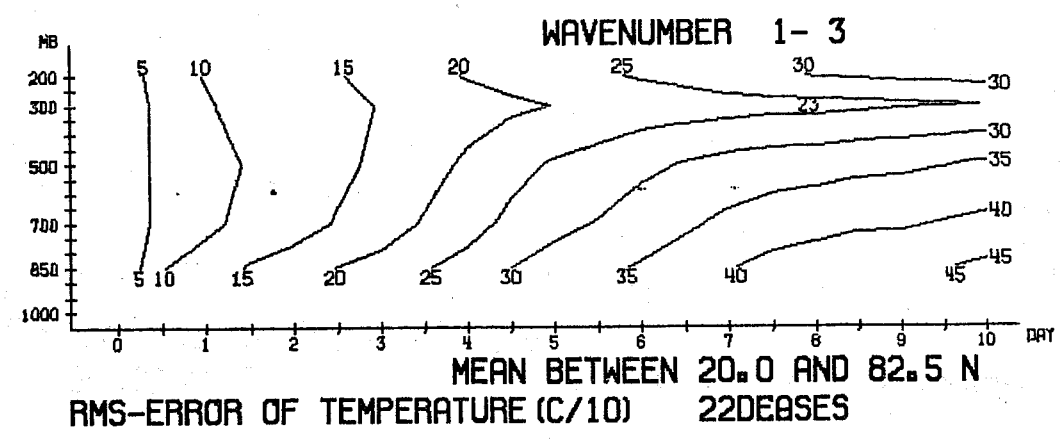
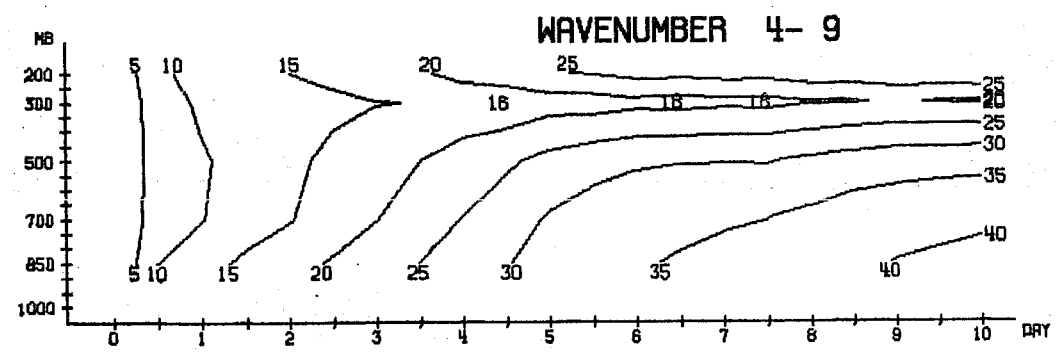
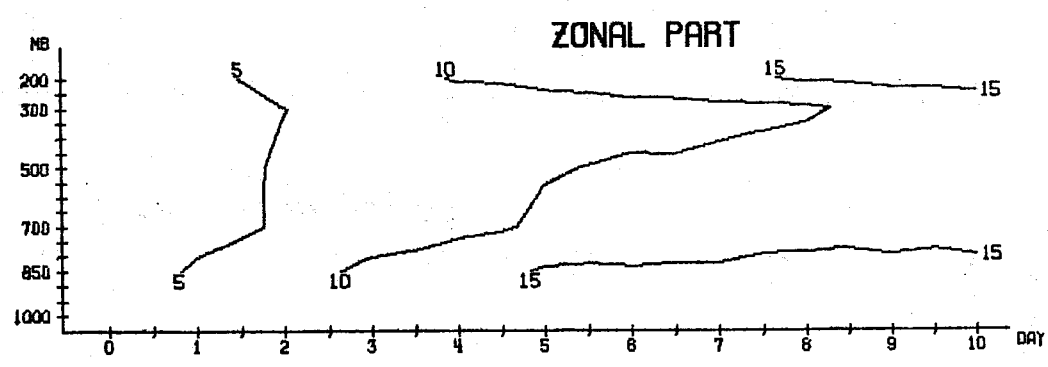
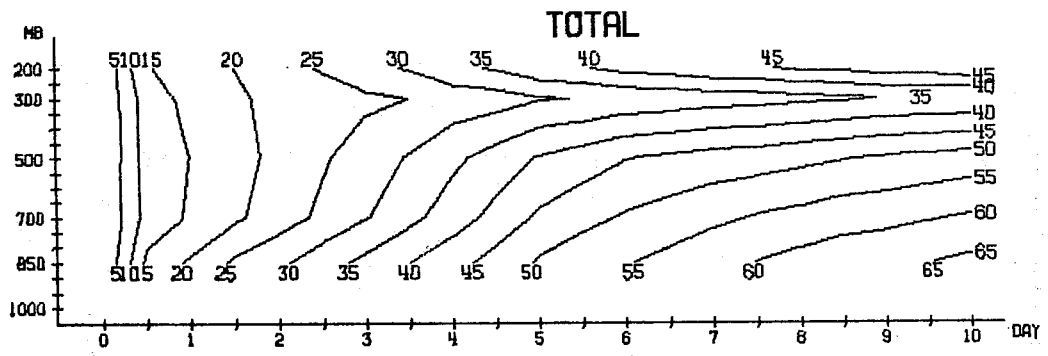
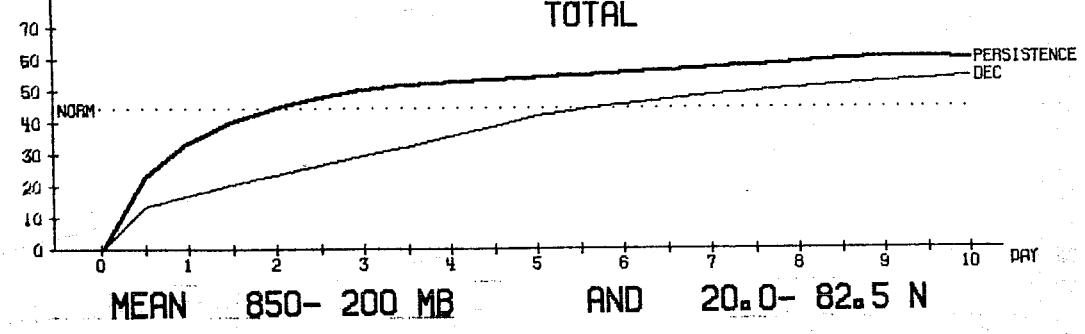


FIG. 3.2

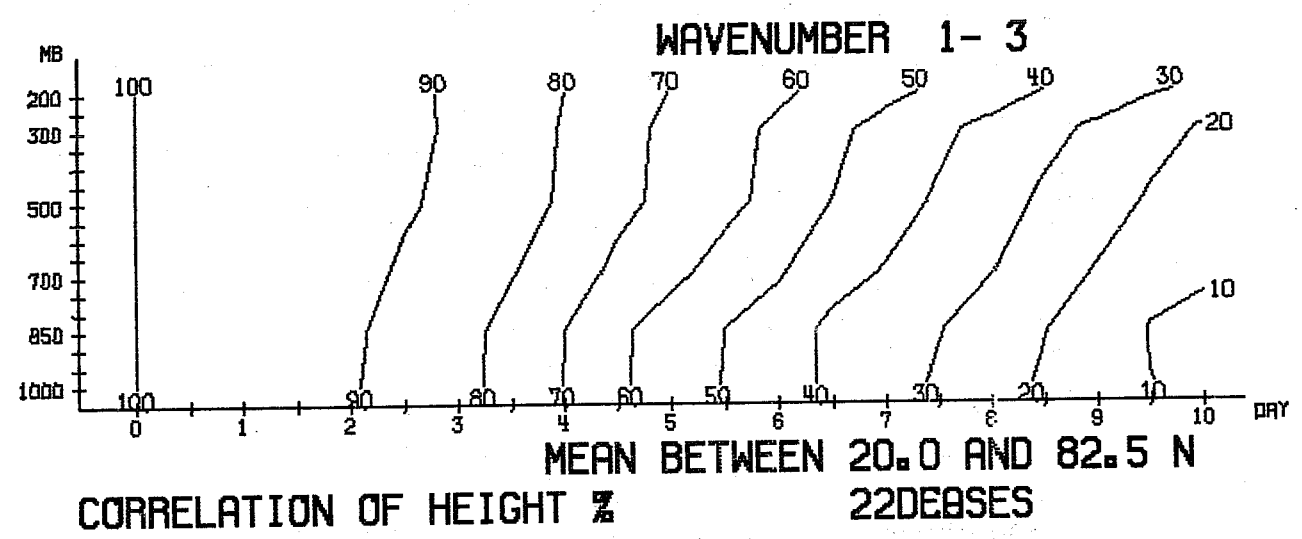
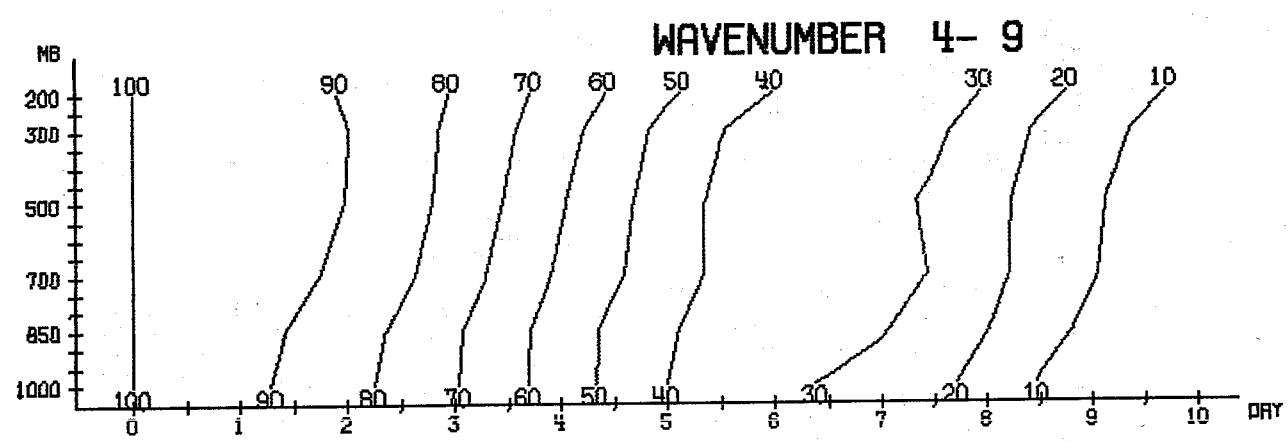
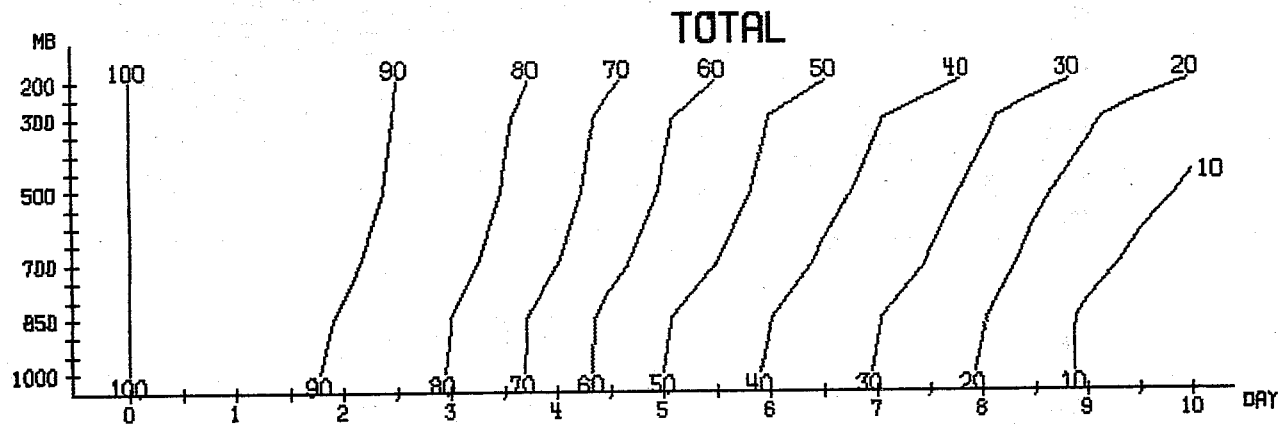
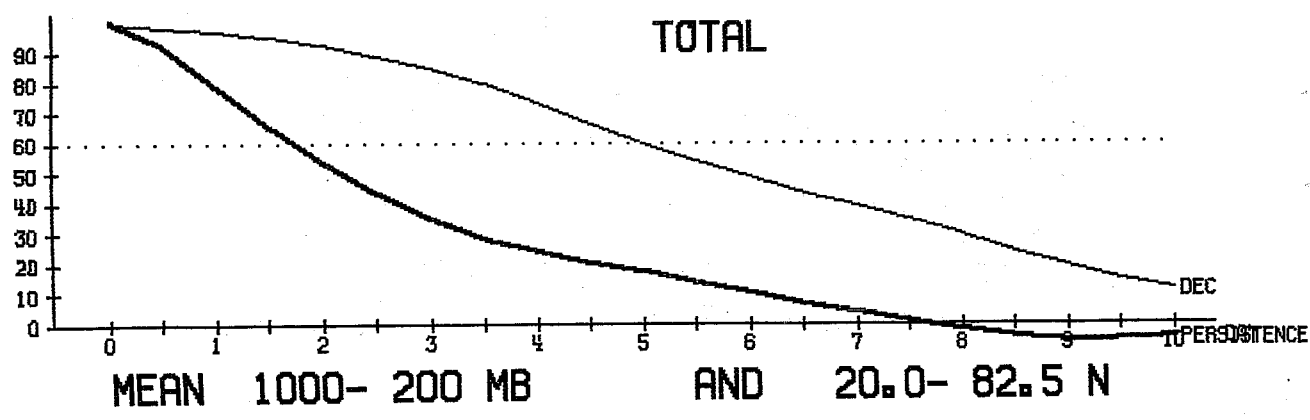


FIG. 3.3

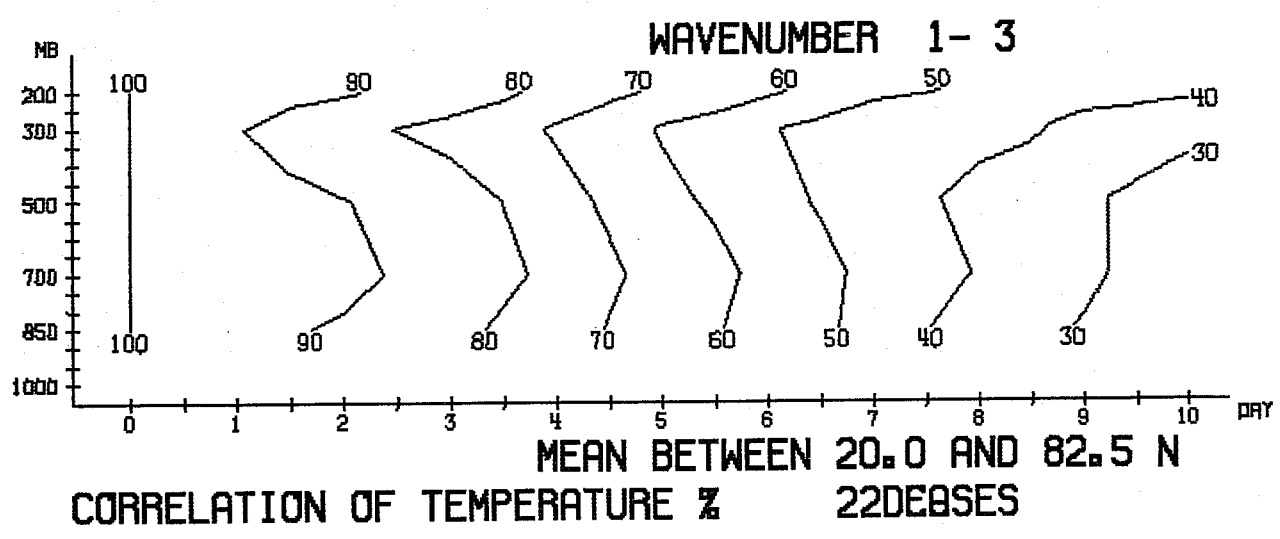
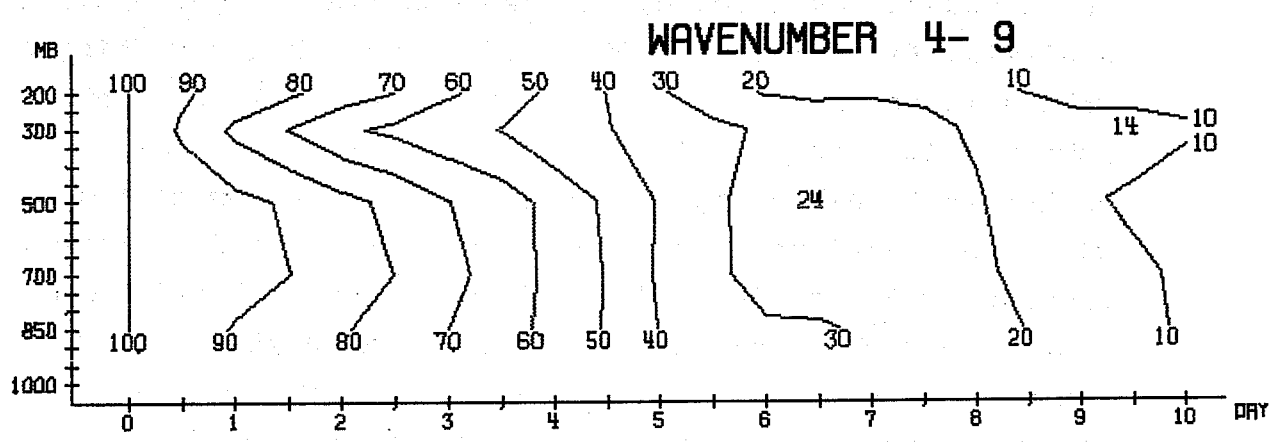
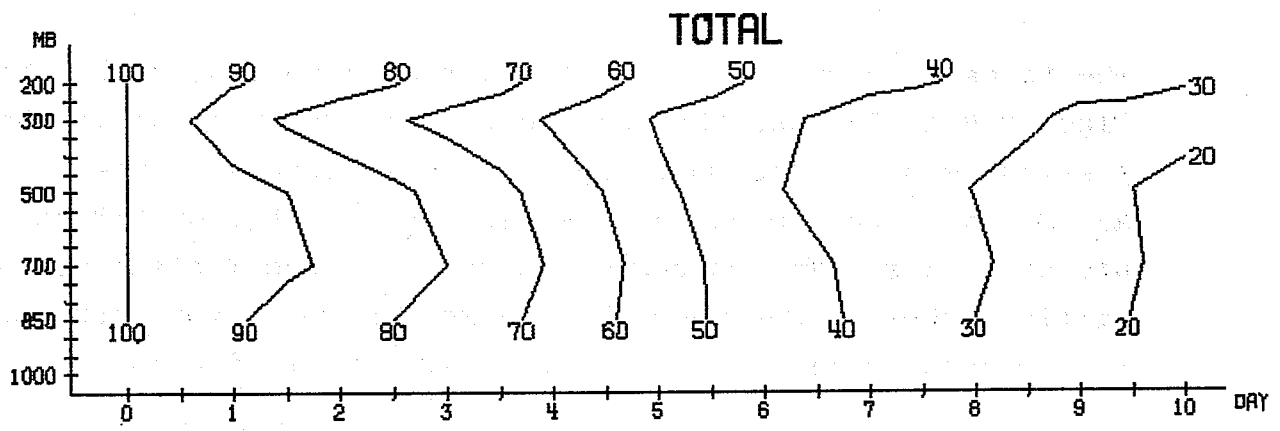
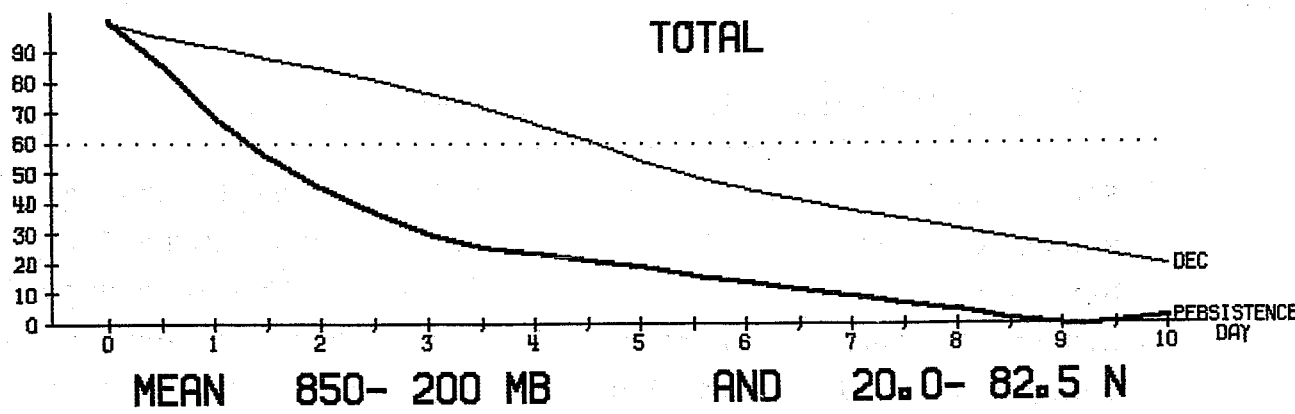


FIG. 3.4

3.2 Verification results of December 1979 for the European area

From daily values of tendency correlation coefficient and standard deviation, Fig. 3.5, we can see that ECMWF forecasts have a high skill at least up to 72 hours. The forecasts for longer periods have more variability from day to day as the daily values of the 144 hour forecast show. This figure also shows the improvement in the forecasts in the second half of the month, already noted in Section 2 above.

The tendency correlation coefficient of geopotential height, Figs. 3.6 to 3.7 has the same feature in December as in the previous month. The most rapid decrease occurs between D+3 and D+6 at lower levels and between D+3 and D+7 or D+8 at higher levels. The values of correlation coefficient are a little higher in December than in November for most part of the forecast period at levels from 1000 mb to 500 mb.

The standard deviation of the geopotential height against analysis, Figs. 3.8 to 3.10, for its part has some higher values in December than in November especially at higher levels. At those levels the persistence error is also higher in December than in November. The crossing point with the normal value for the height error is in December close to D+5½ at 850 mb level, D+6 at 700 mb level, and D+6½ at 500 mb level, and still later at higher levels. The most significant differences between December and November can be seen in the temperature error, Figs. 3.11 to 3.12. The RMS error values are over 0.7 °C higher at 1000 mb level in December than in November. This same difference can also be found between the persistence errors. The RMS error is still 0.5 °C higher in December at 700 mb level after D+7, but it is decreasing when the upper levels are considered. The crossing point with the normal value of temperature is close to D+4½ at 850 mb level, D+5 at 700 mb level, and D+6 at 500 mb level. This is remarkably earlier than in November.

Chart
Well
Graph Data Ref. 5501

mm, 1/2 and 1 cm

ECMWF DECEMBER 1977

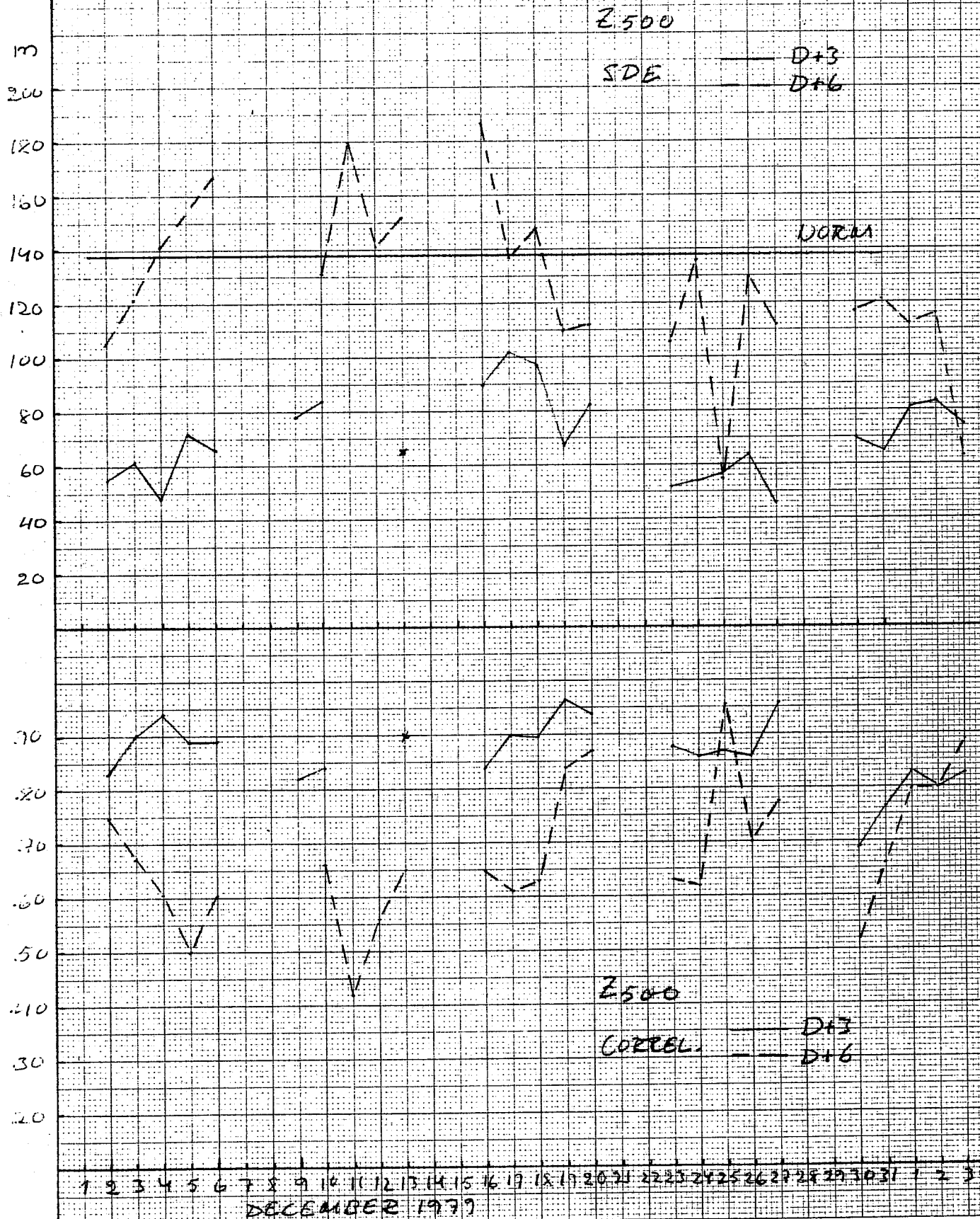


FIG. 3.5

ECMWF DECEMBER 1979

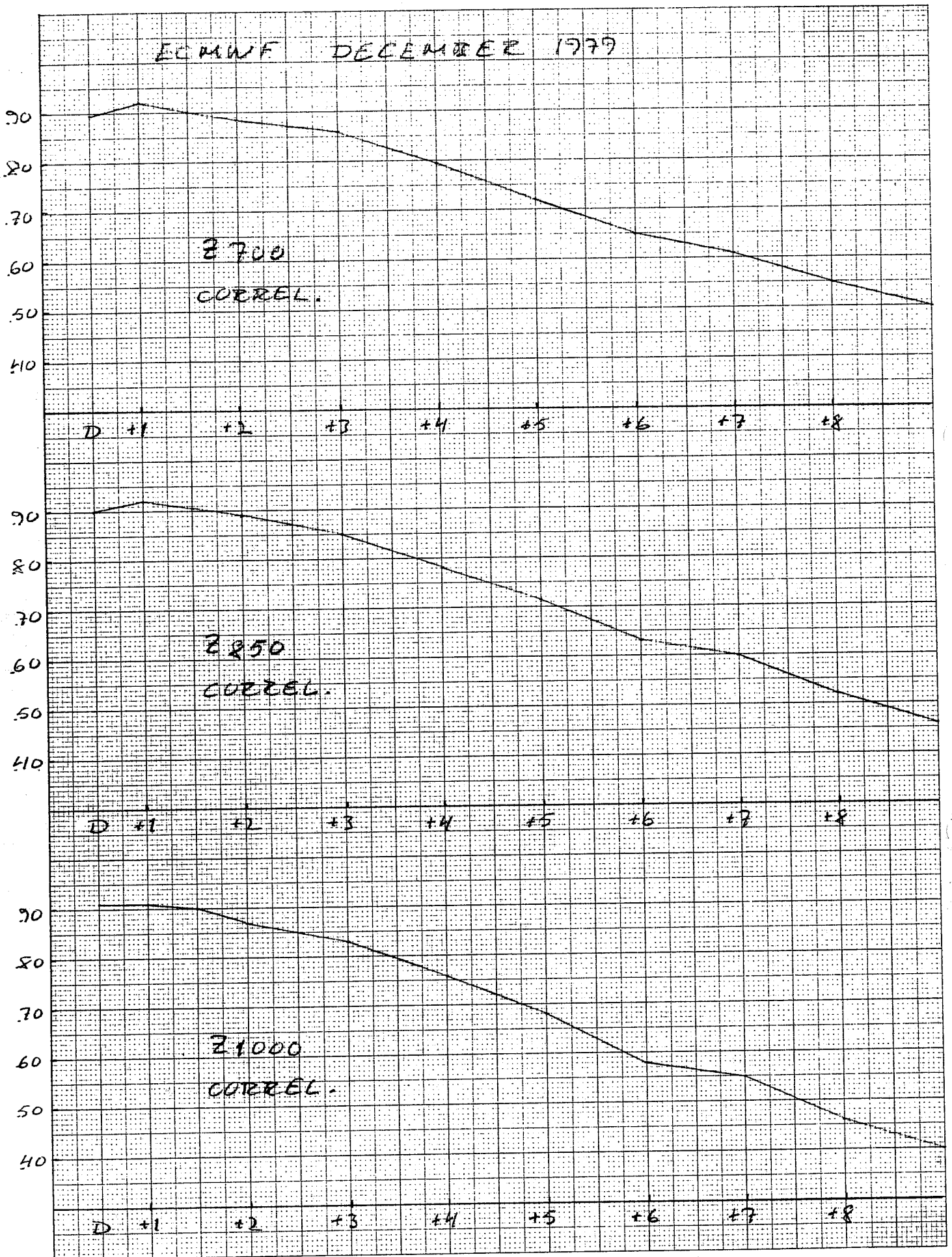


FIG. 3.6

ECMWF DECEMBER 1979

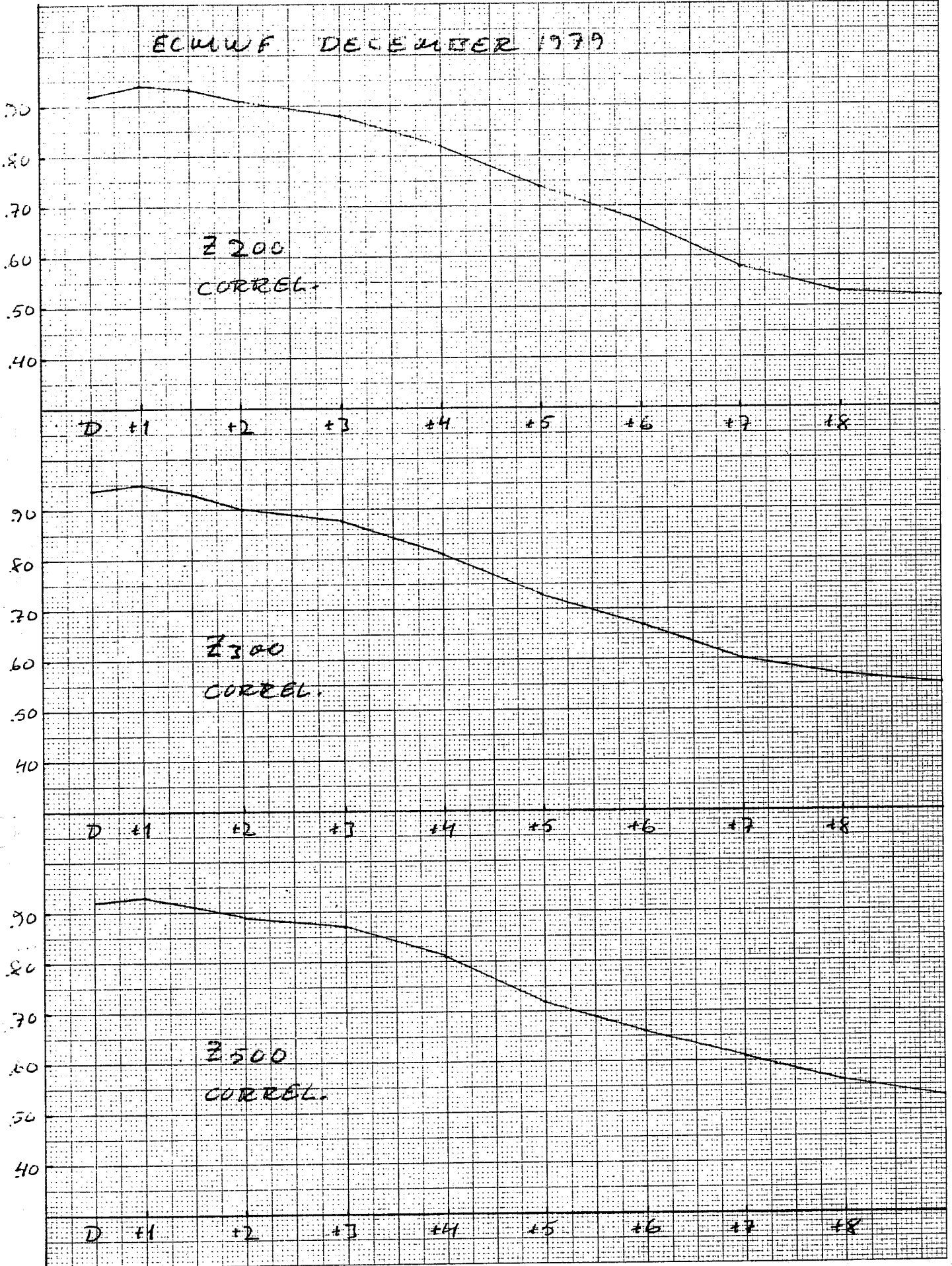


FIG. 3.7

ECMWF DECEMBER 1979

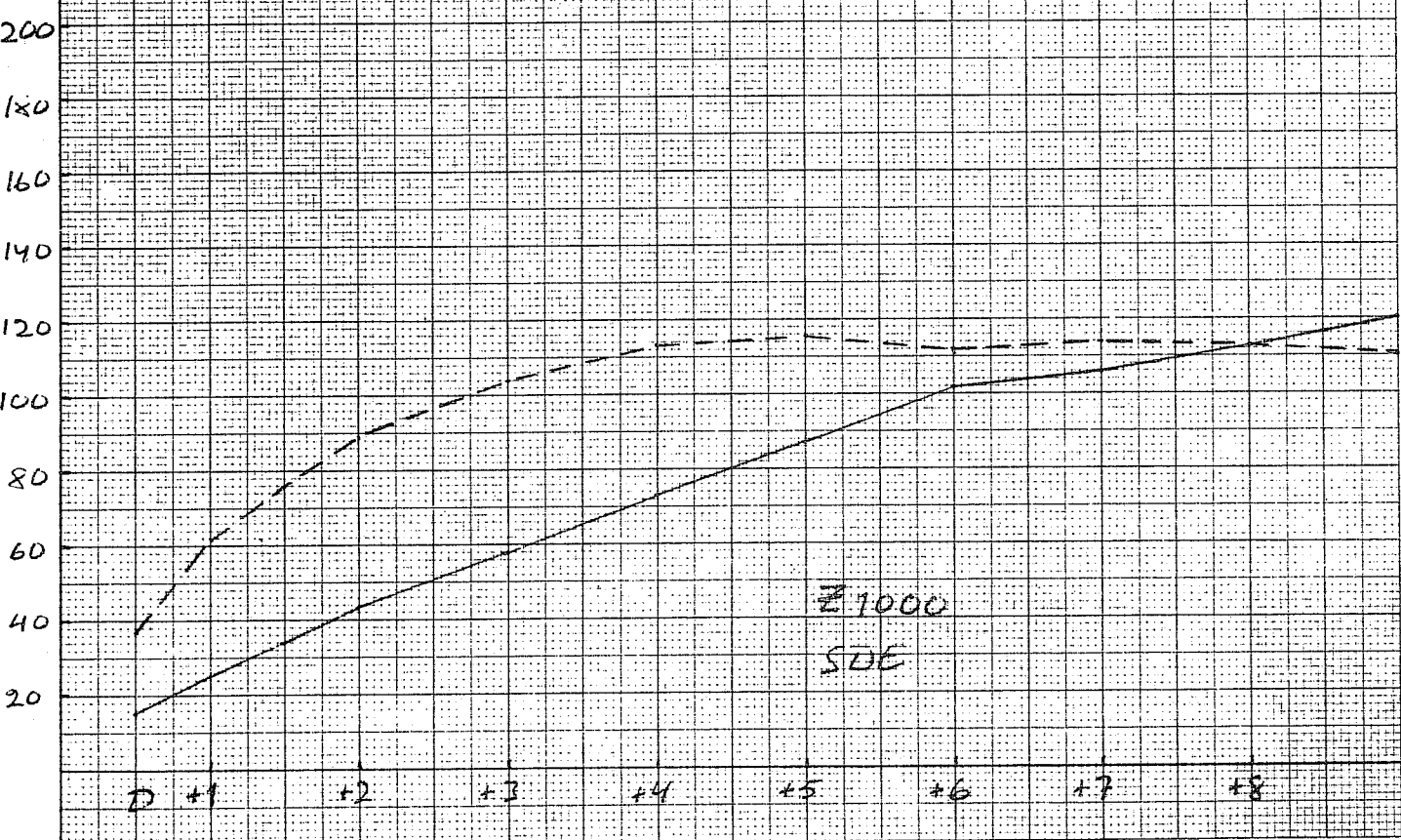
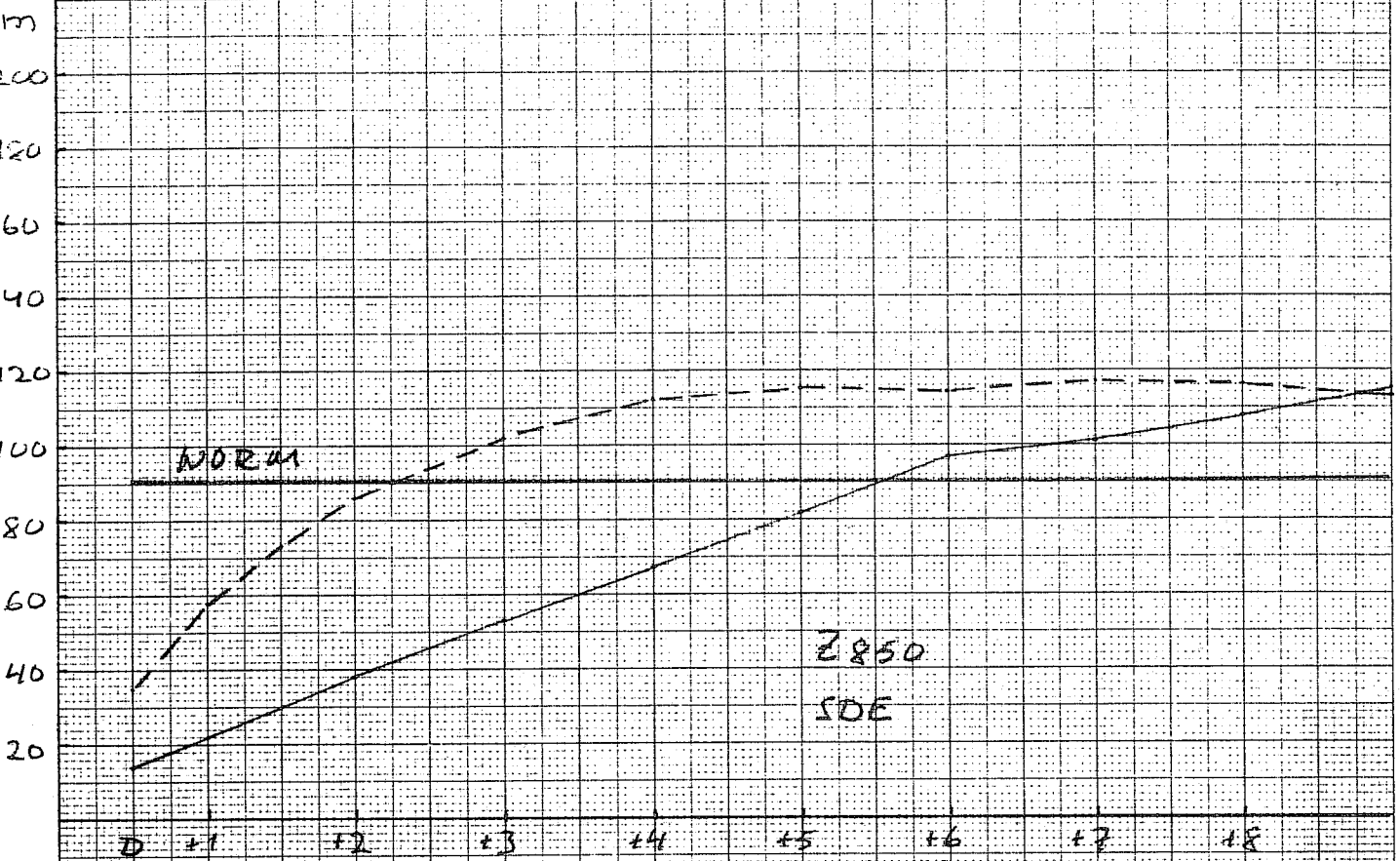


FIG. 3.8

mm. $\frac{1}{2}$ and 1 cm

Graph Data Ref. 5501

CHA
WELL

ECMWF DECEMBER 1979

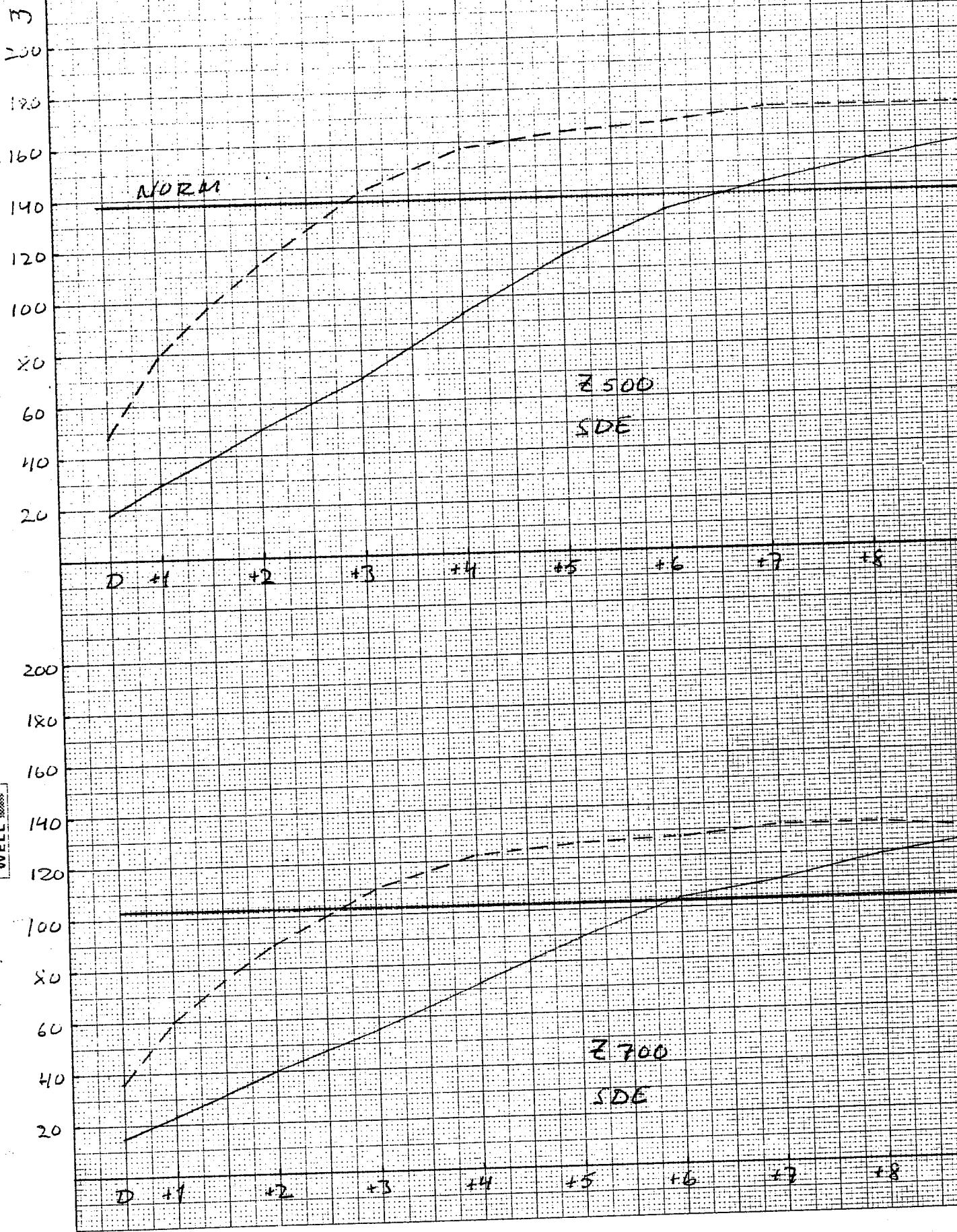


FIG. 3.9

ECMWF DECEMBER 1979

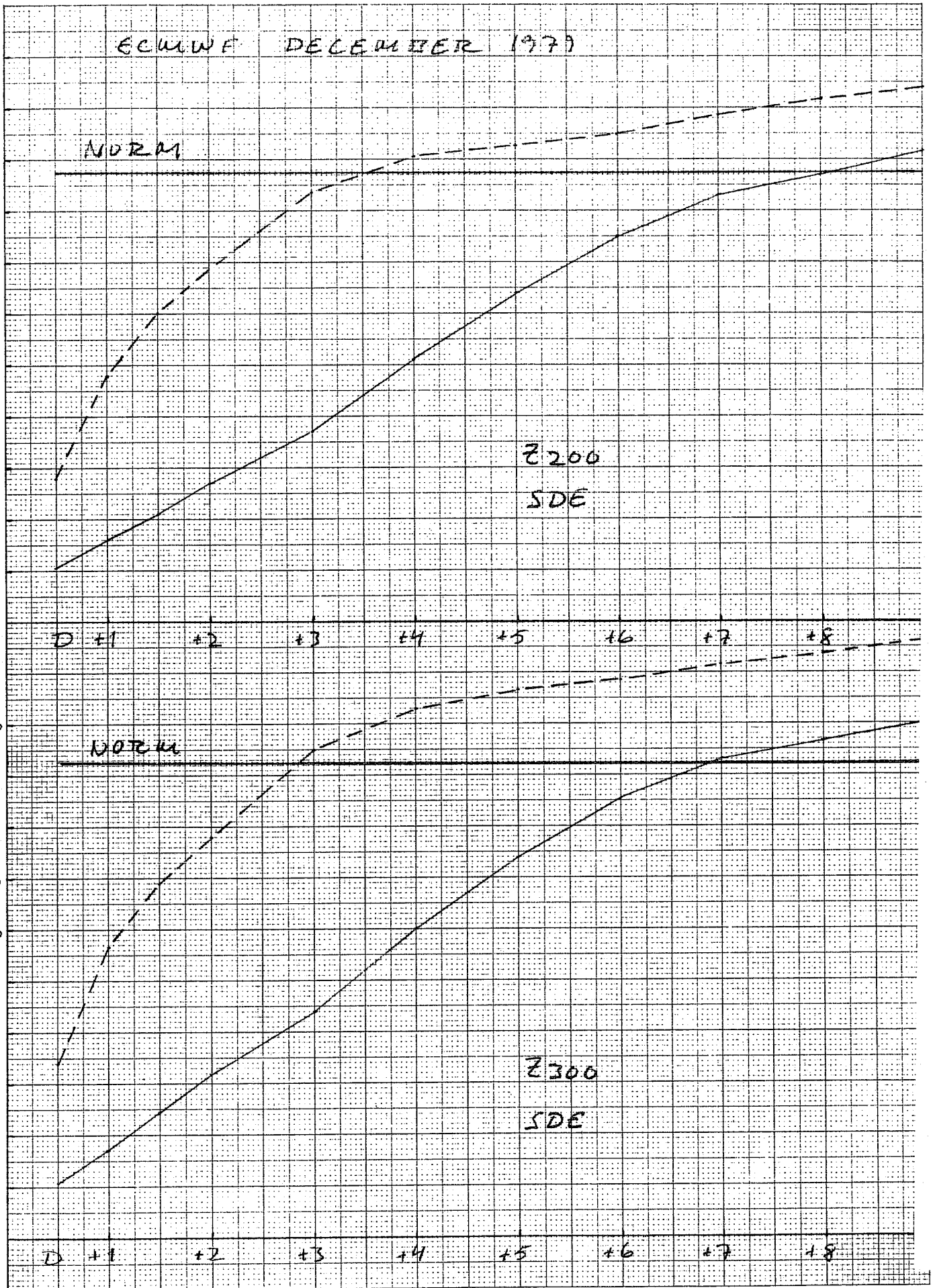


FIG. 3.10

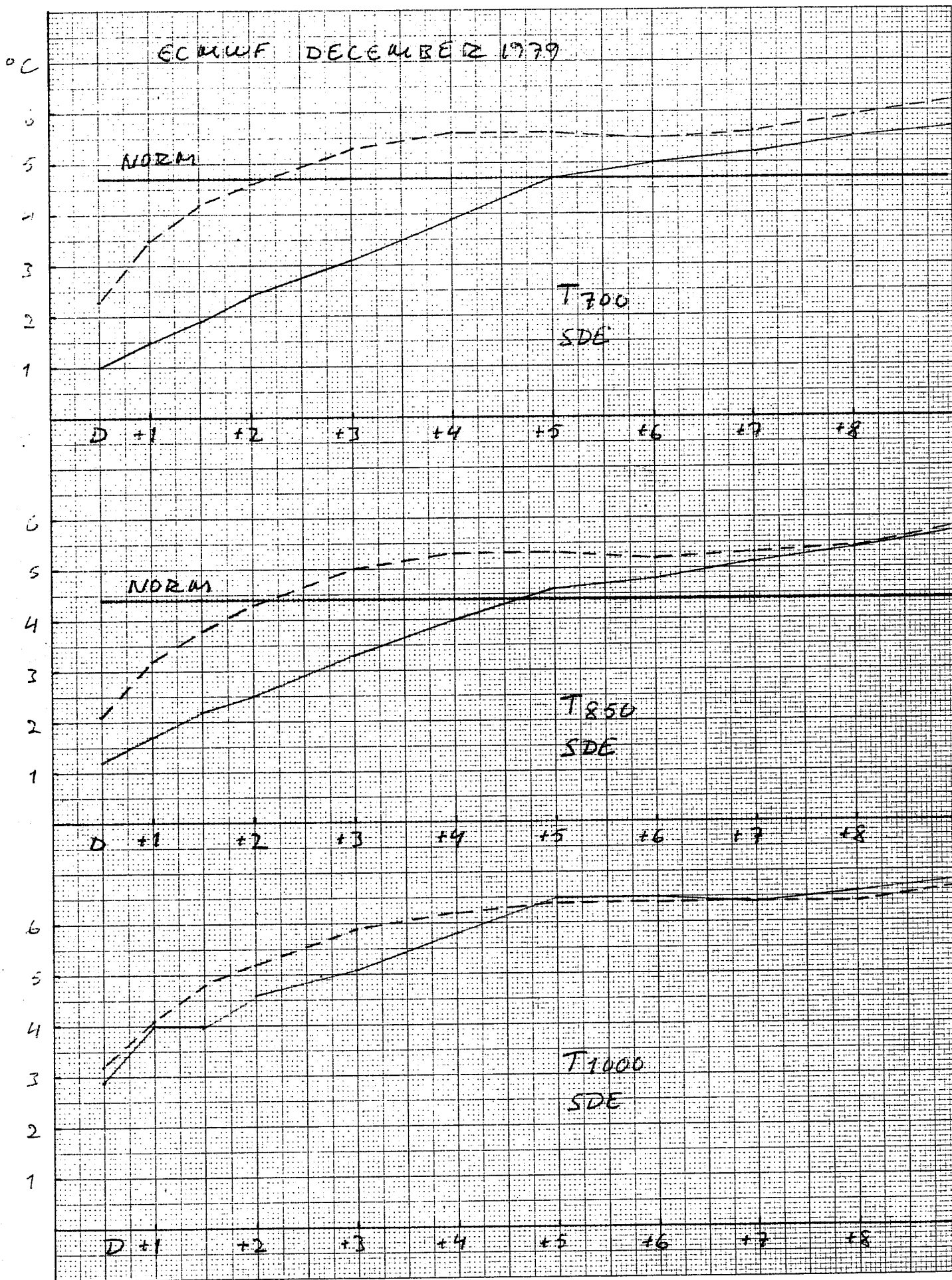


FIG. 3.11

ECMWF DECEMBER 1979

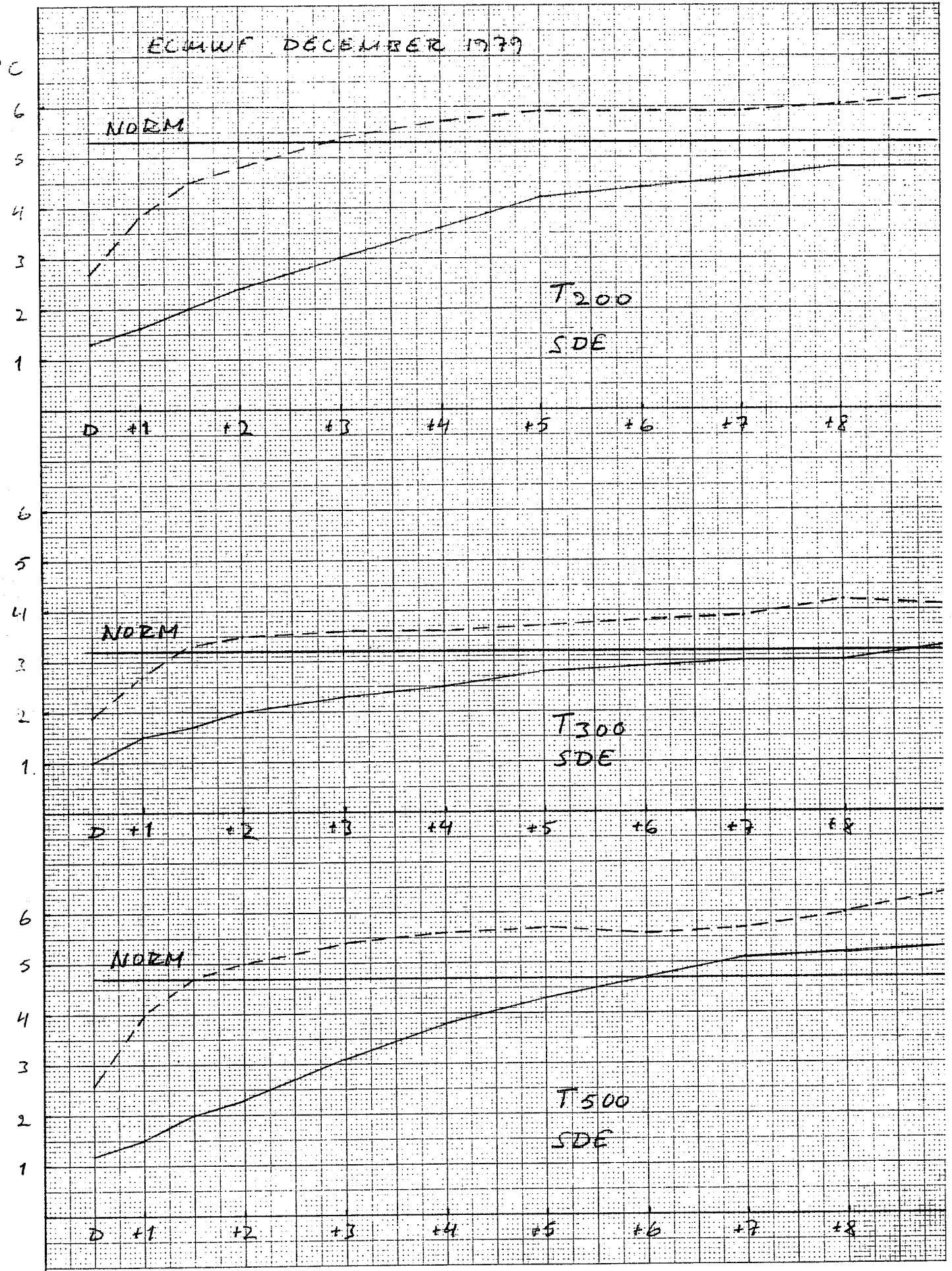


FIG. 3.12

4. SYSTEMATIC ERRORS

4.1 Mean and difference maps of 500 and 1000 mb height and 850 mb temperature

In this Section we present maps of both the observed and forecast mean 500 mb height (Fig. 4.1) and their difference (Fig. 4.2), the observed and forecast mean 1000 mb height (Fig. 4.3) and their difference (Fig. 4.4), the observed and forecast mean 850 mb temperature (Fig. 4.5) and their difference (Fig. 4.6) plus maps of the RMS errors in these fields (bottom part of Figs. 4.2, 4.4, 4.6), all evaluated for day 7 of the forecast period. Contrary to previous reports we have chosen and shall present in the future day 7 instead of day 10 because it is closer to our predictability limit and more suitable for use by meteorologists. To ease the transition the maps for day 10 shall be presented and compared in the special topics Section 5.1.

Looking at the 500 mb height fields (Fig. 4.1), it is quite apparent that the model fails to maintain the observed diffluence over the Pacific and also to a lesser extent over Europe. This leads to a well defined pattern of errors (Fig. 4.2) over these regions with broad negative centres in northern latitudes and positive centres to the south. Turning our attention to the two main observed troughs positioned over the eastern coasts of Asia and North America, we note an eastward displacement of their forecast counterparts born out by positive error centres over these regions and negative centres further east. Displacement errors are even more apparent on the northern side of the mean jet with absence of ridging over the Rocky Mountains and lack of tilting of the trough over Europe.

The pattern of error for 1000 mb height (Figs. 4.3, 4.4) has a very similar structure leading to the conclusion that the error has a large barotropic component. Note in particular the lack of ridging on a line going from Central North-America

to Eastern Siberia, suggesting insufficient topography forcing.

Temperatures at 850 mb (Figs. 4.5, 4.6) show the tendency for the forecasts to be colder than observed over most of the northern hemisphere except over the Polar Cap and Eastern Canada.

4.2 North-south profiles and cross-sections

In this Section we present north-south profiles of both forecast and observed temperature at 850 mb and 500 mb, zonal wind at 300 mb and height at 1000 mb (Fig. 4.7) and cross-sections of temperature, zonal wind and stability deviations from observed, (Fig. 4.8) all averaged between day 4 and 7.

From the north-south profiles, and cross-sections it is apparent that the forecast bias toward colder temperatures extends over the whole troposphere and into the stratosphere with a gap near the tropopause level (see also mean stability deviations) and is almost uniform between 20° and 60° N. Northward shift of the mean jet, larger winds in middle latitudes and weaker ones at both southern and northern latitudes (increased confinement) is seen to be a feature not only of the 300 mb level but again leading to an error very much barotropic in character (Fig. 4.8). Height departures at 1000 mb are very much indicative of excessive zonal surface winds in middle latitudes and suggest lack of effective surface drag as part of the problem.

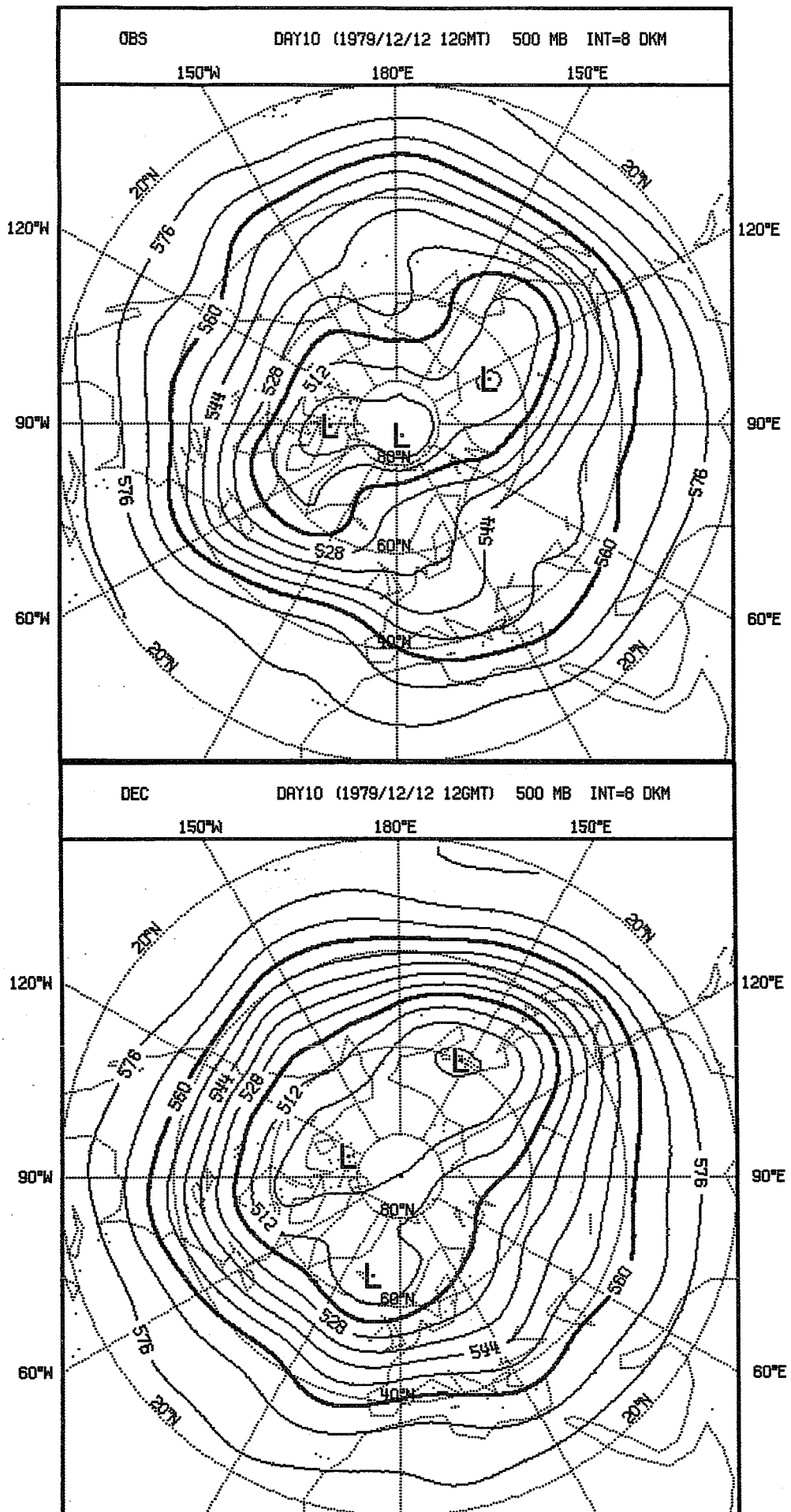


FIG. 4.1

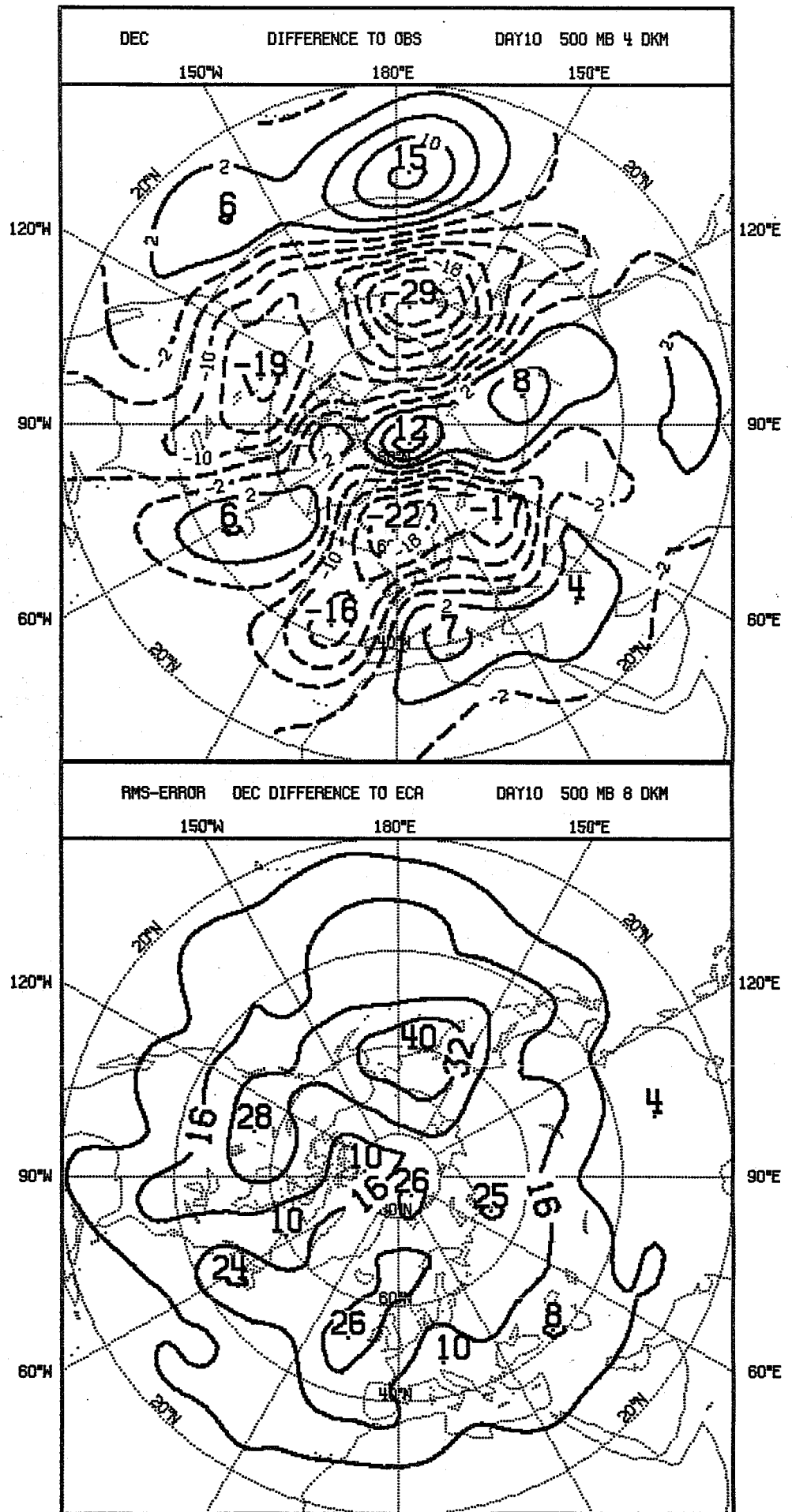


FIG. 4.2

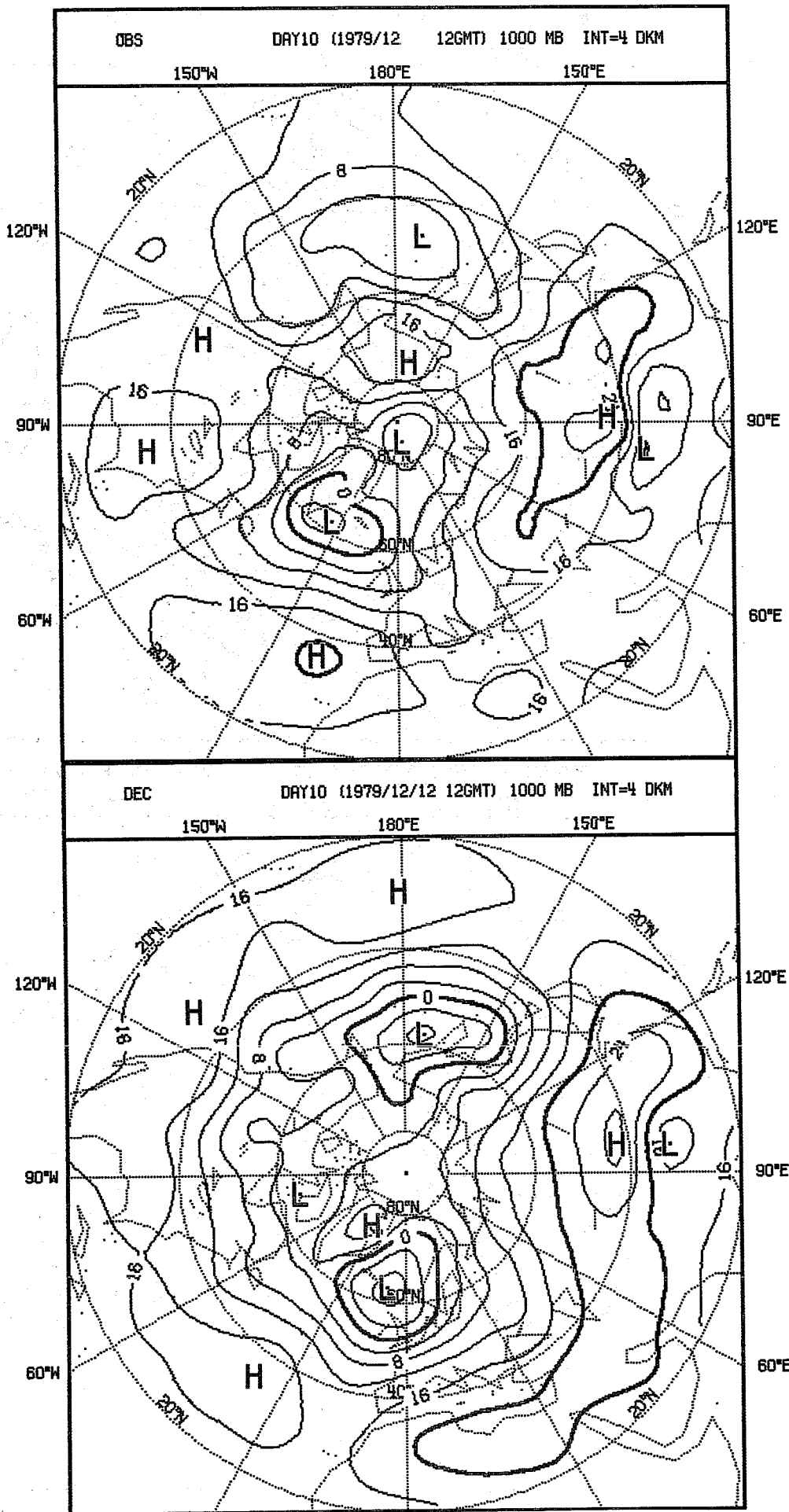


FIG. 4.3

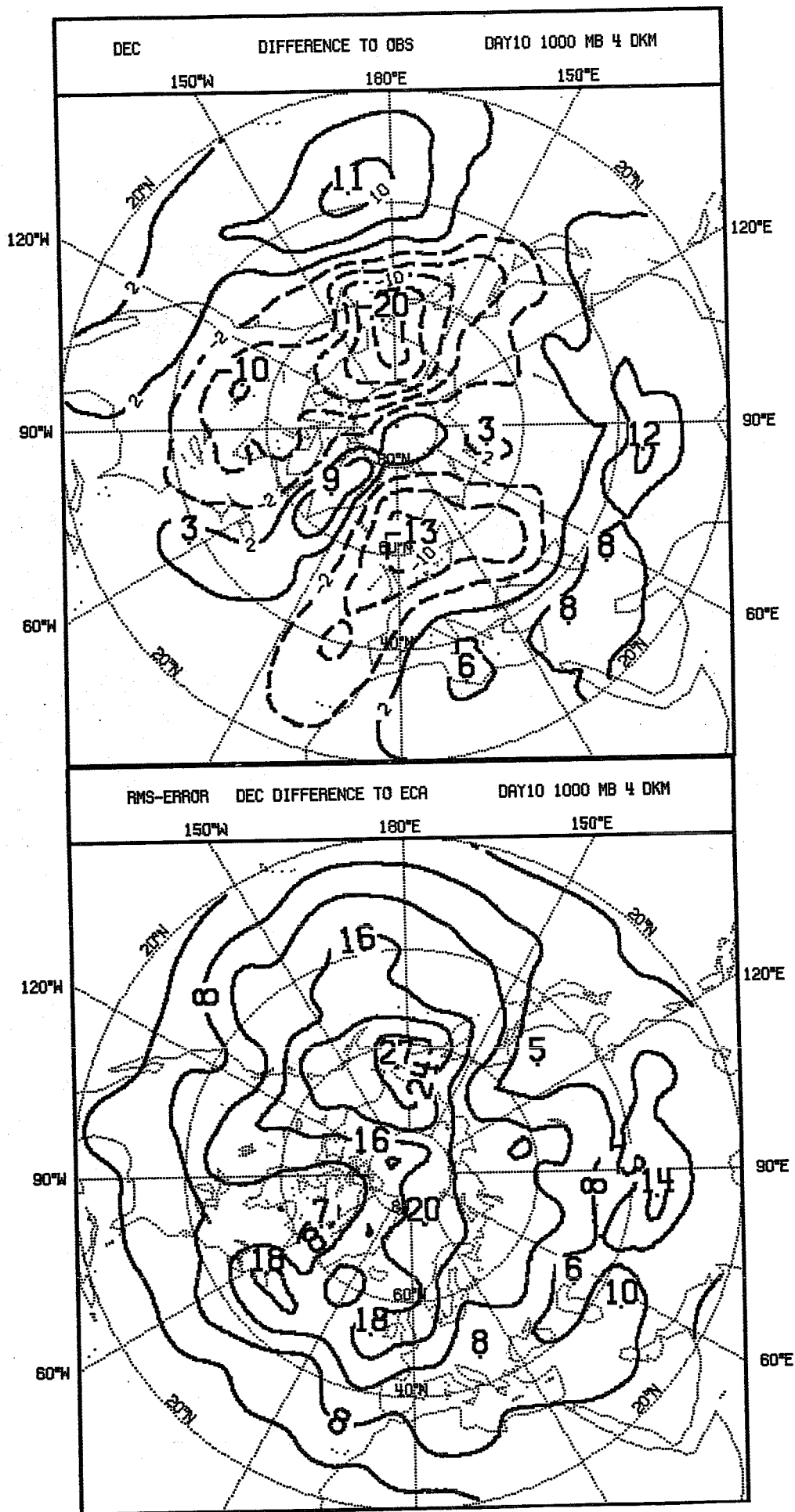


FIG. 4.4

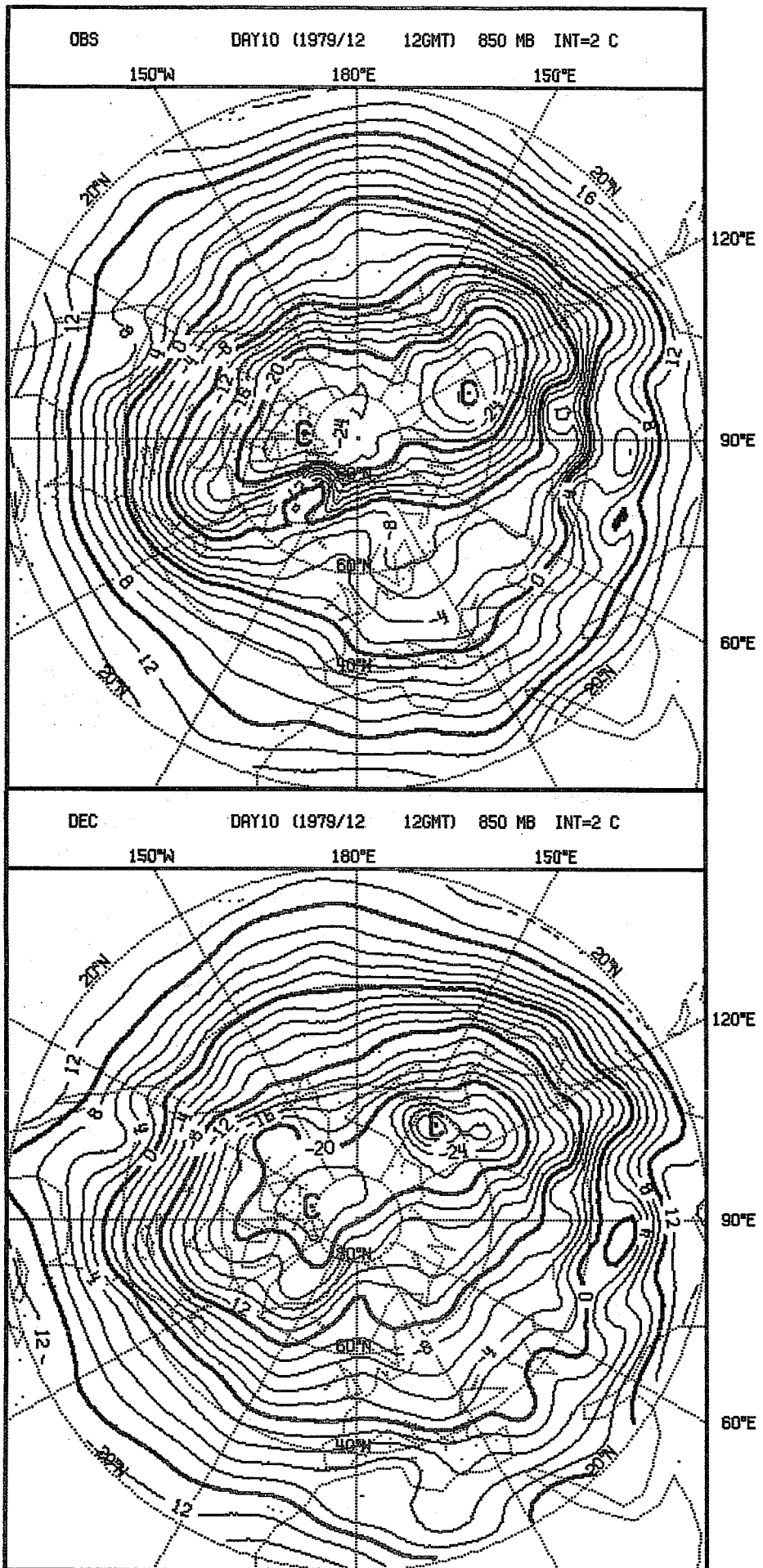


FIG. 4.5

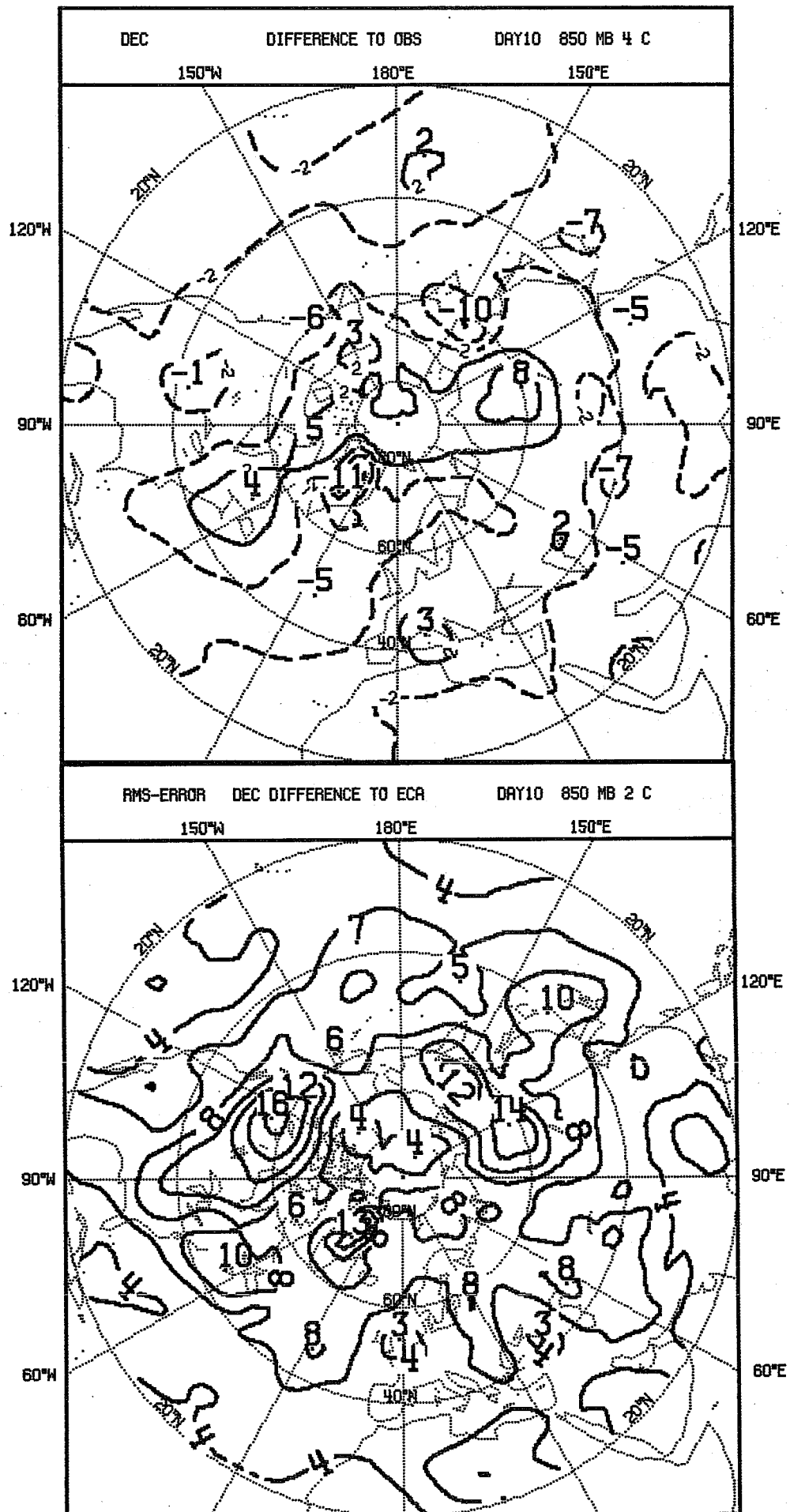


FIG. 4.6

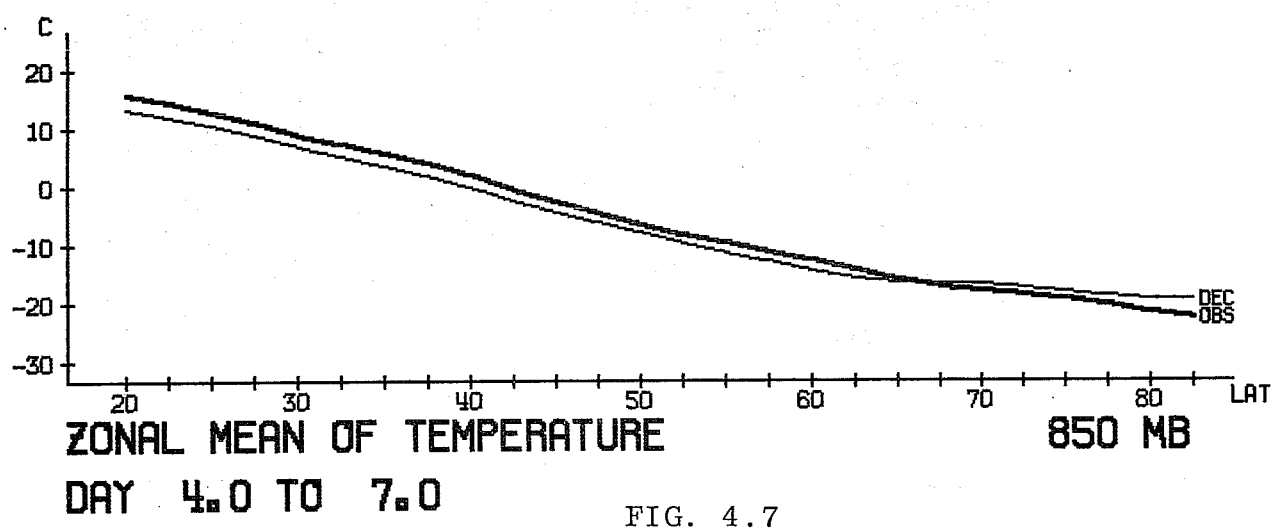
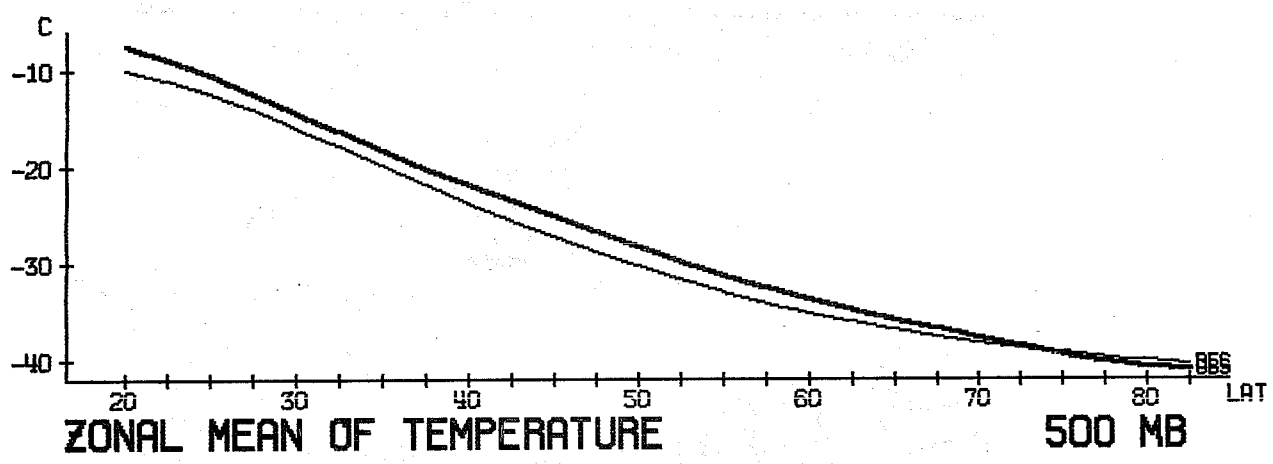
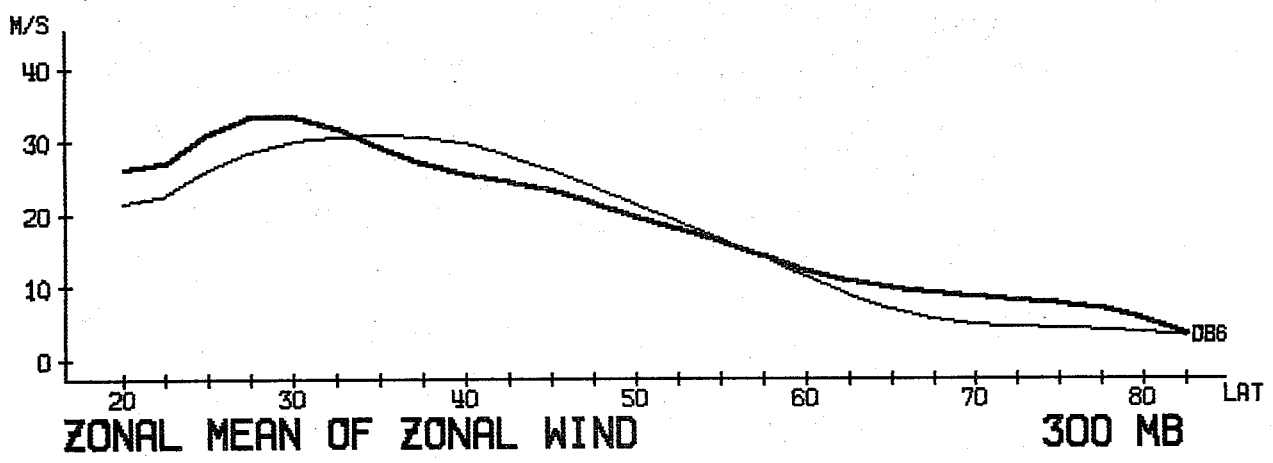
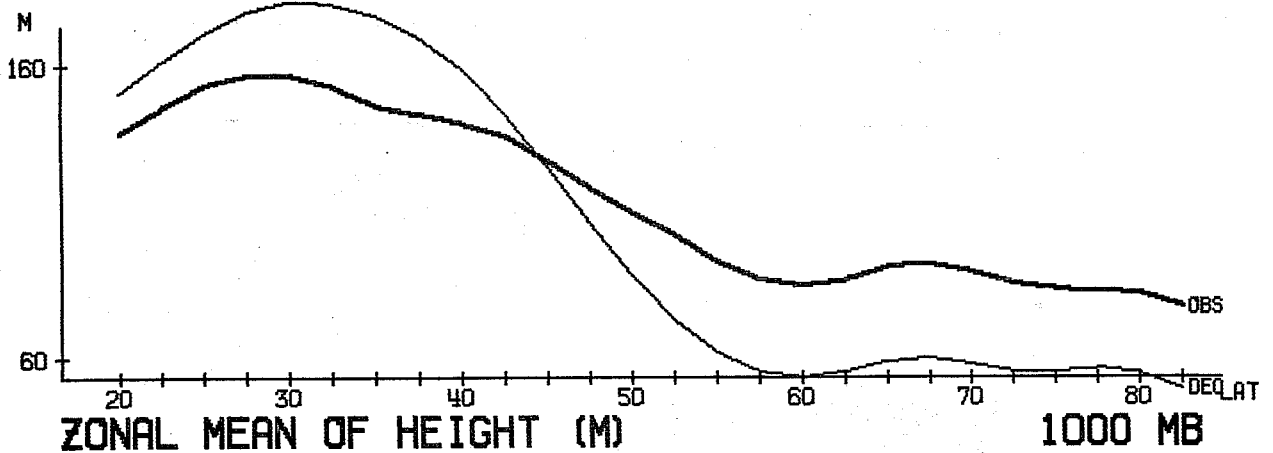
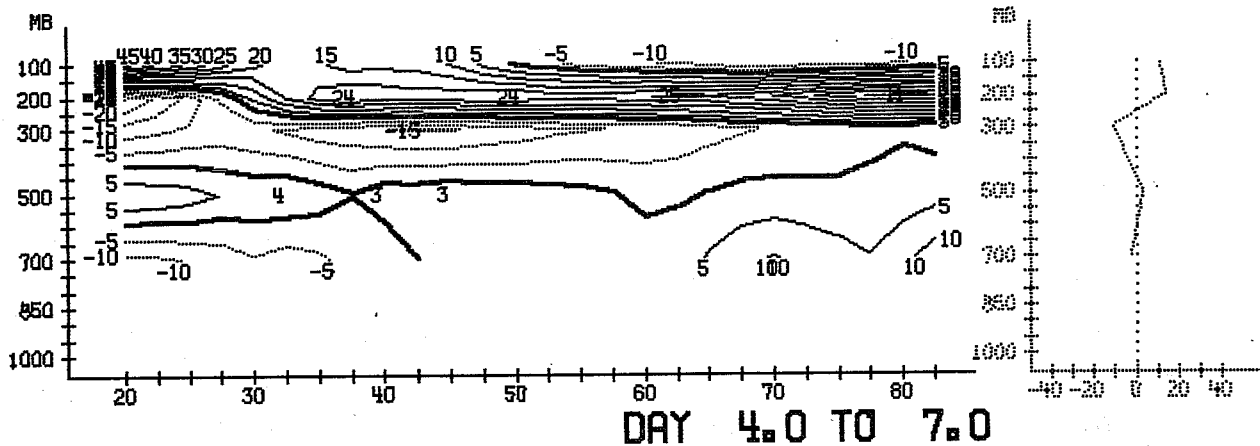
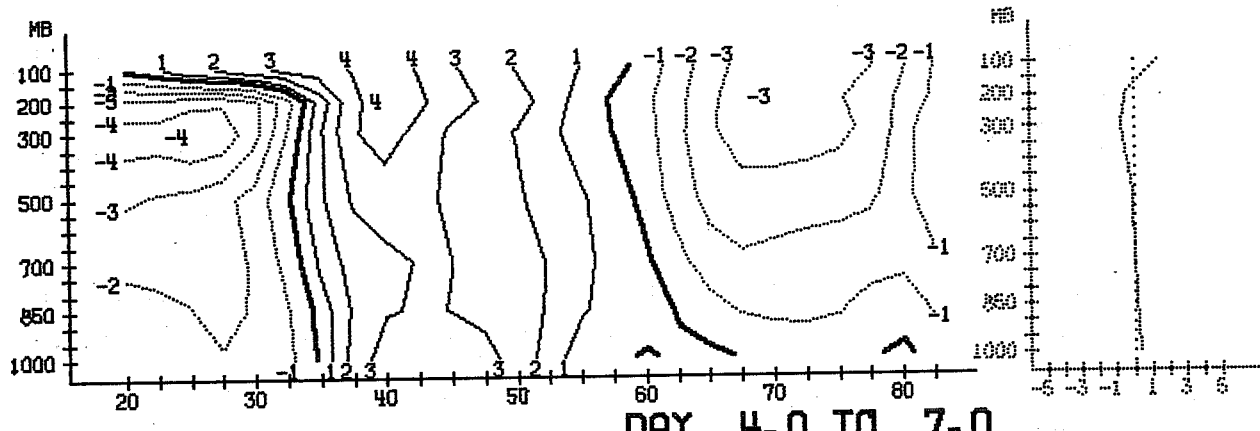


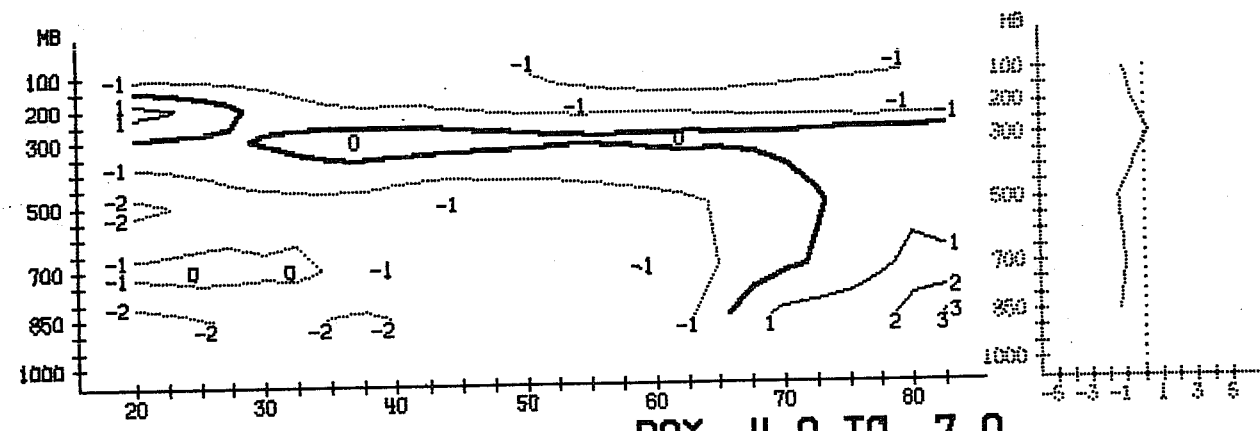
FIG. 4.7



DAY 4.0 TO 7.0
MEAN VERT STABILITY DEVIATION FROM OBS



DAY 4.0 TO 7.0
ZONAL MEAN OF U DEVIATION FROM OBSERVED GEOSTR



DAY 4.0 TO 7.0
ZONAL MEAN OF T DEVIATION FROM OBSERVED

FIG. 4.8

5. SPECIAL TOPICS

5.1 Comparison of the systematic errors, days 4-7 and 7-10

Figs. 5.1 to 5.6 show the same fields as Figs. 4.1 to 4.6 except averaged between forecast days 7-10 instead of days 4.7. Note in particular the remarkable similarity of the error patterns between forecast days 10 and 7. Note also the intensification of the two north-south oriented error dipoles over the Pacific and Europe - North-Africa for both 500 and 1000 mb height fields.

The north-south profiles and cross-sections (Figs. 5.7, 5.8) show that additional cooling has been much smaller in the latter part of forecasts. Zonal mean wind errors have also but slightly increased, their character remaining the same.

Although the errors are larger between days 7-10 and the mean forecast fields between days 7-10 are perhaps closer to the model "climatology", the similarities of the errors between days 4-7 with those at 7-10 are large enough that we can use either indifferently in first analysis.

5.2 Zonally averaged energetics

Figs. 5.9 to 5.20 show as usually the zonally averaged energetics for days 7 to 10. Contrary to what was seen in the previous months the zonal kinetic energy is underestimated in the forecast. But the observed values are far larger than in November, the model values lying somewhere between November and December observations in both months. So, like for its position (see November report) the jet's intensity in the model seems to have a preferred value with a rapid convergence towards it during the course of the forecast. The eddy kinetic energy is underestimated as in previous cases. The diagram for CK does not show any dramatic

northward shift of the main negative centre as in November; there is an attempt to produce a positive centre but with less success than in October. The better positioning of these centres is in some contradiction with the fact that we still have a northward shift of the jet (see above)

The available potential energy show a good repartition both in height and latitude but as always with a systematic underestimation, although less important than in previous months. CA is good as usual.

The term UV is well represented except for the high latitude negative cell which is hardly present in the model's integrations. The term TV in the model is very similar to the model one for other months but this time in disagreement with observations: weakened long wave effect in the stratosphere comparatively to November, the model having not been able to capture this change.

5.3 Tropospheric energy spectra

Figs. 5.21 to 5.29 show the time evolution of the different energy spectra. Looking first at day 7 to 10 one can see a marked improvement against past months: there is still an underestimation, but it is no more localised in a certain part of the spectrum. Furthermore this lack of intensity, noticeable in the higher atmosphere is less than previously and there is no overestimation of KE at 1000 mb. The 500 mb height spectrum is good as well. Unfortunately the study of the time sequence indicate that during days 0-3 there was too much KE at 1000 mb in the model; therefore the better results at the end of the forecast period might have been obtained for the wrong reasons.

The spectra of the standing waves are quite similar to the ones presented before (no figure shown for the standing waves) except for wavenumber 2 which has a most surprising behaviour: quick decrease of intensity in the beginning of the forecast period but then strong rebuilding in the lower layers only with a still low stationary value on the high atmosphere

5.4 Time evolution of the energetics

Figs. 5.30 to 5.33 show the time evolution, with wavenumber decomposition of KE, CK, AE, CA. Compared with November we have for KE an improvement of the zonal term and less dramatic losses for the medium waves but a stronger under-estimation of long waves; CK is slightly improved although the type of error remains the same; AE shows very good quality especially for the medium waves but hardly any improvement for the long waves; CA although quite acceptable is not as good as in November.

5.5 Estimates for the non-adiabatic forcing

Figs. 5.34 and 5.35 show the ensemble mean kinetic energy dissipation, net diabatic heating and net humidity source vertical profiles averaged over land and ocean areas, for 12 GMT analyses (31 cases) and 1 day and 4 day forecasts (21 cases) within December 1979. They are calculated as residuals in the energy balance equations determining the local energy changes, horizontal and vertical flux divergences and internal sources (generation $W \cdot \nabla \phi$ for kinetic energy, conversion $-\alpha \omega$ for enthalpy) from the gridpoint wind, temperature and humidity data.

The kinetic energy dissipation is stronger in the model boundary layer than in the analyses, especially over land ($- 28 \text{ W/m}^2$ and $- 14 \text{ W/m}^2$ respectively in the surface). In the 600-800 mb layer the dissipation remains rather constant in the forecasts

while in the analyses there is a local minimum, even positive dissipation over oceans. A secondary maximum in the 250 mb level can be found both in analyses and forecasts. When averaged globally the dissipation has the largest value of -3.4 W/m^2 for day 4 forecasts, being -1.6 W/m^2 in the analyses and -2.2 W/m^2 in the day 8-10 forecasts.

The net diabatic heating profiles (temperature budget residual) show a general cooling for the forecasts, stronger over land and for 24 h forecast. Global cooling rate for the 24 h forecast is -48 W/m^2 ($\sim 0.4 \text{ deg/day}$). The forecast heating profiles are rather similar over land and sea having a radiative cooling peak in 80 mb level (model level 2).

The humidity net source (humidity budget residual) is proportional to evaporation minus precipitation. The 24 h forecasts show a large excess of evaporation over condensation in the surface layer, especially over oceans, wherefrom the extra moisture is transported upwards. Above the boundary layer the condensation in the forecasts is larger than in the analyses. The condensation values over land are quite large in the 4 day forecasts; this is mainly balanced by excessive horizontal humidity transport from ocean areas to land areas.

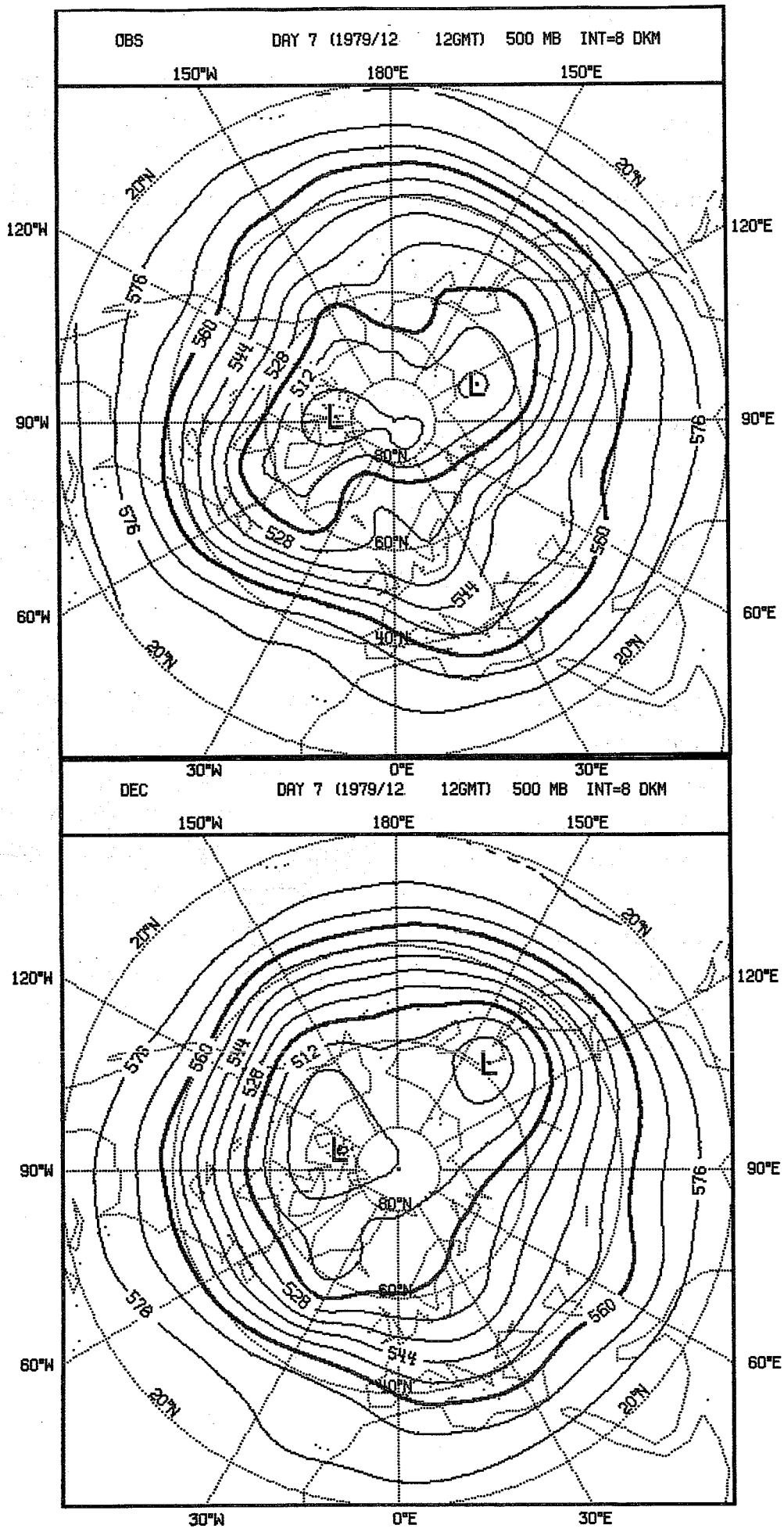


FIG. 5.1

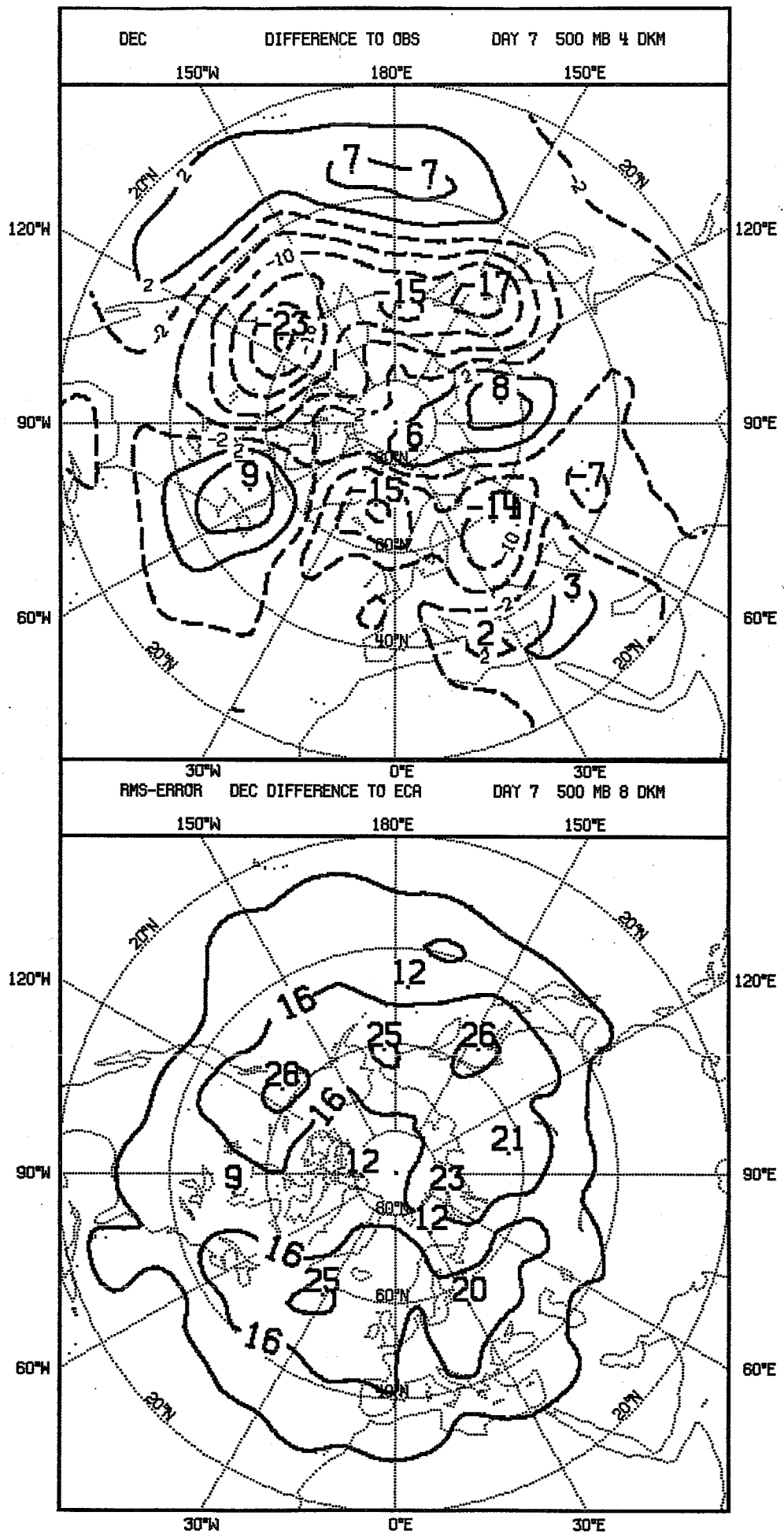


FIG. 5.2

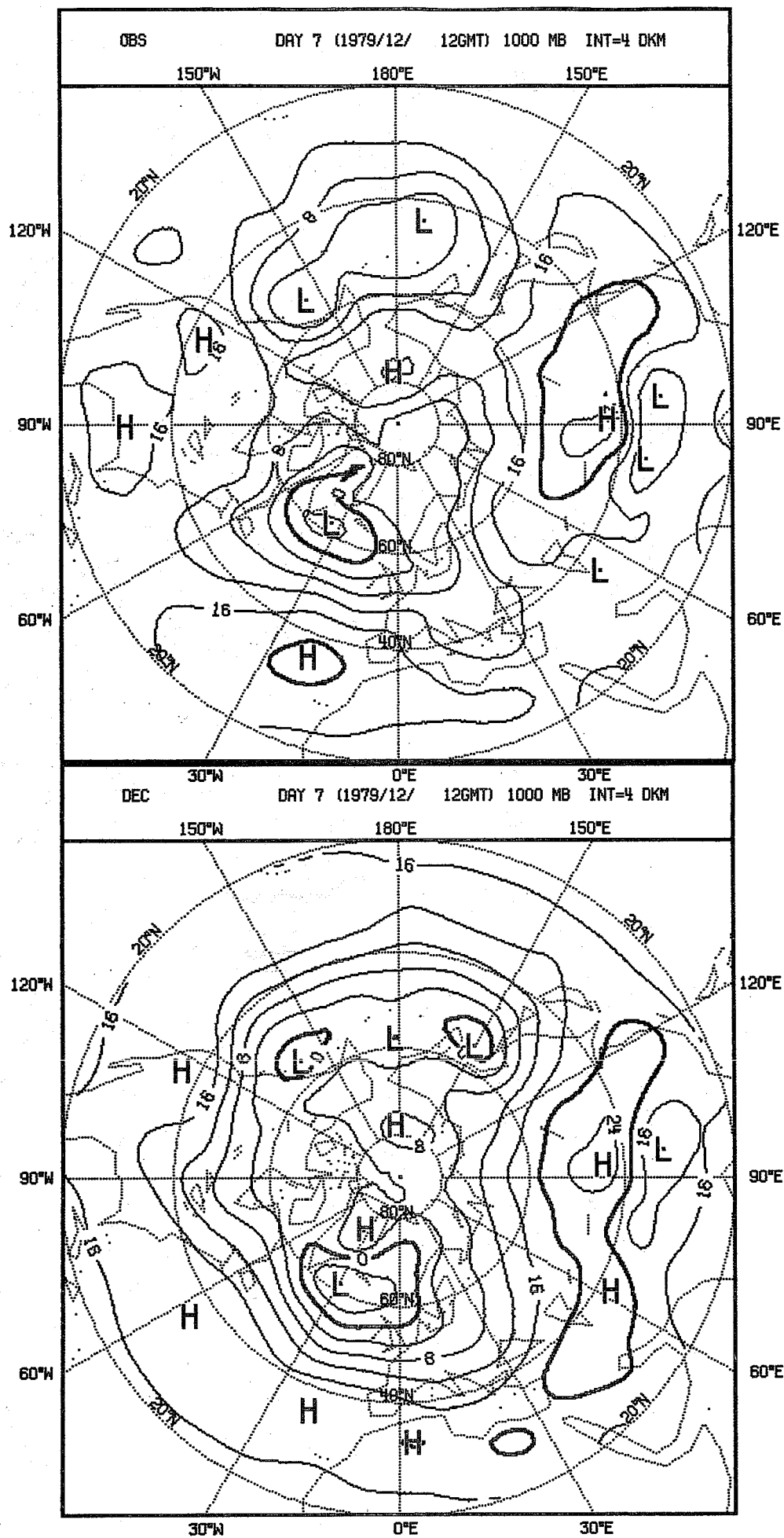


FIG. 5.3

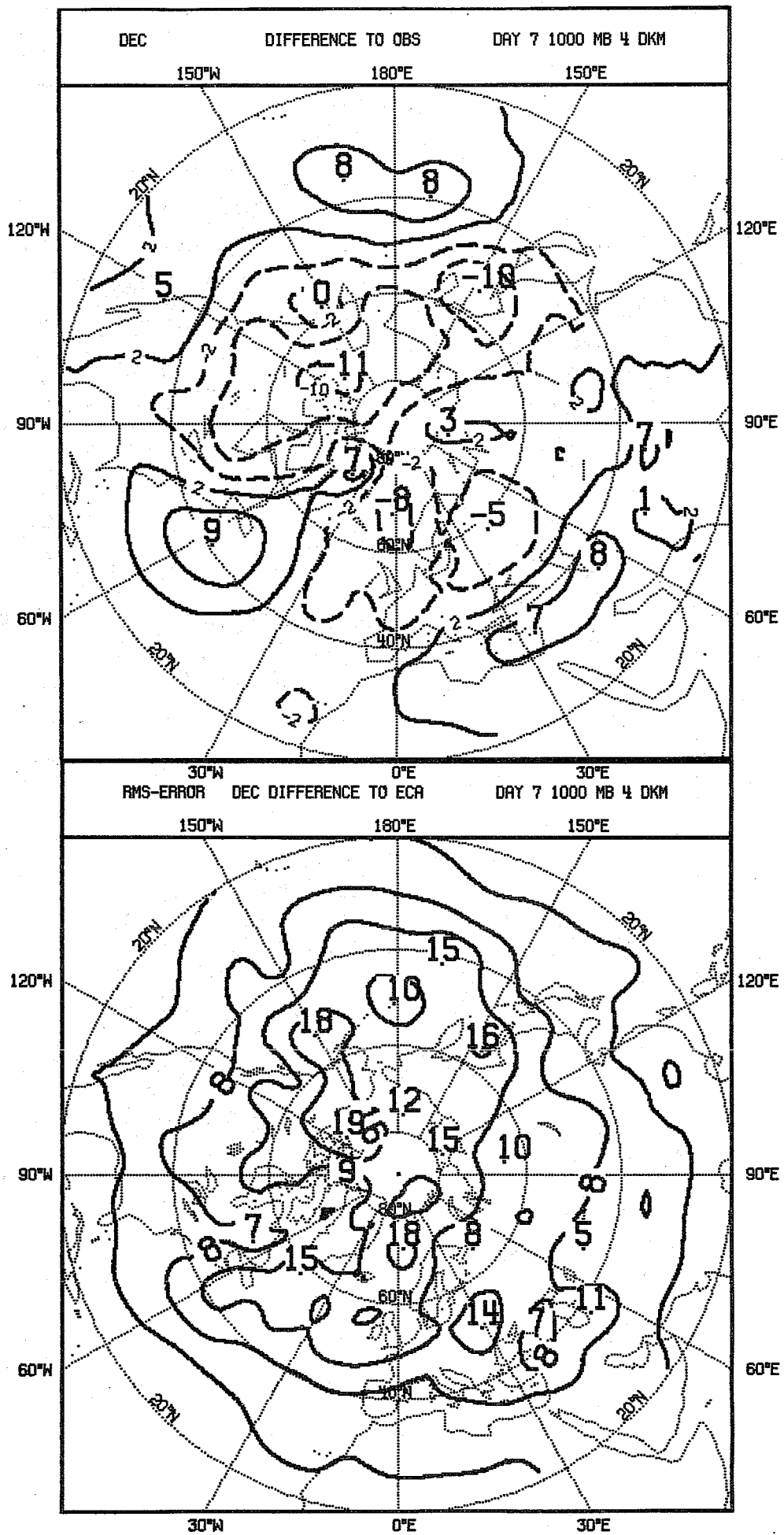


FIG. 5.4

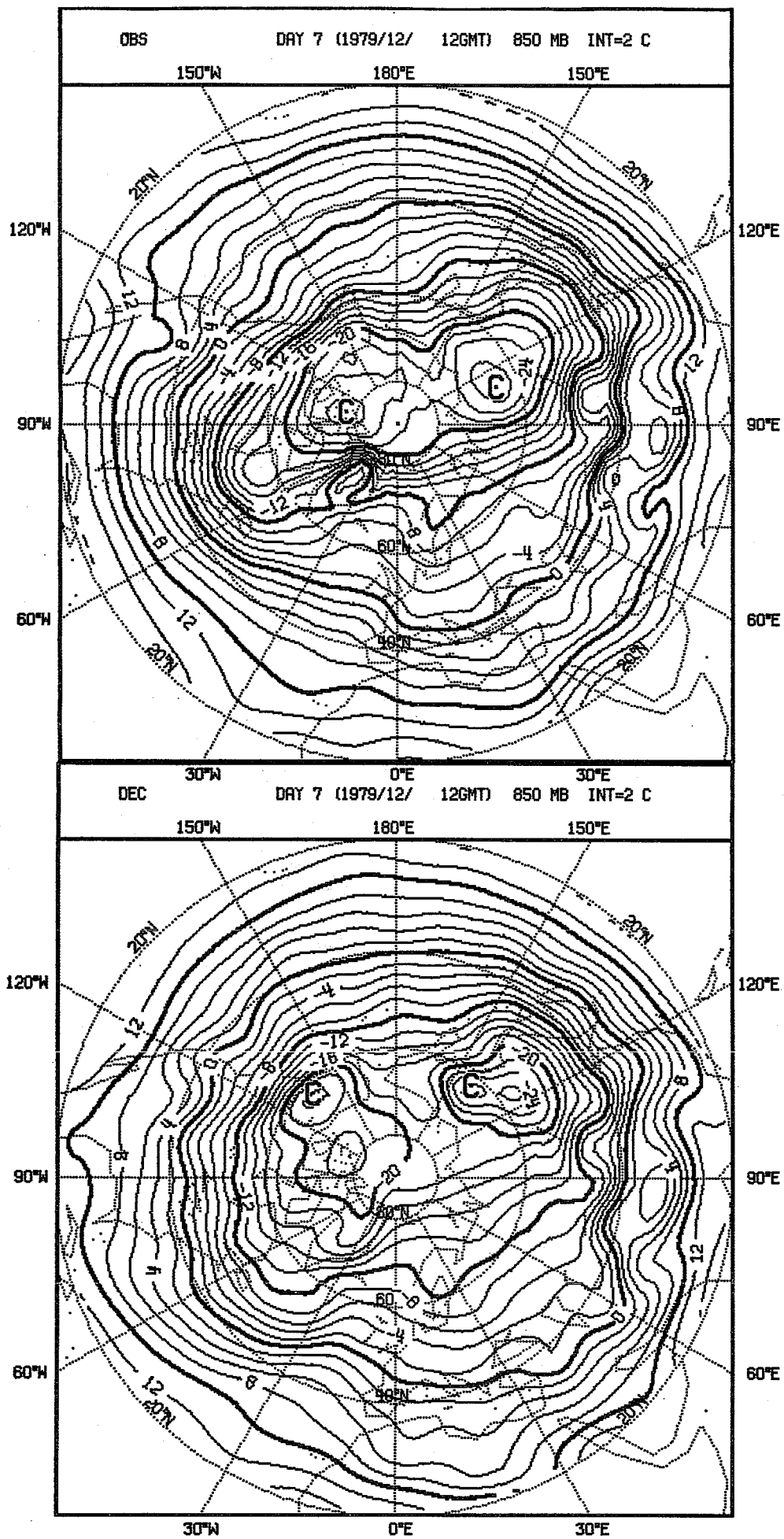


FIG. 5.5

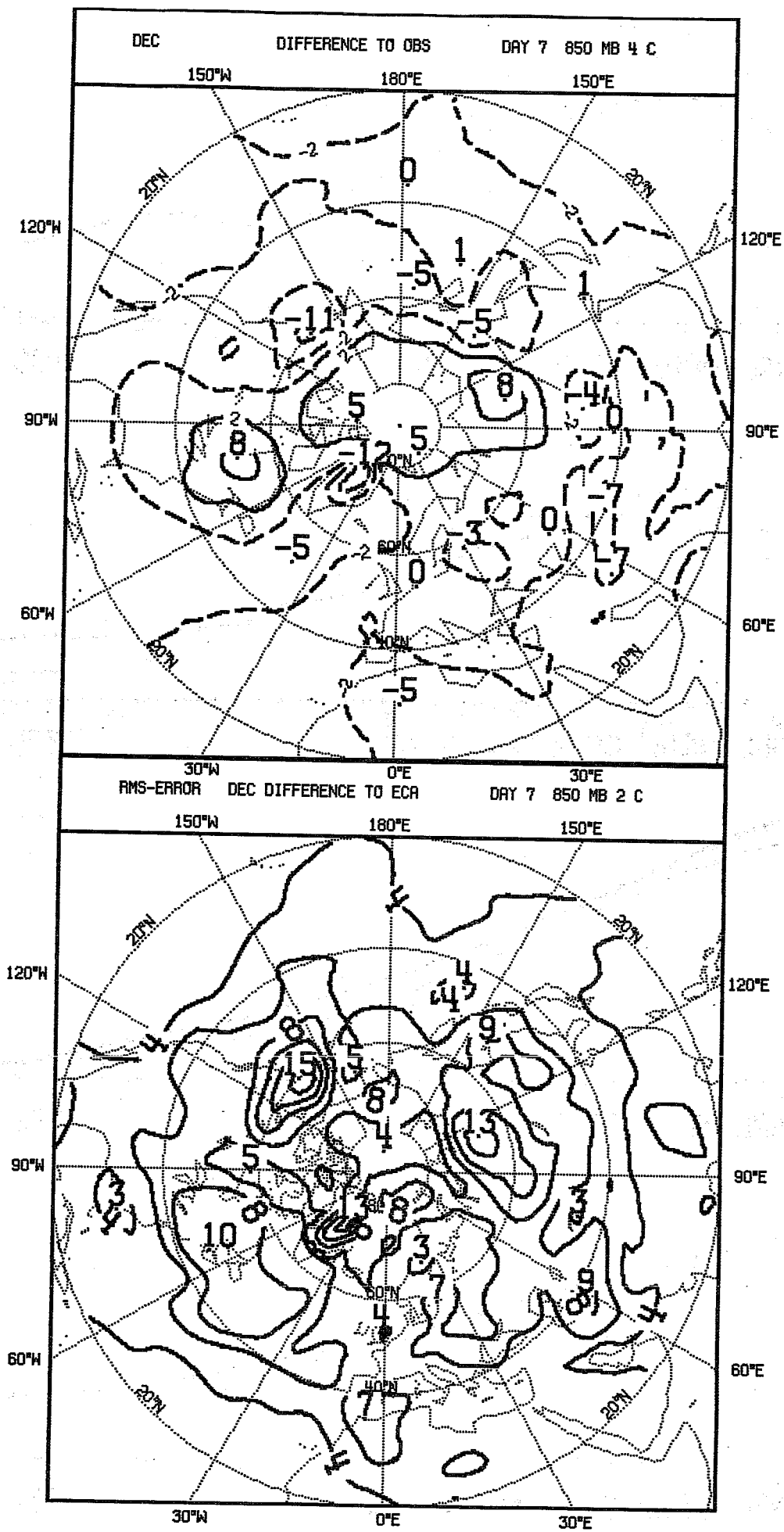


FIG. 5.6

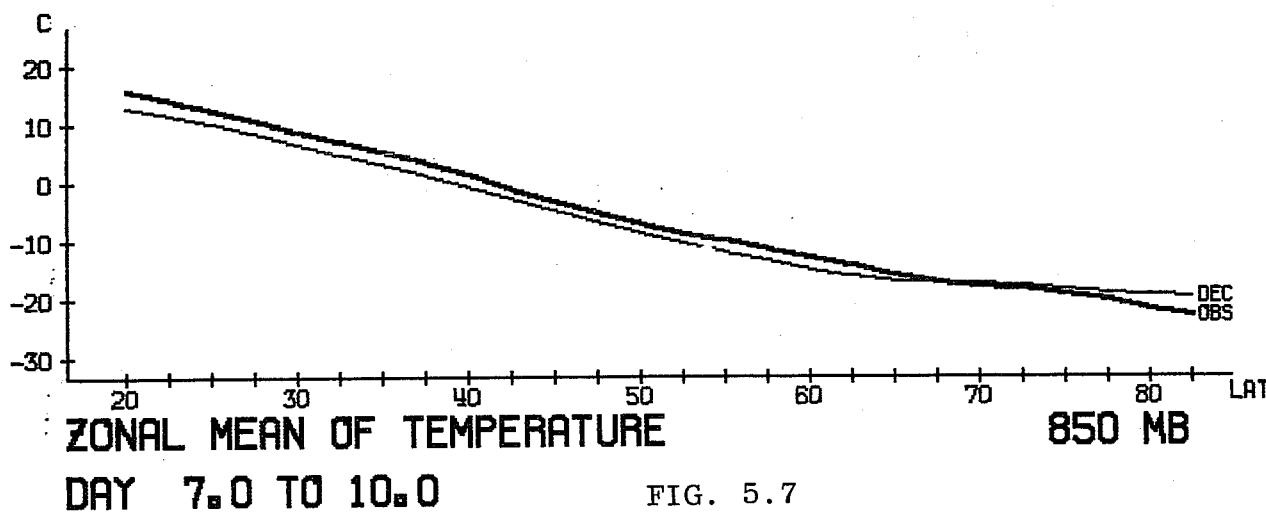
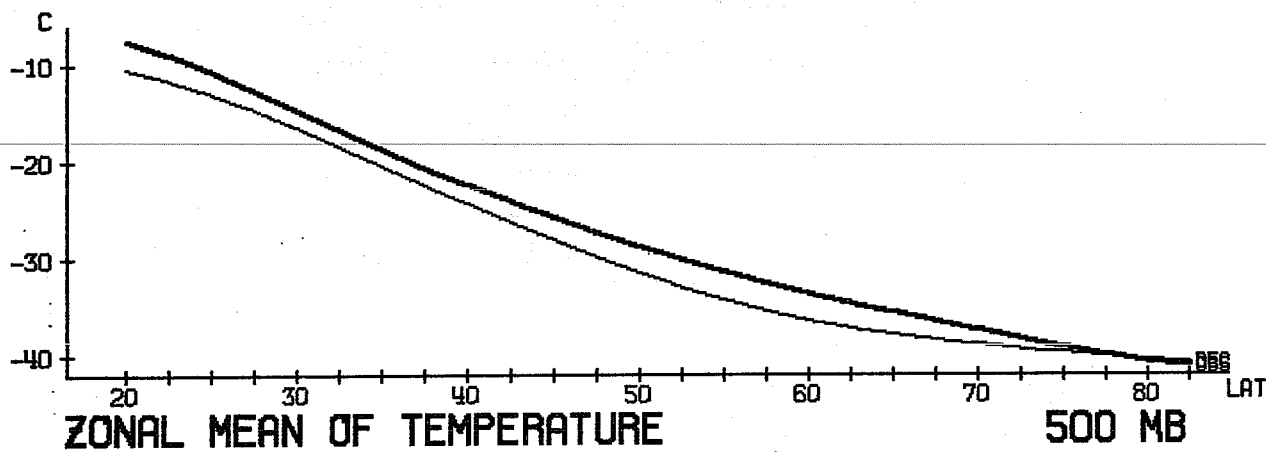
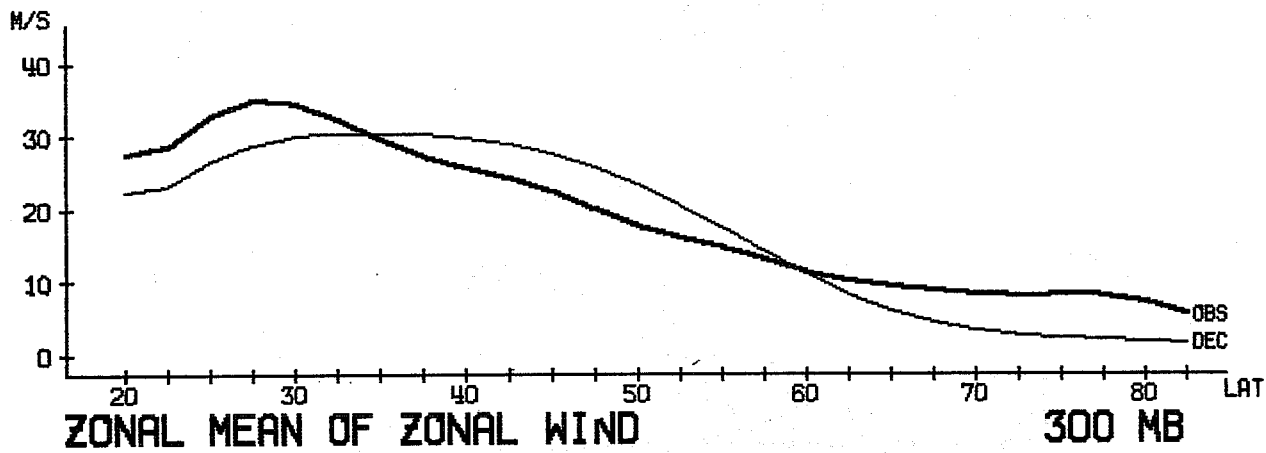
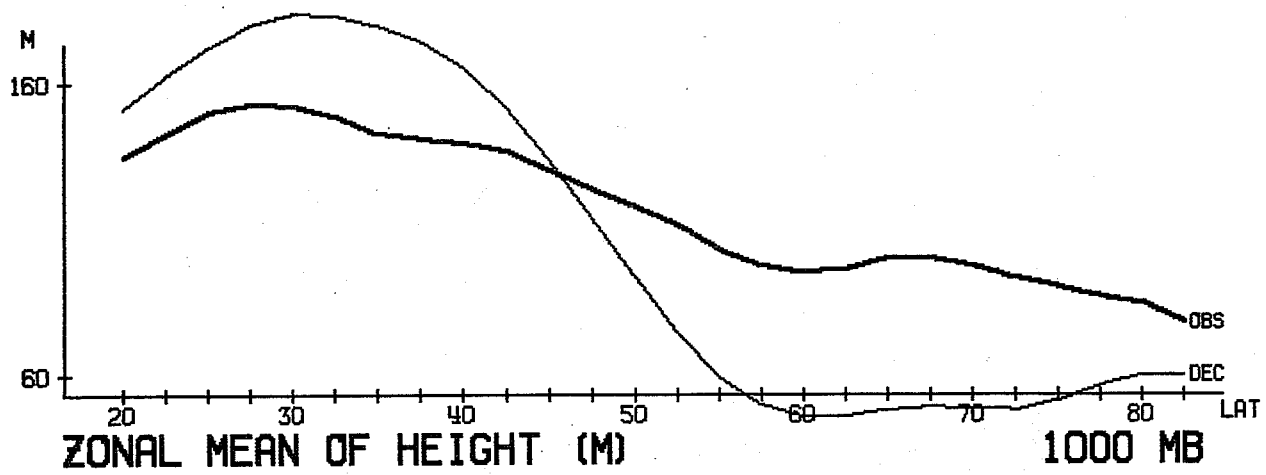
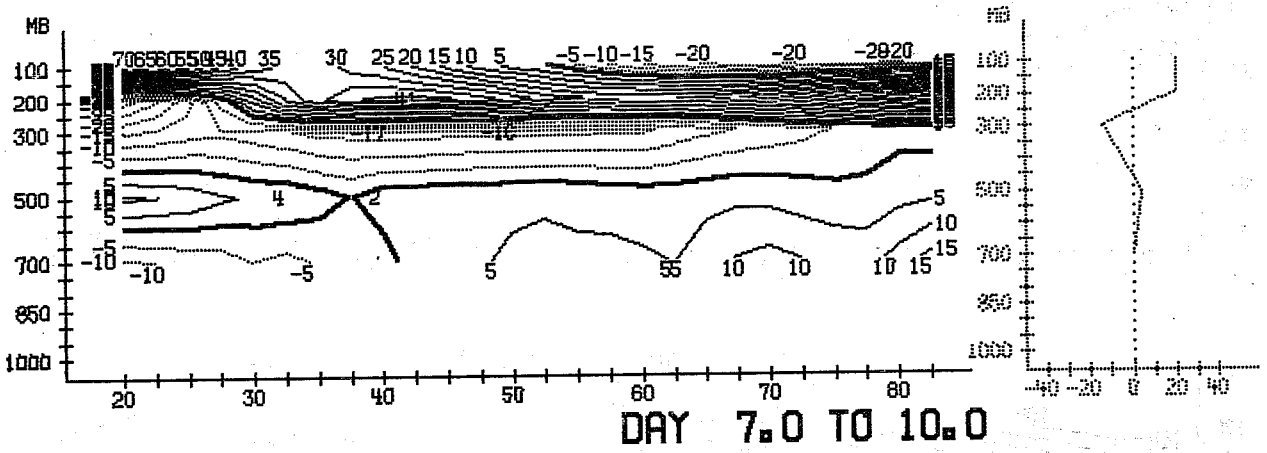
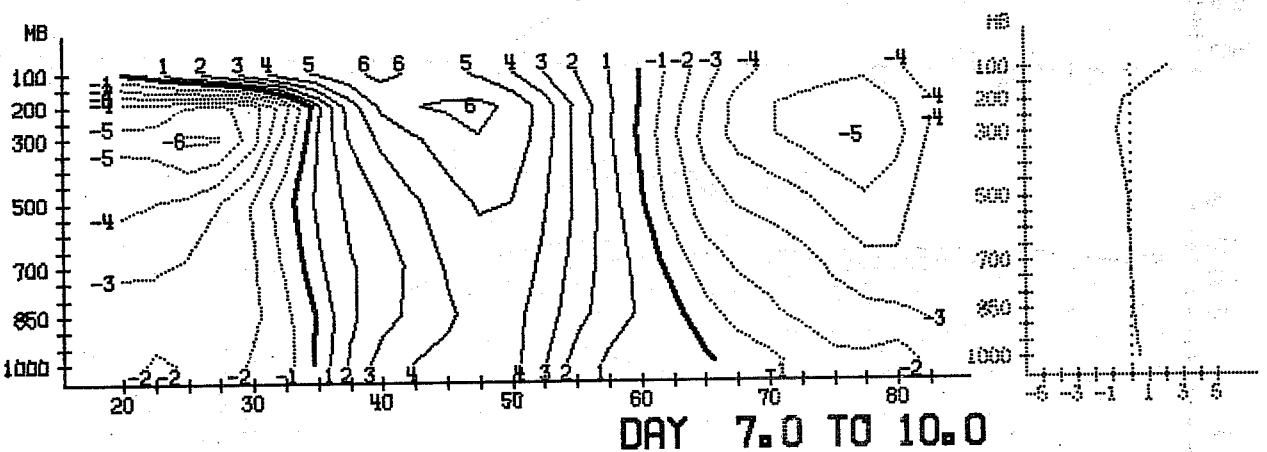


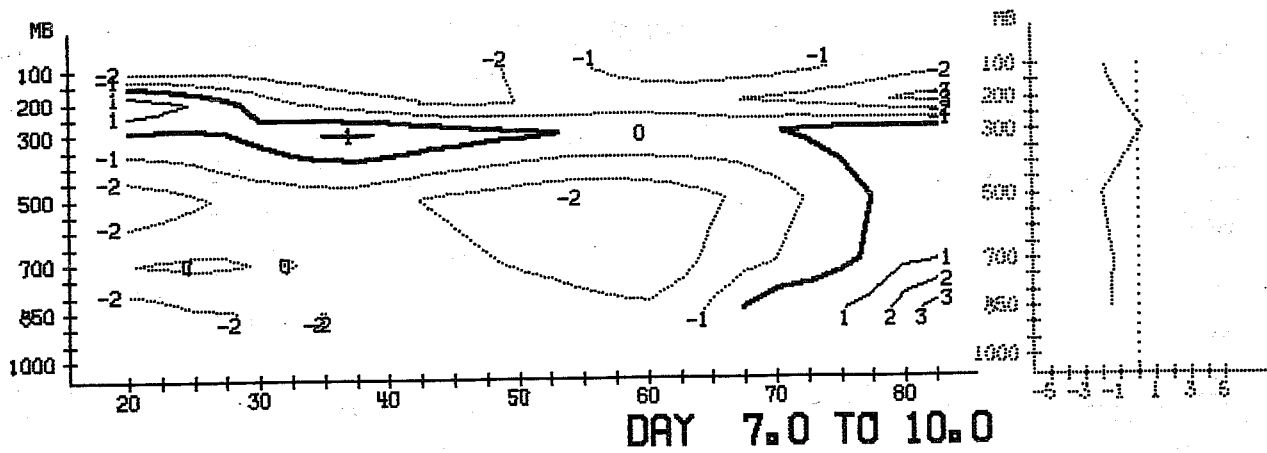
FIG. 5.7



MEAN VERT STABILITY DEVIATION FROM OBS



ZONAL MEAN OF U DEVIATION FROM OBSERVED GEOSTR



ZONAL MEAN OF T DEVIATION FROM OBSERVED

FIG. 5.8

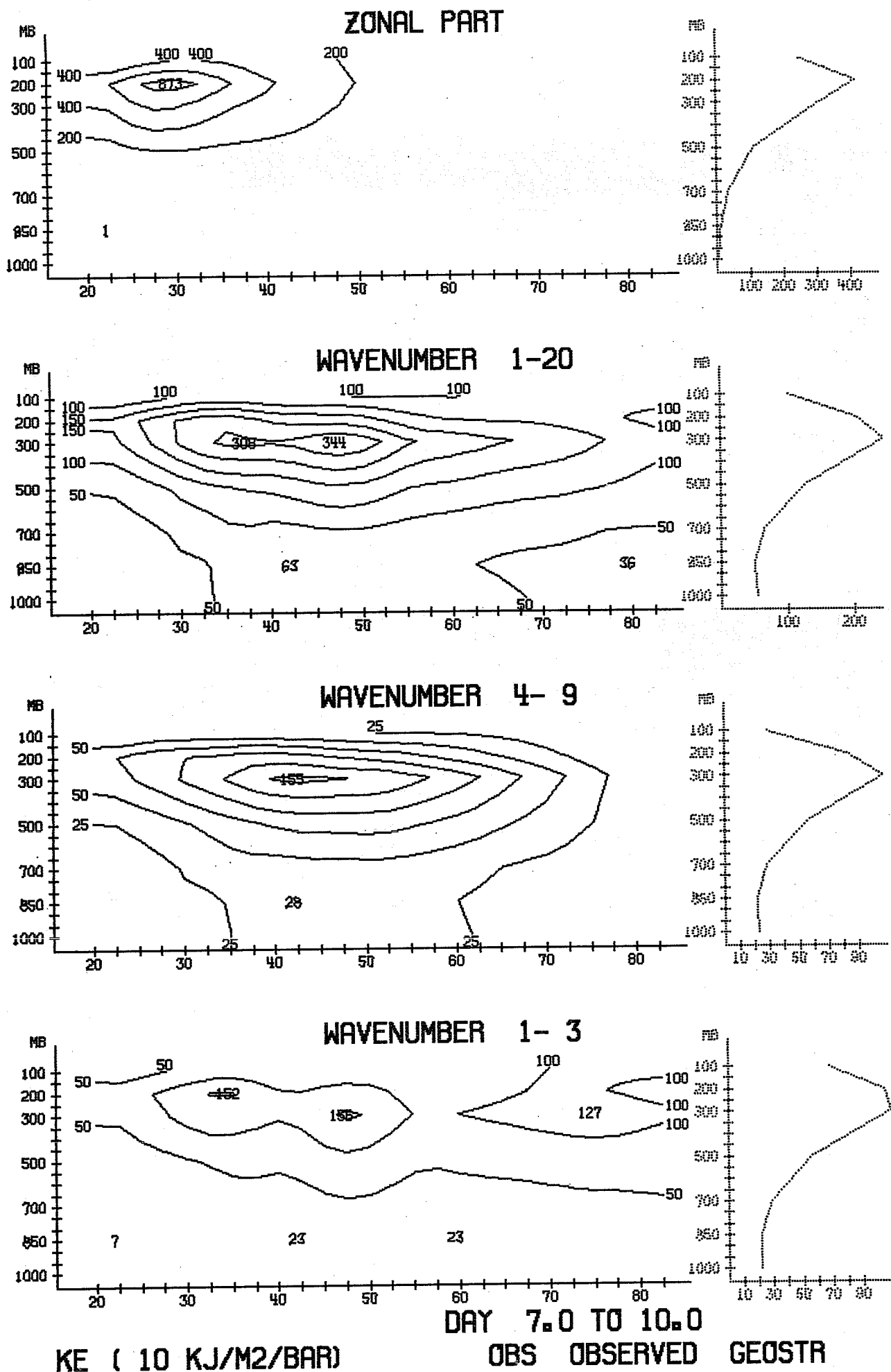


FIG. 5.9

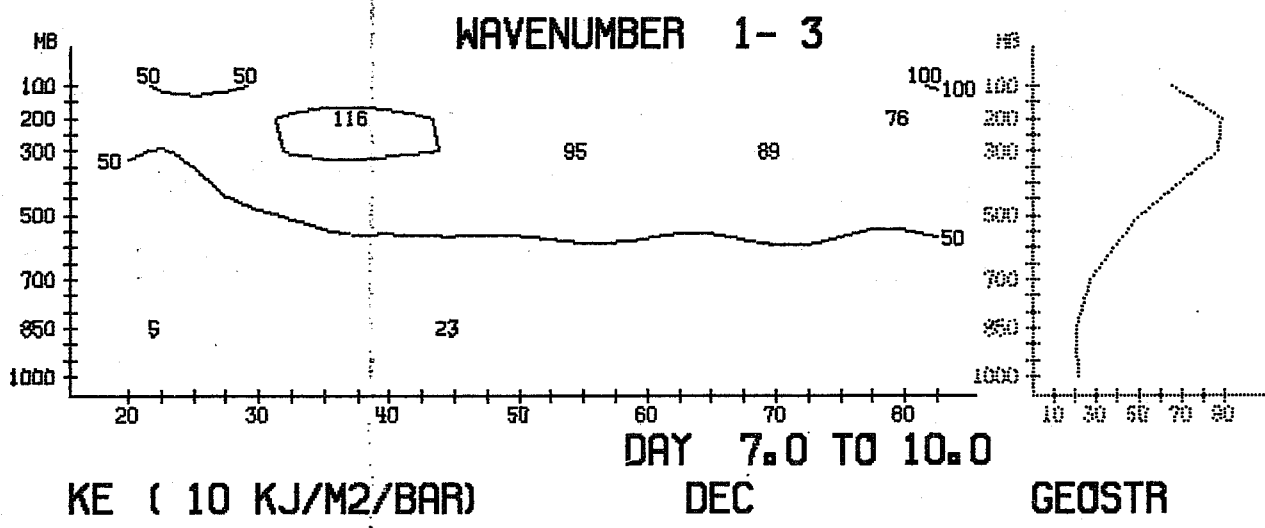
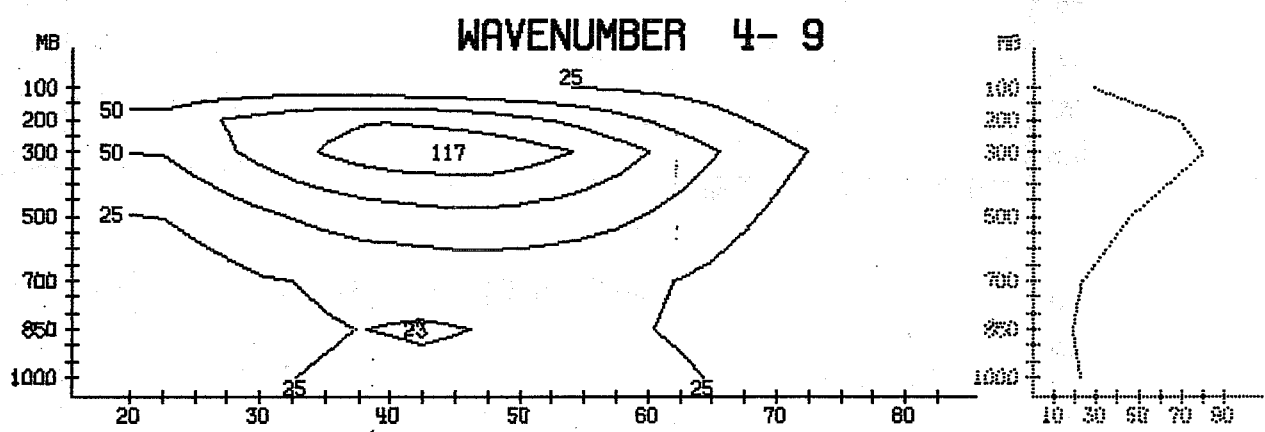
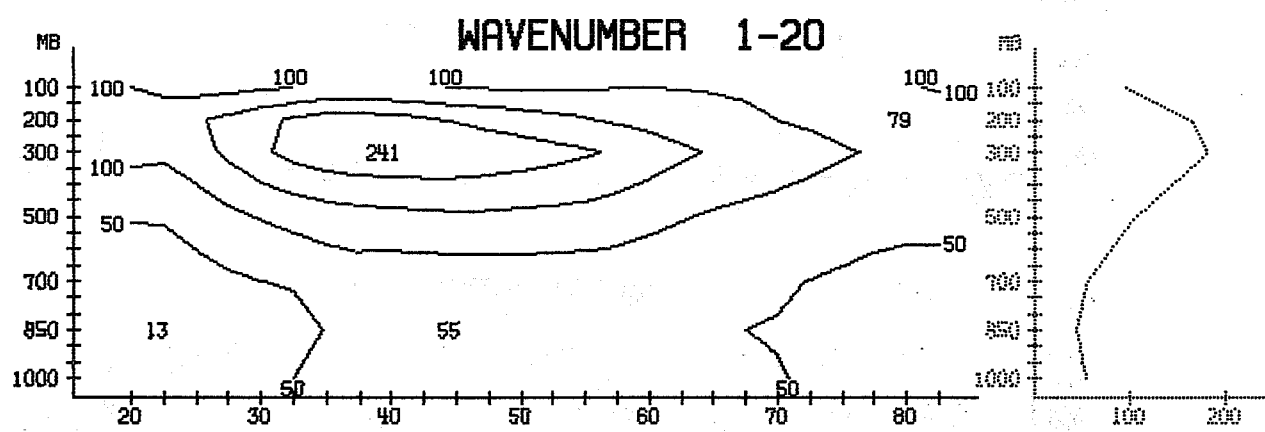
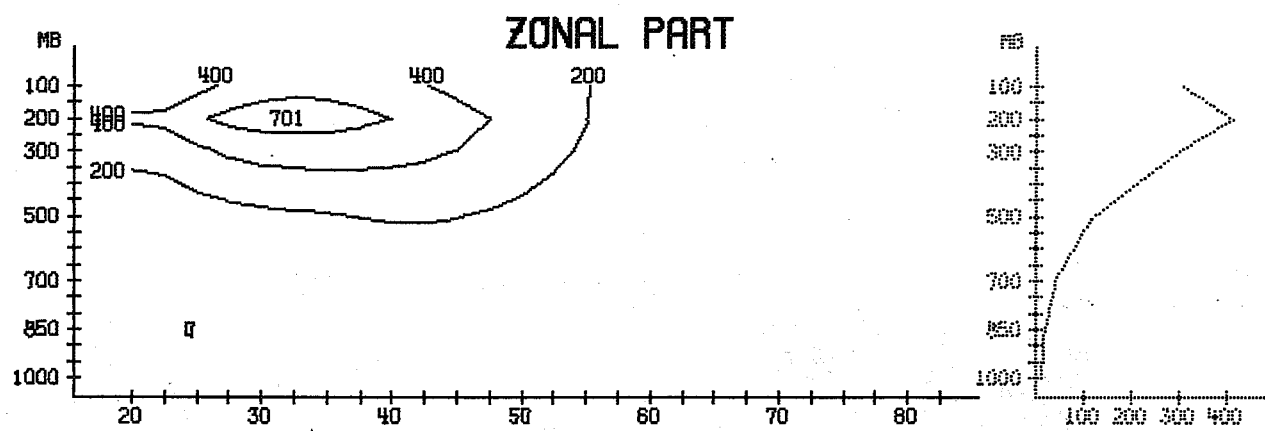
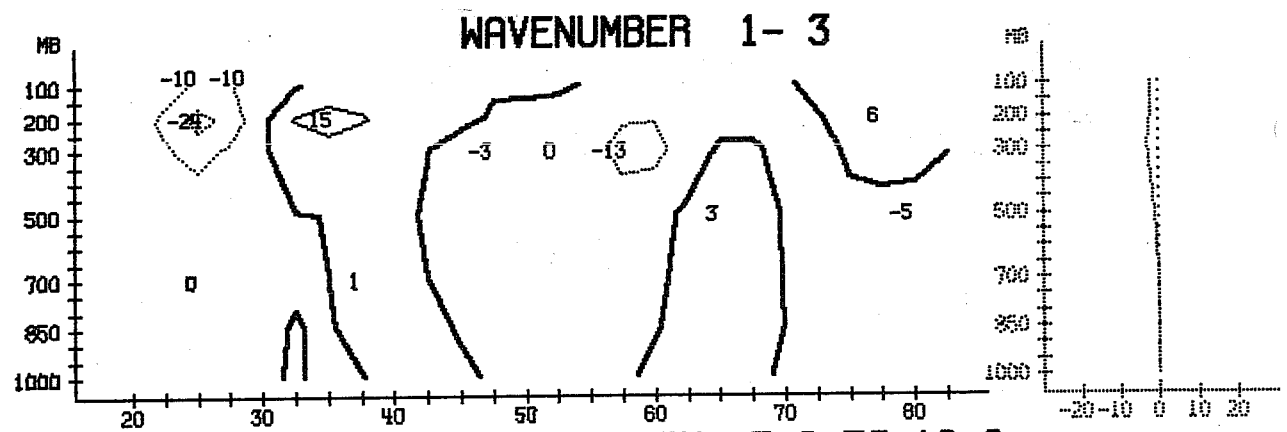
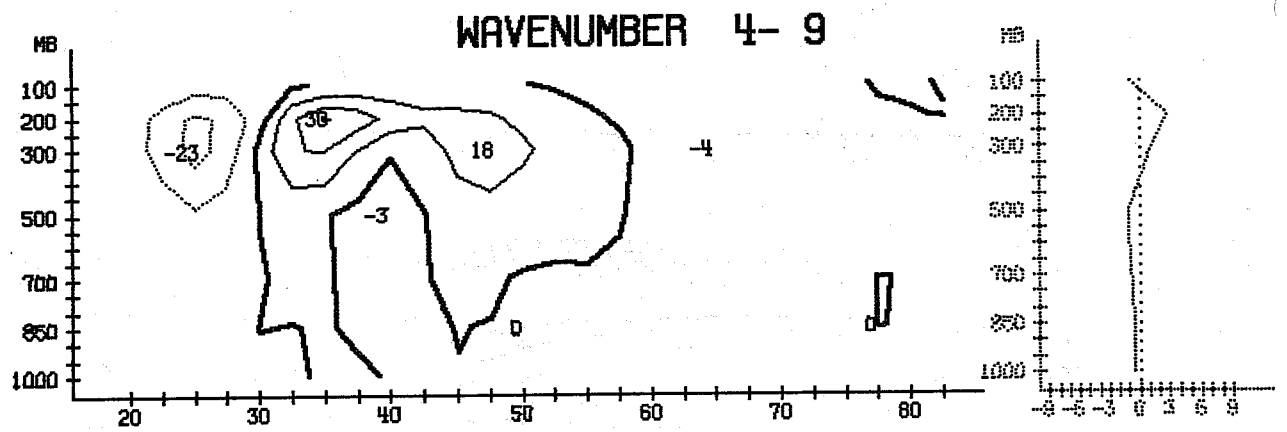
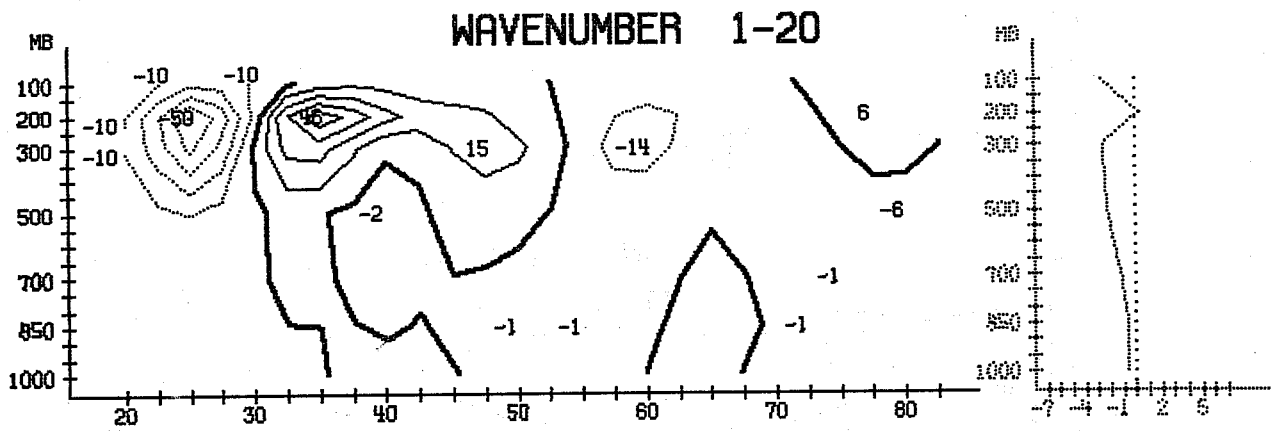


FIG. 5.10



DAY 7.0 TO 10.0
CK (1/10 WATT/M2/BAR) OBS OBSERVED GEOSTR

FIG. 5.11

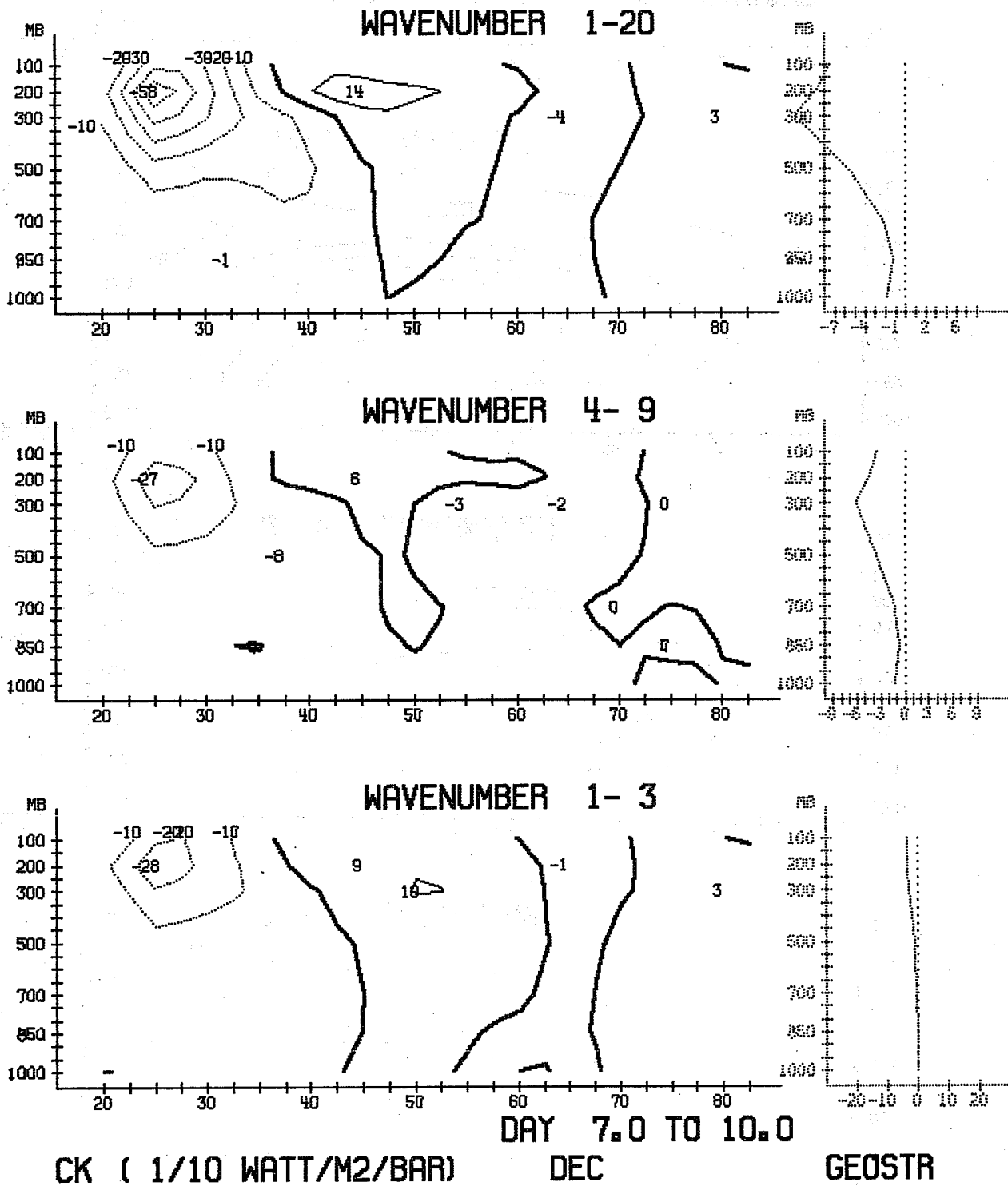
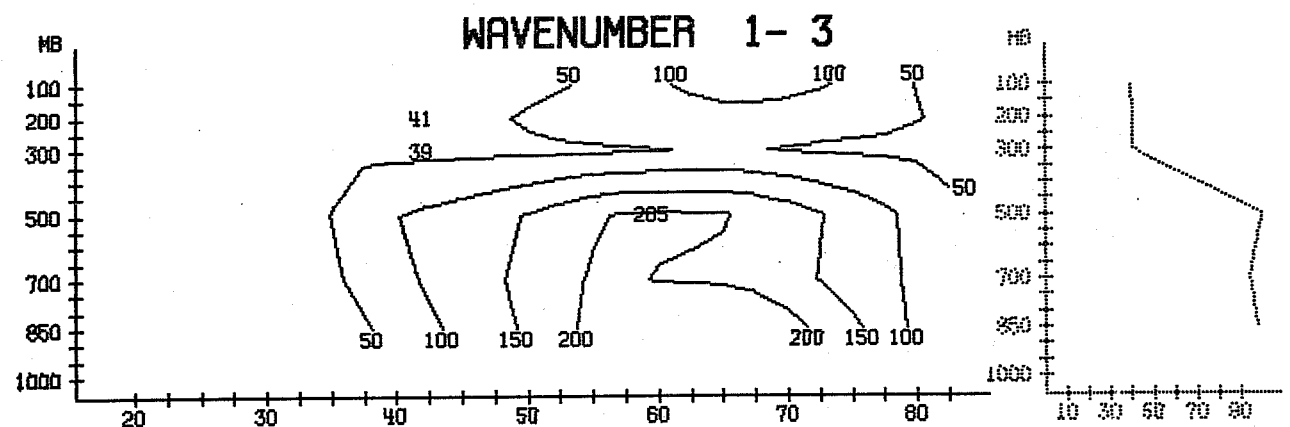
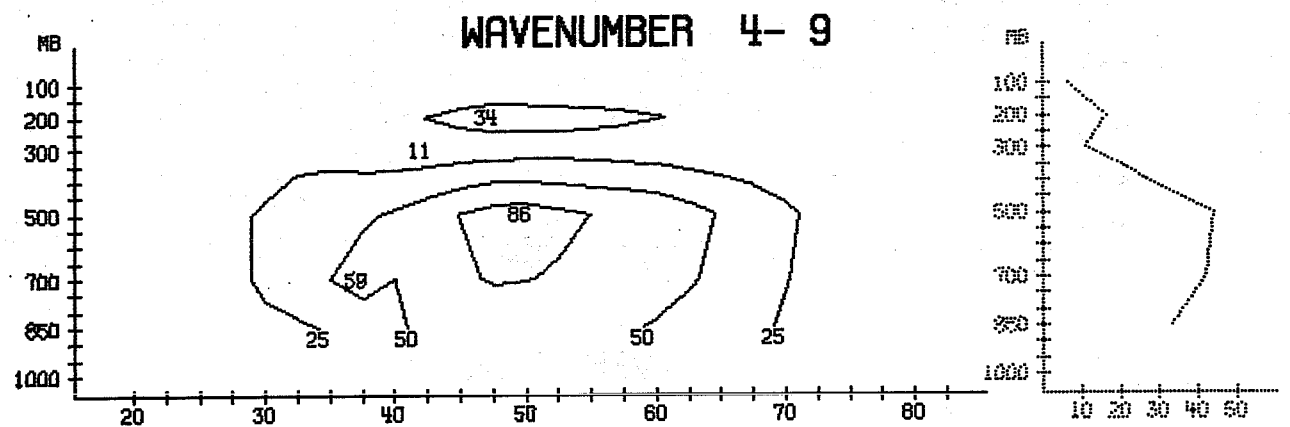
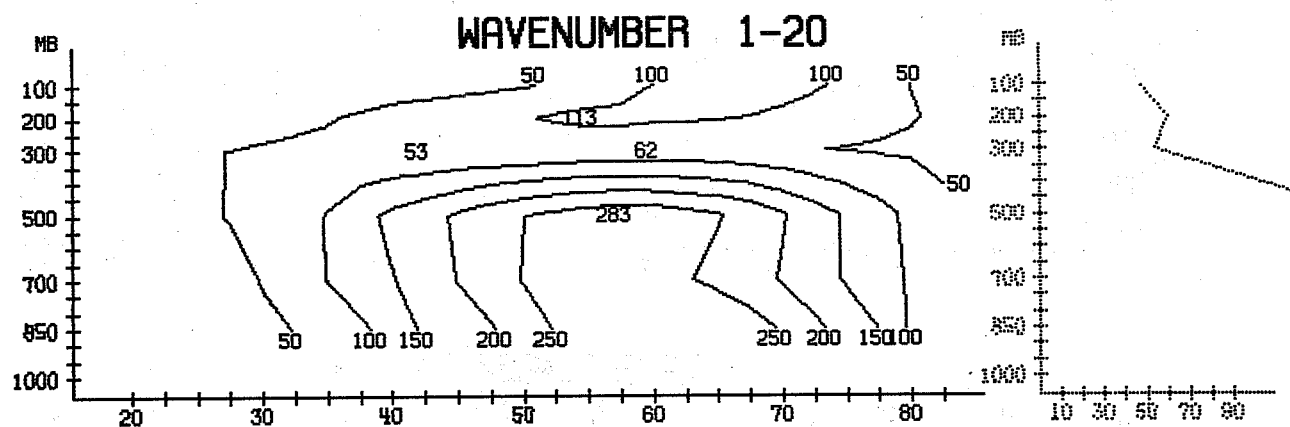
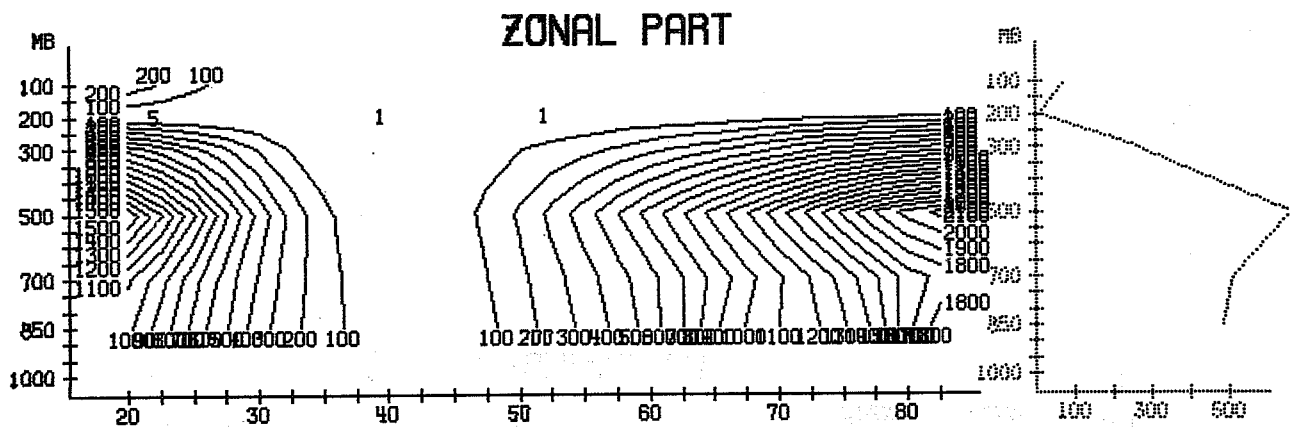


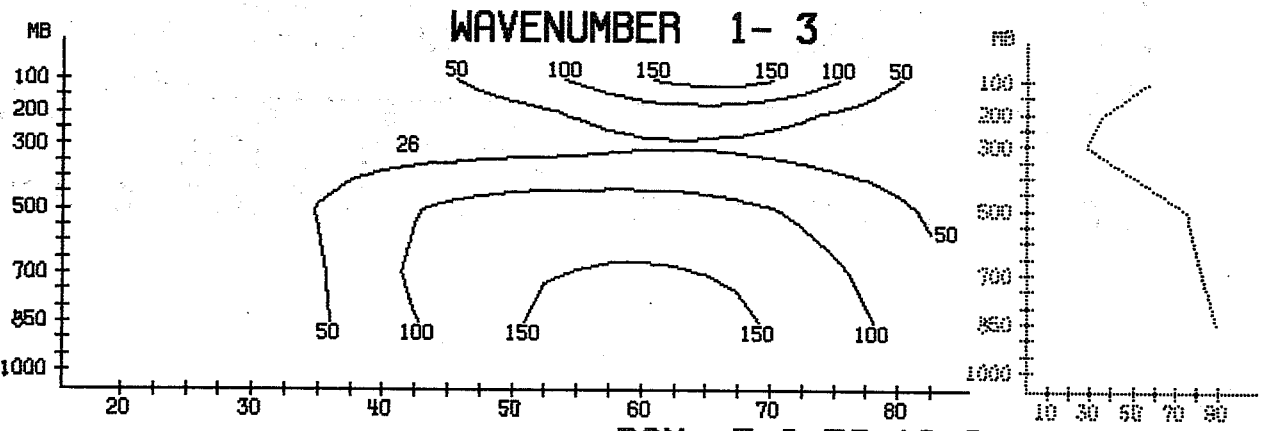
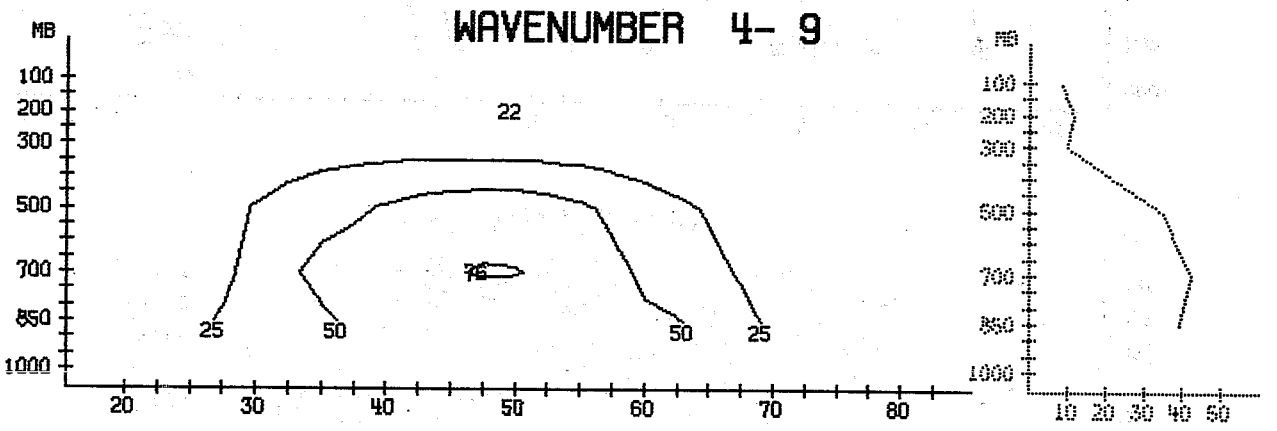
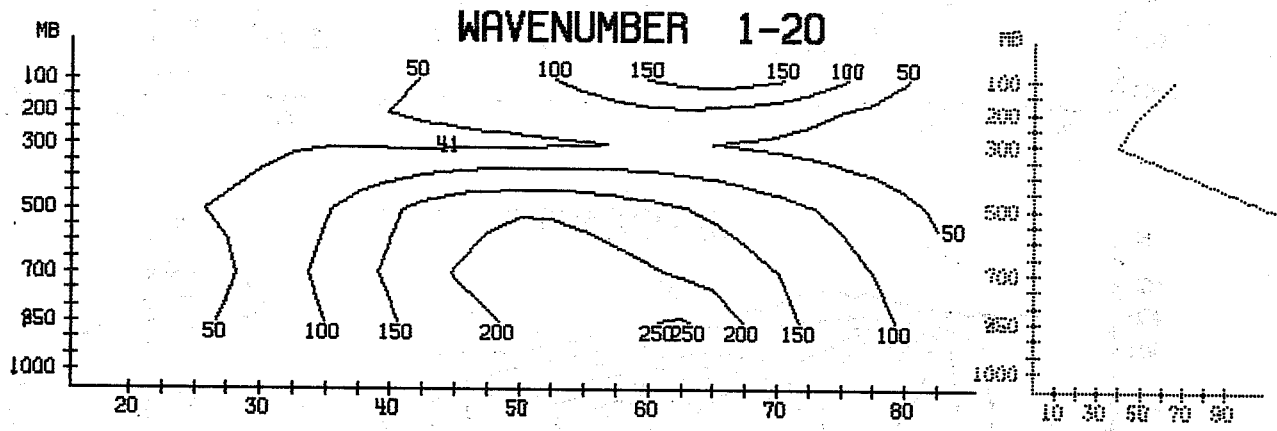
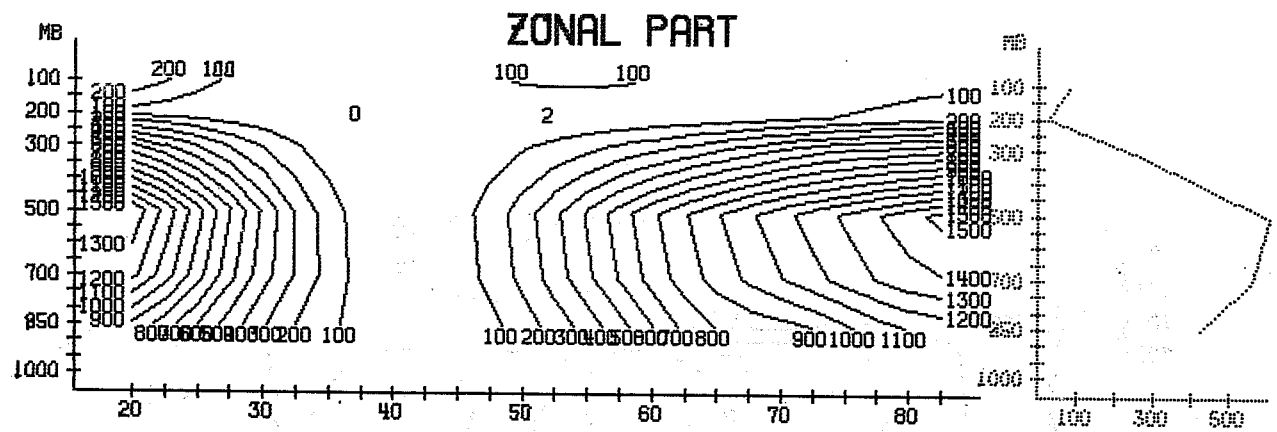
FIG. 5.12



DAY 7.0 TO 10.0
OBS OBSERVED

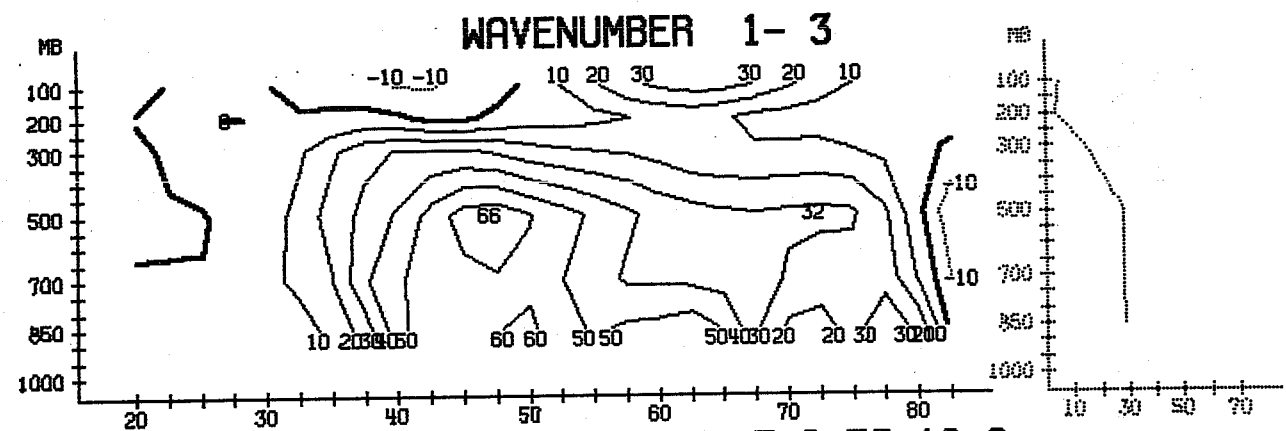
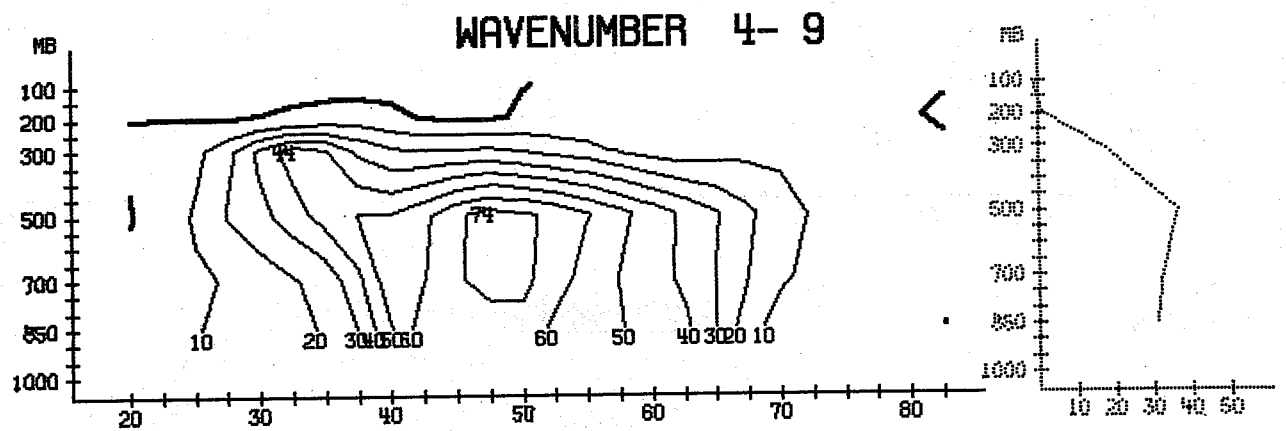
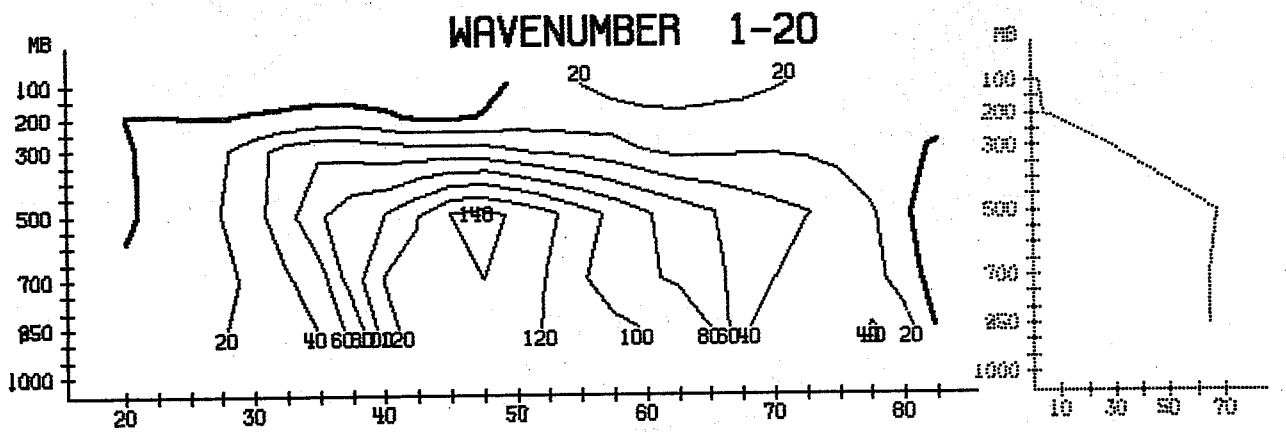
AE (10 KJ/M2/BAR)

FIG. 5.13



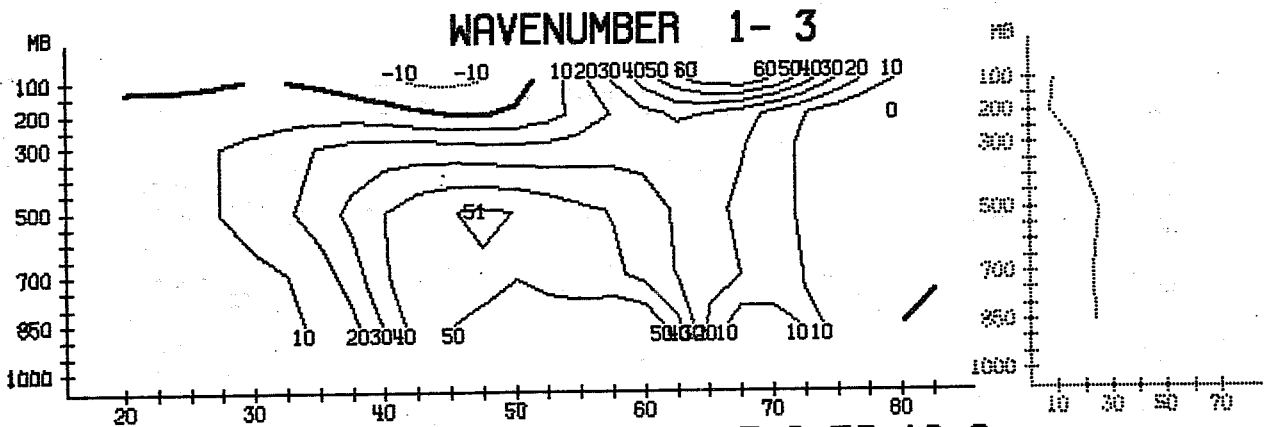
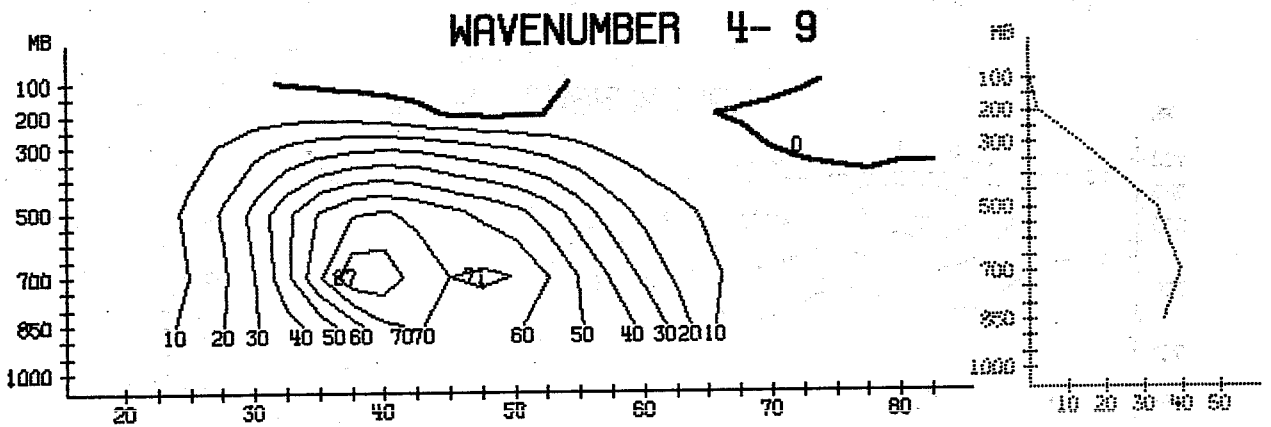
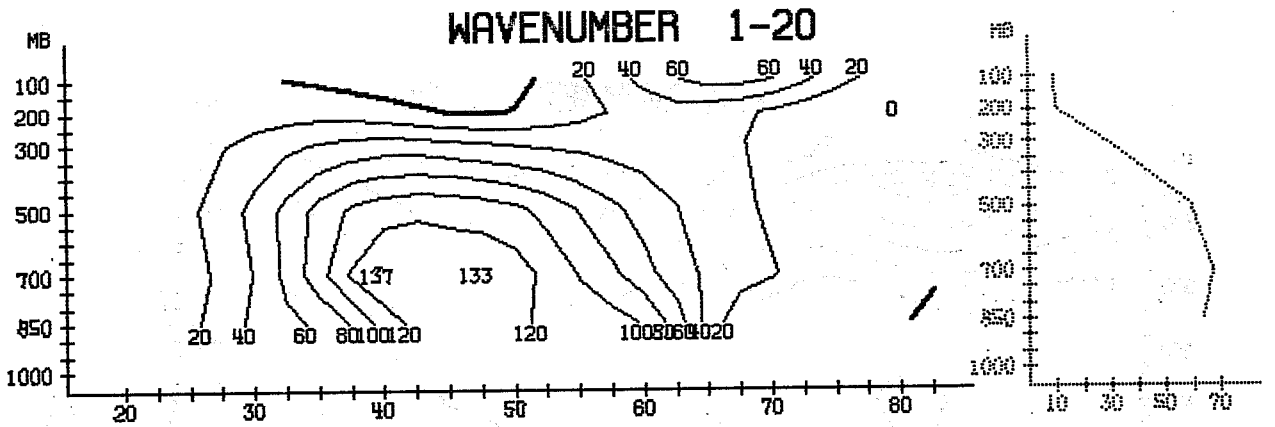
DAY 7.0 TO 10.0
 RE (10 KJ/M2/BAR) DEC

FIG. 5.14



DAY 7.0 TO 10.0
 CA (1/10 WATT/M2/BAR) OBS OBSERVED GEOSTR

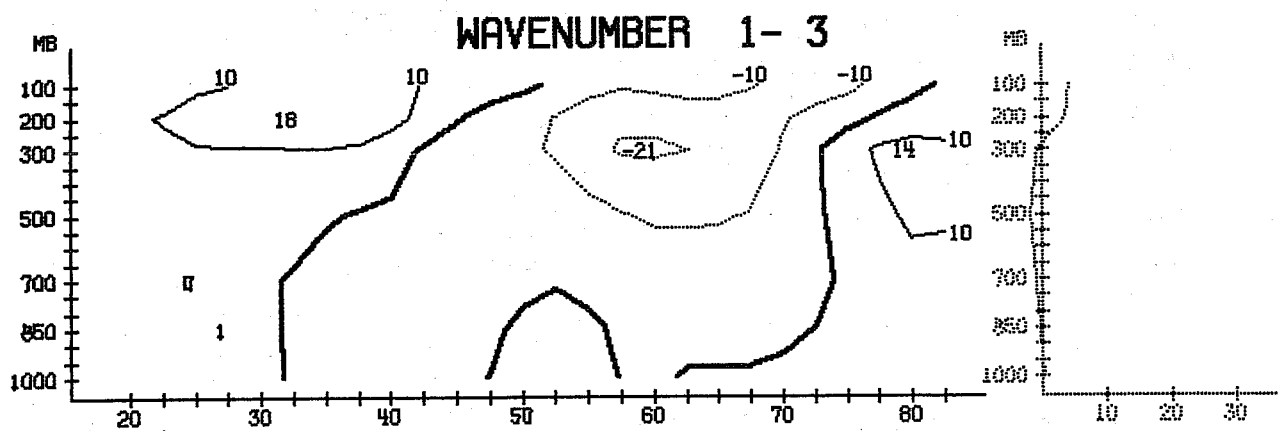
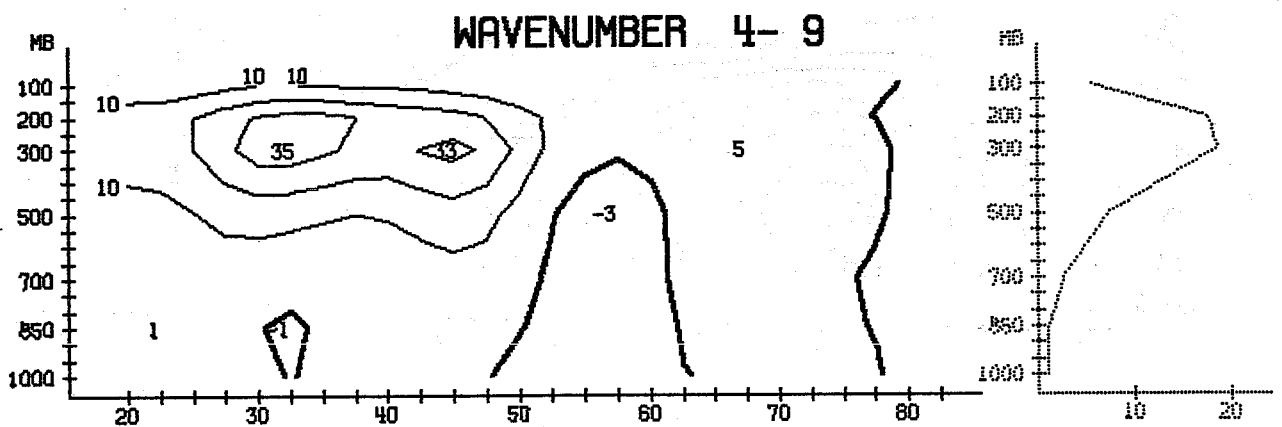
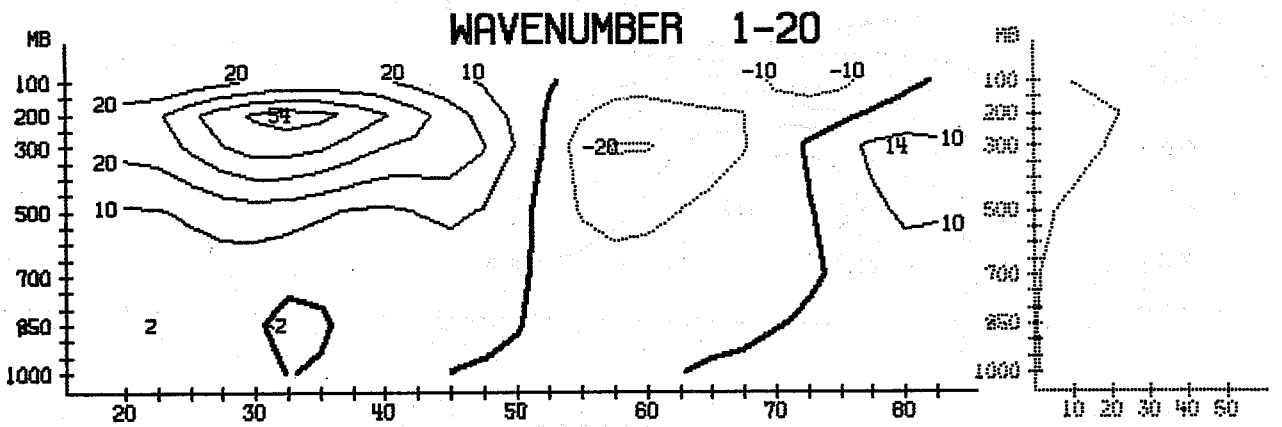
FIG. 5.15



DAY 7.0 TO 10.0

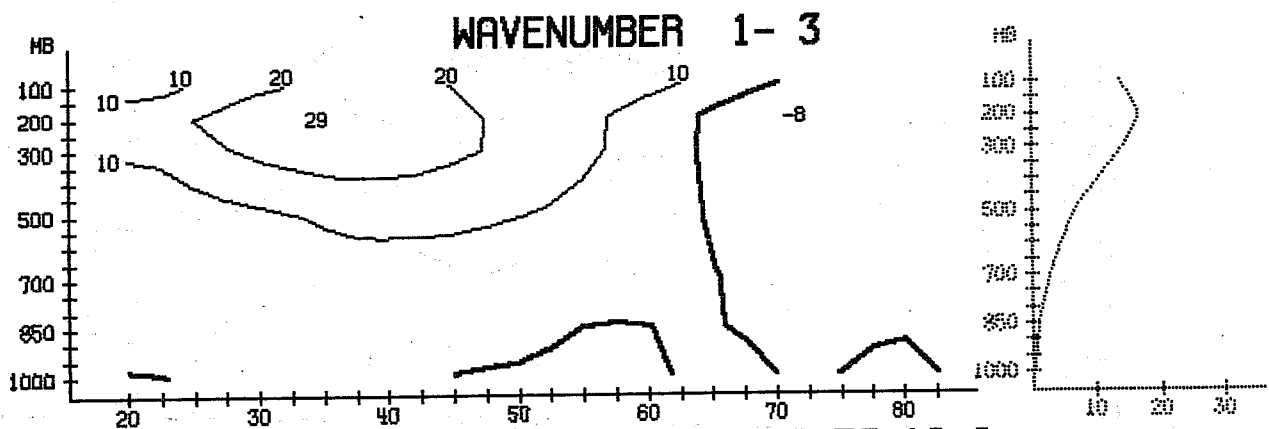
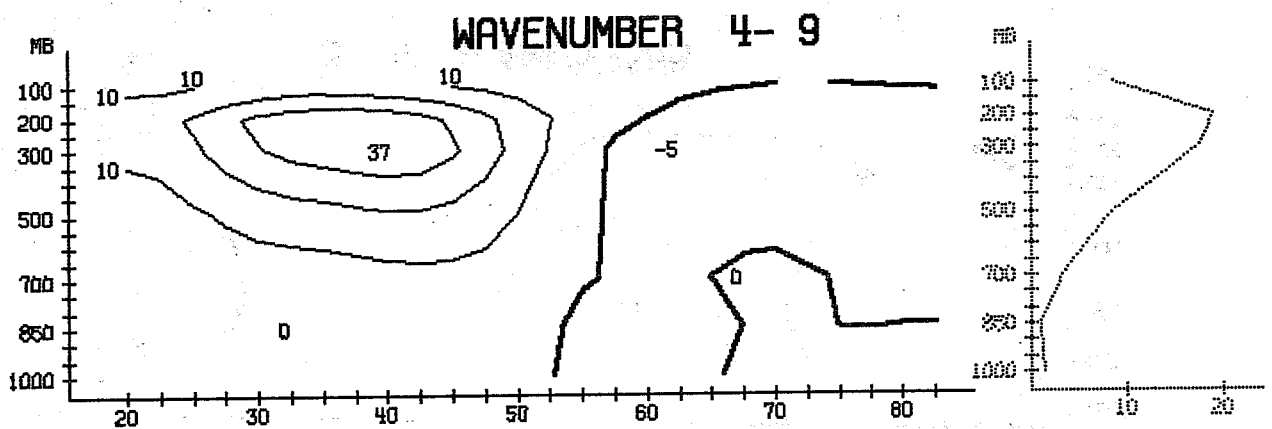
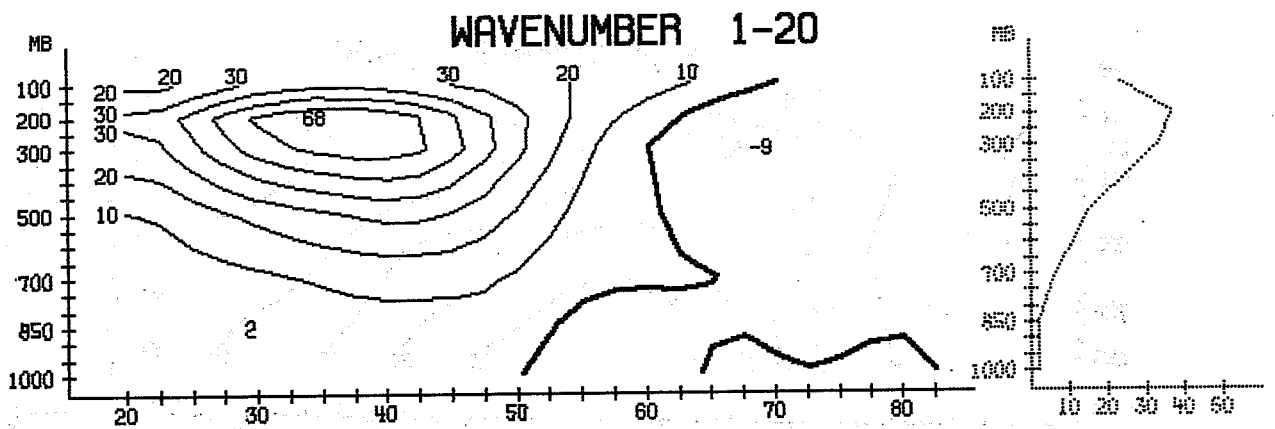
CA (1/10 WATT/M2/BAR) DEC GEOSTR

FIG. 5.16



DAY 7.0 TO 10.0
MOMENTUM-FLUX UV (M2/S2) OBS OBSERVED GEOSTR

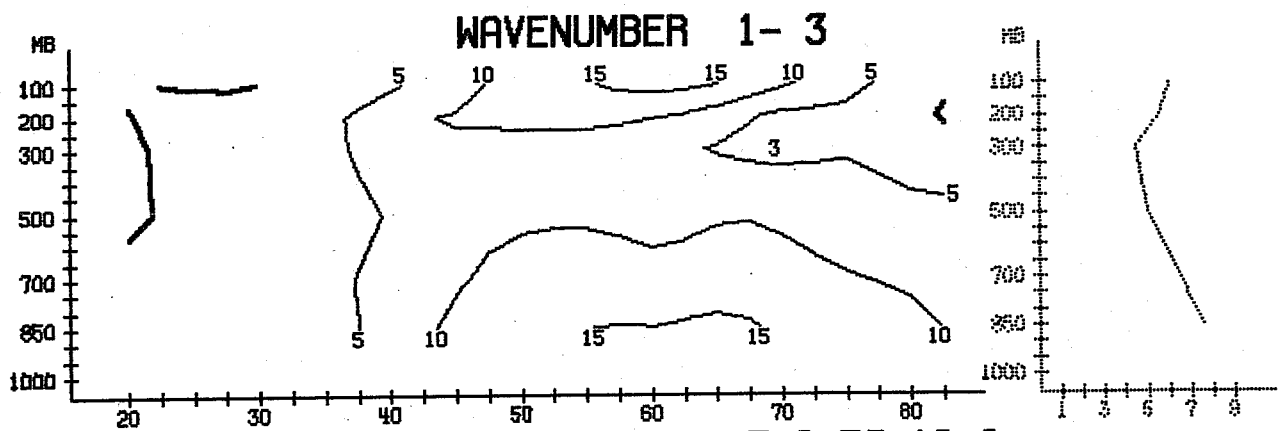
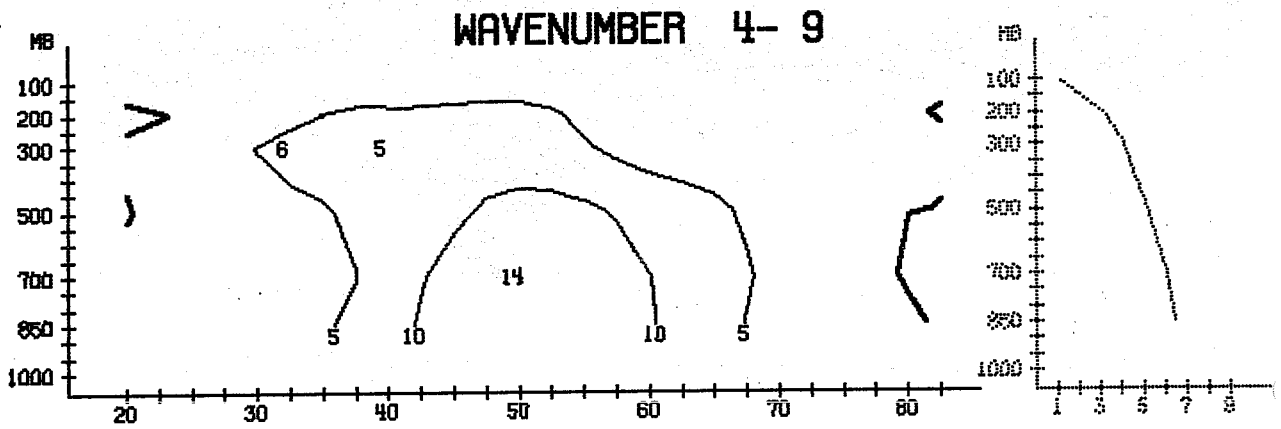
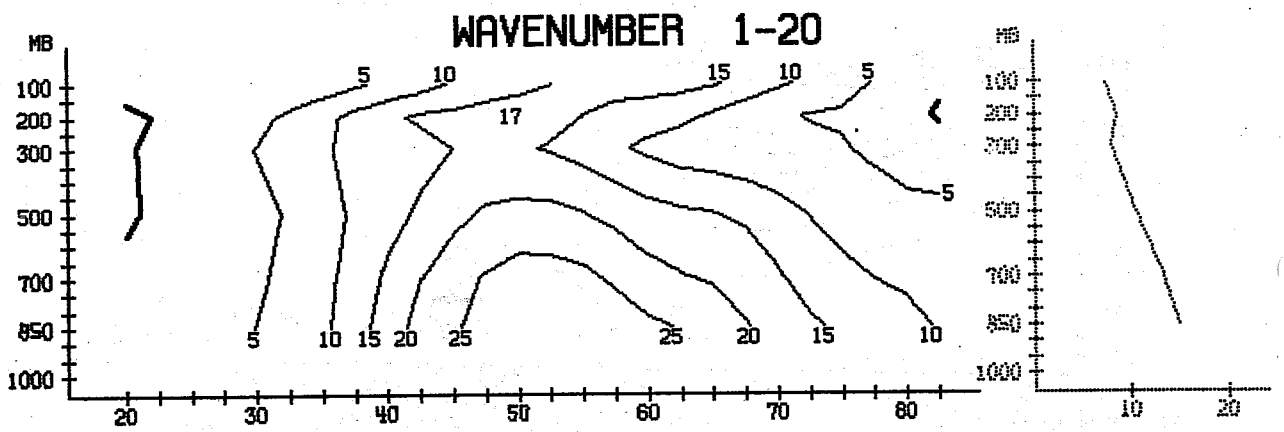
FIG. 5.17



DAY 7.0 TO 10.0

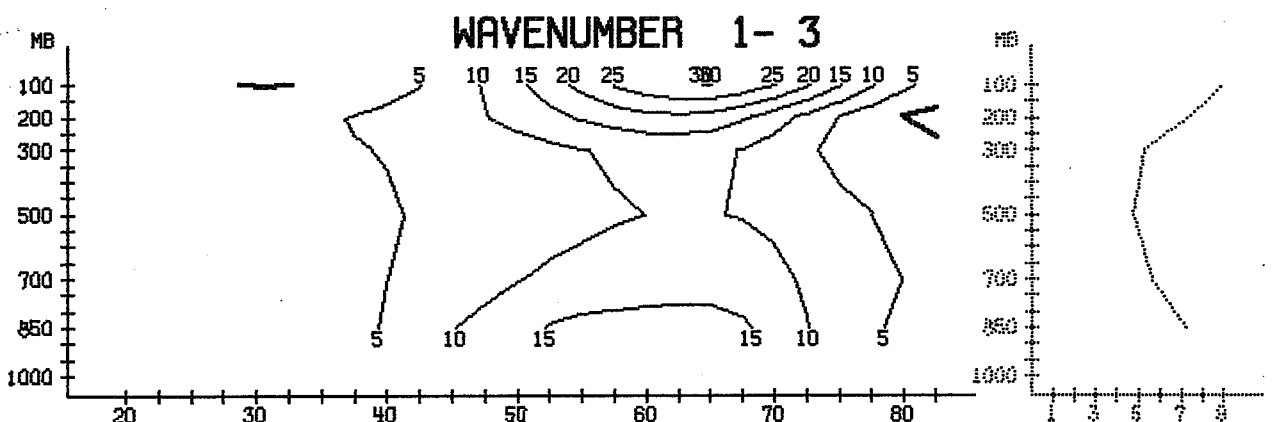
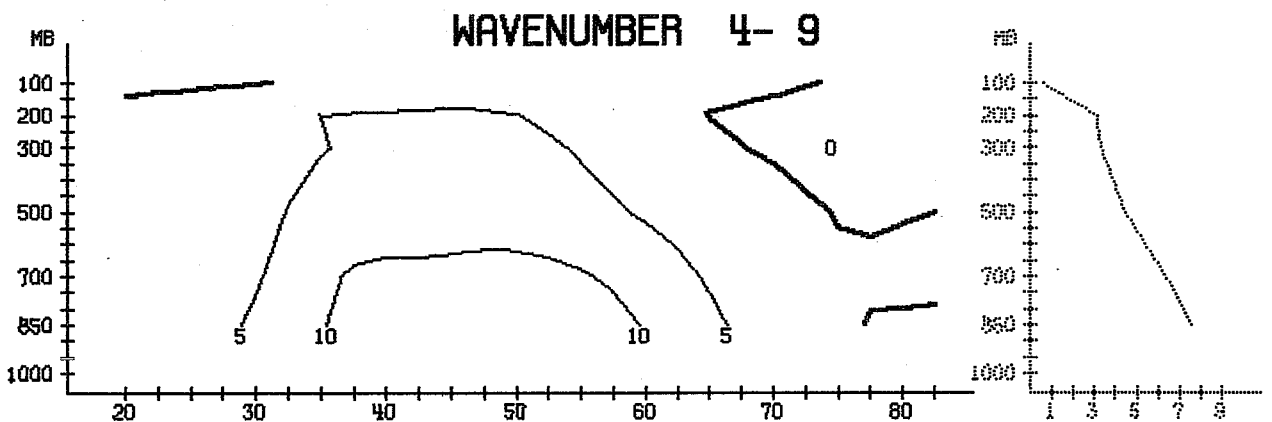
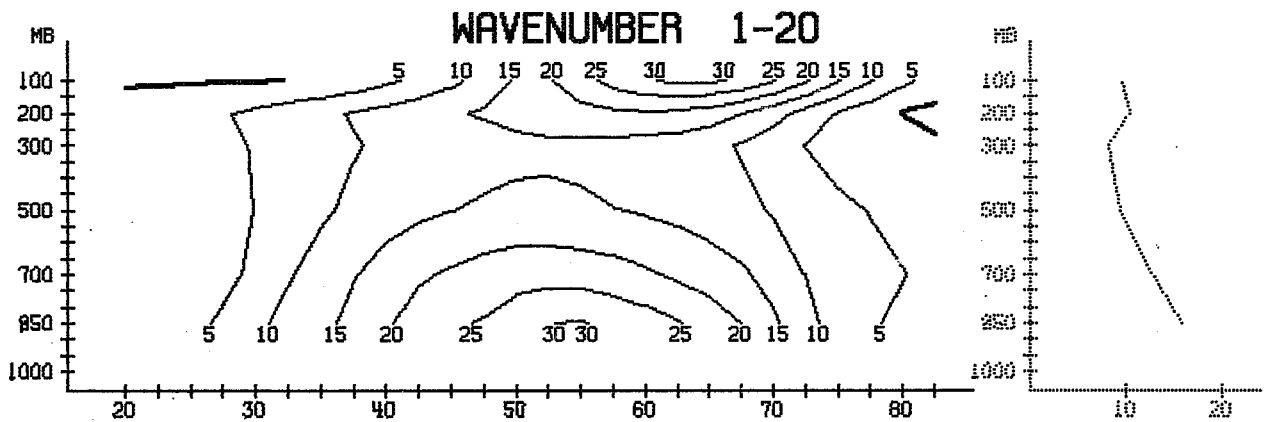
MOMENTUM-FLUX UV (M2/S2) DEC **GEOSTR**

FIG. 5.18



DAY 7.0 TO 10.0
SENSIBLE HEAT-FLUX TV (K*M/MS) OBSERVED GEOSTR

FIG. 5.19



DAY 7.0 TO 10.0
SENSIBLE HEAT-FLUX TV (K*M/SEC)

GEOSTR

FIG. 5.20

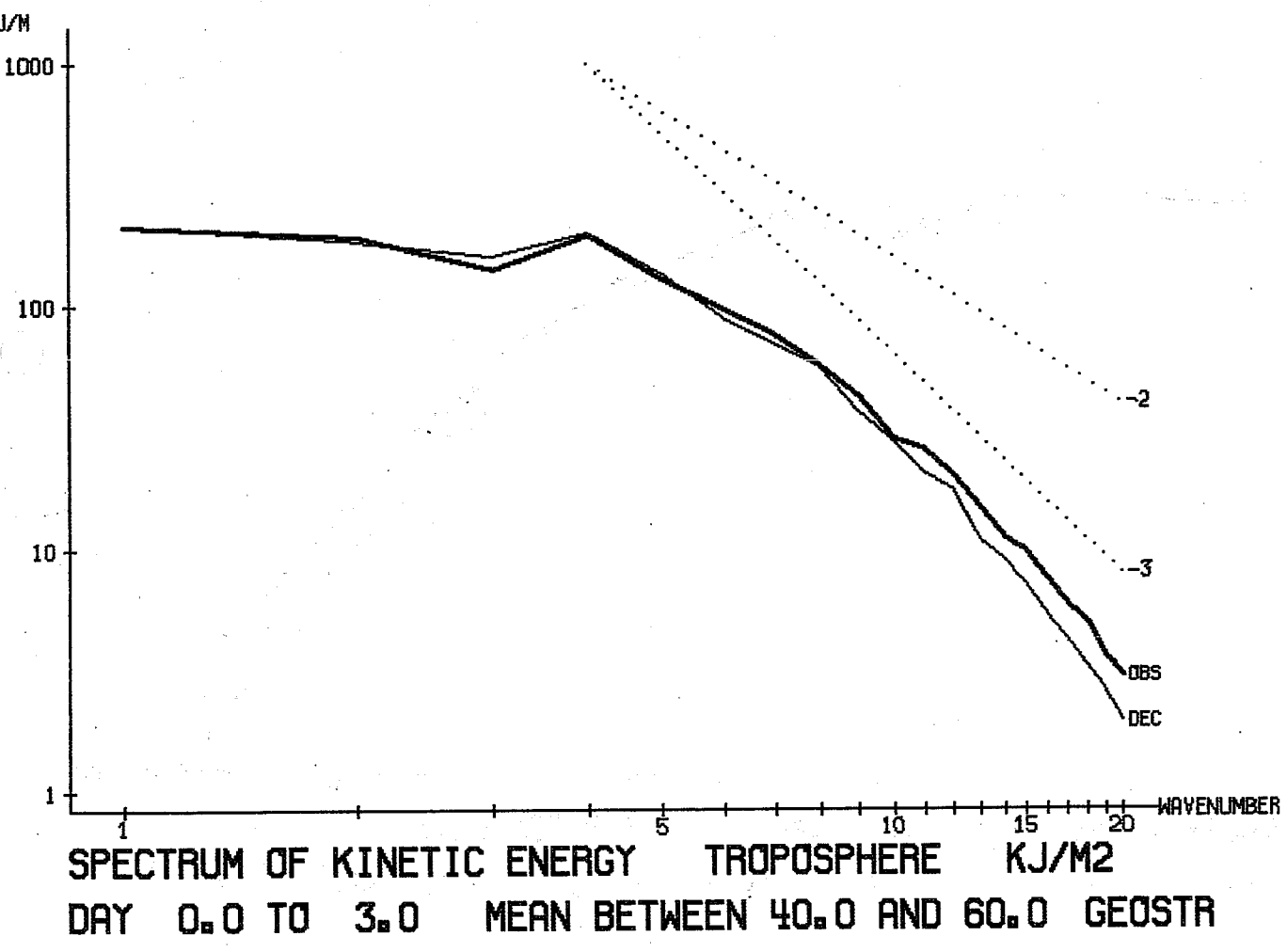
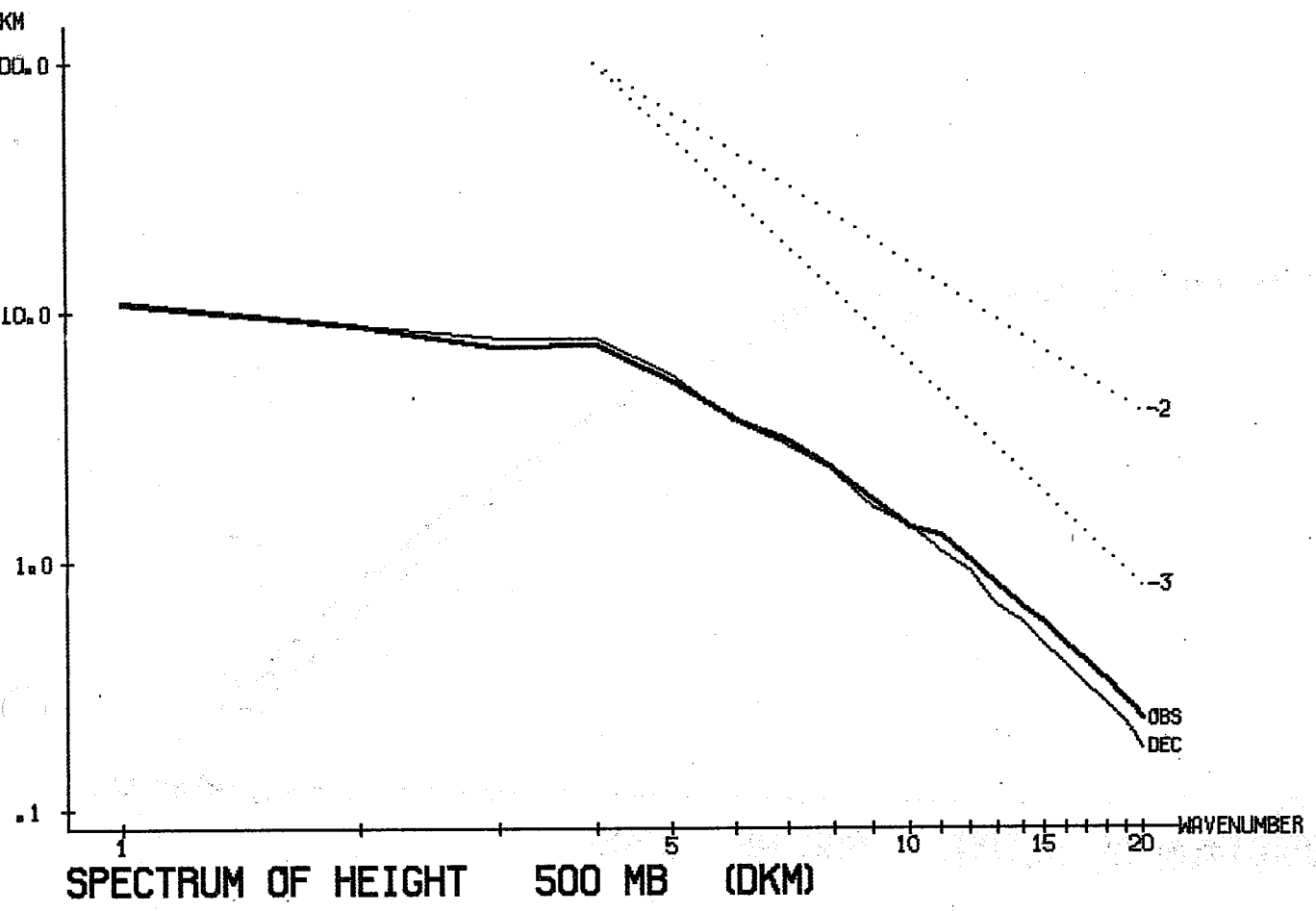


FIG. 5.21

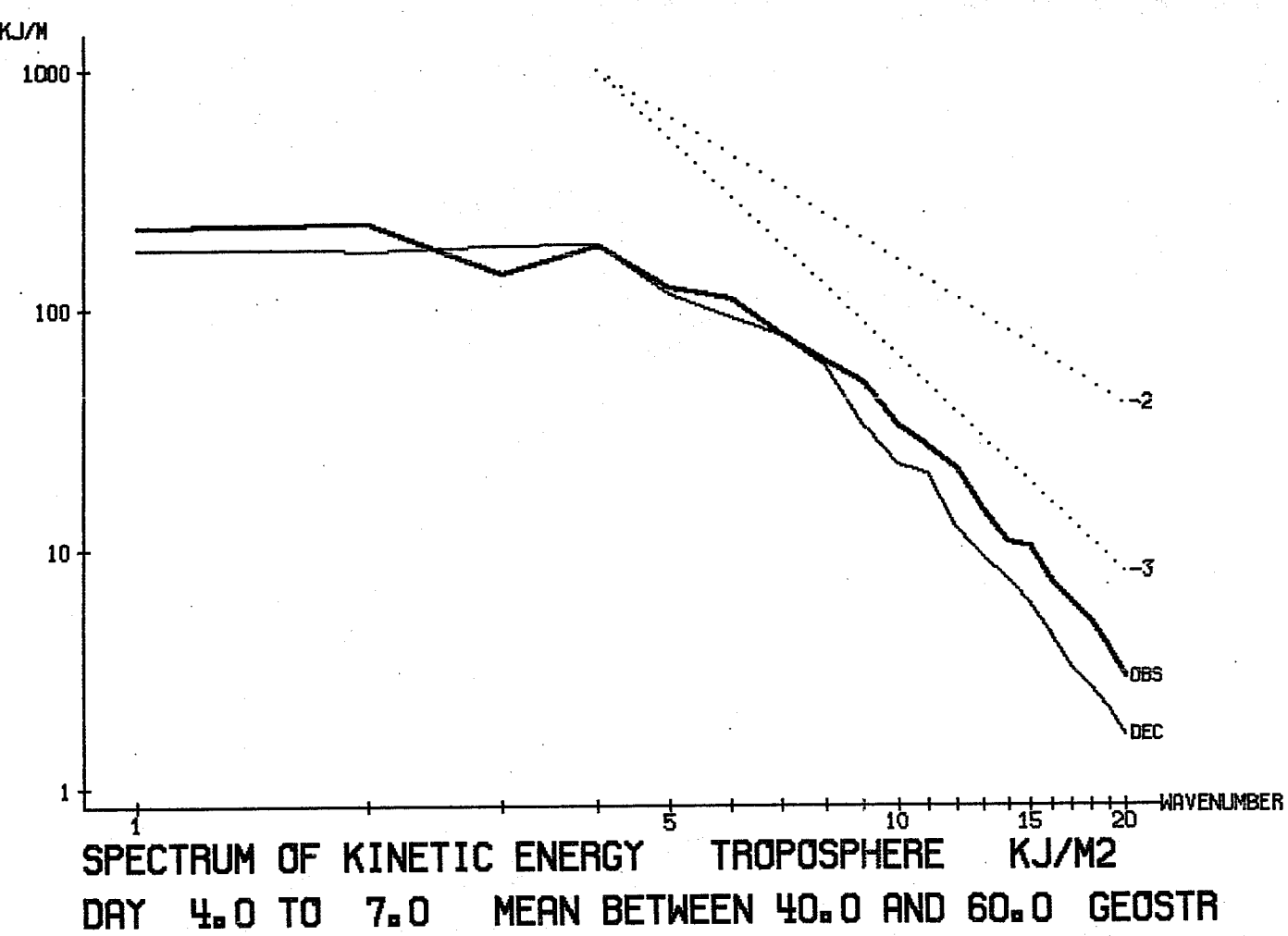
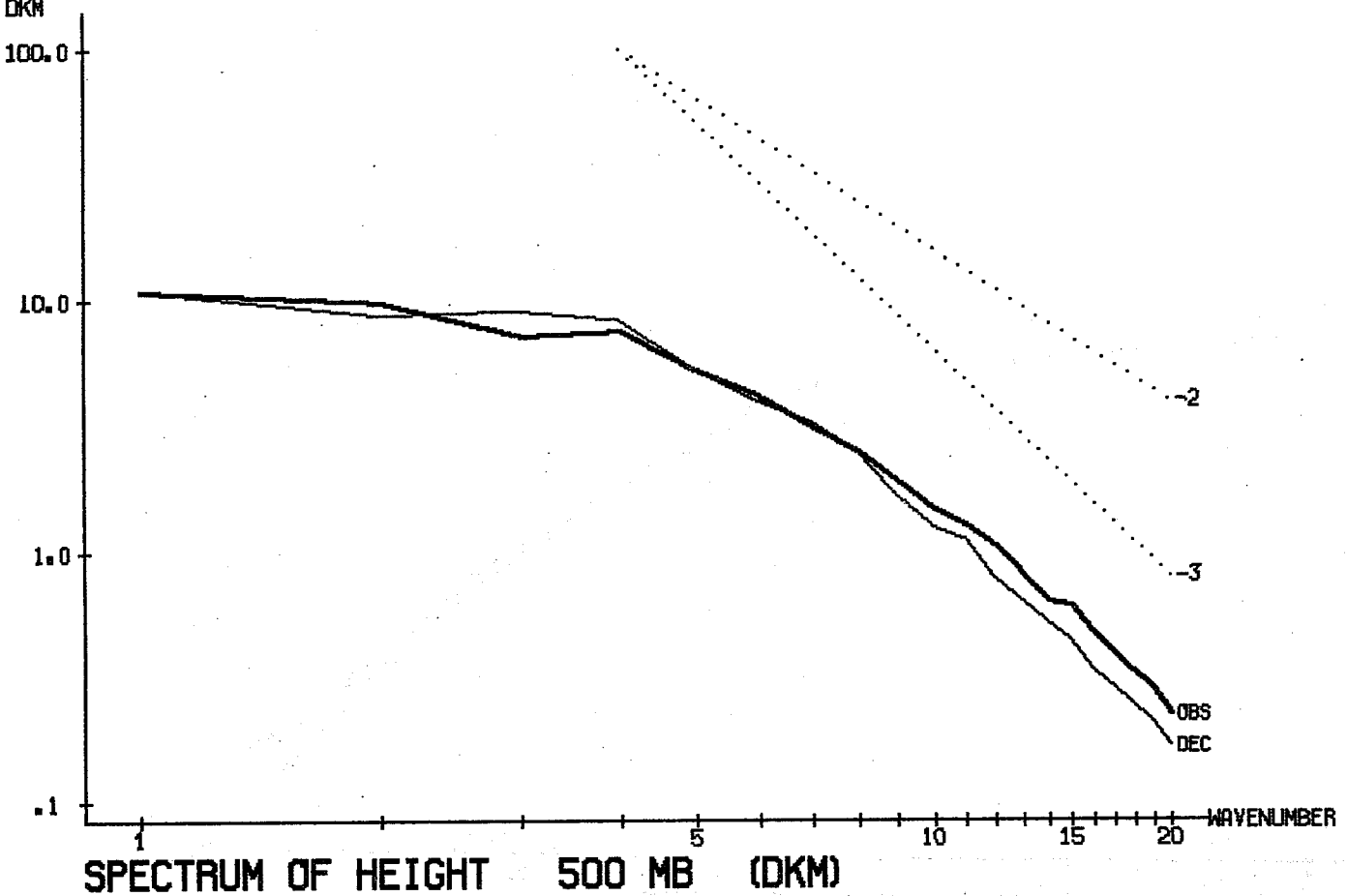


FIG. 5.22

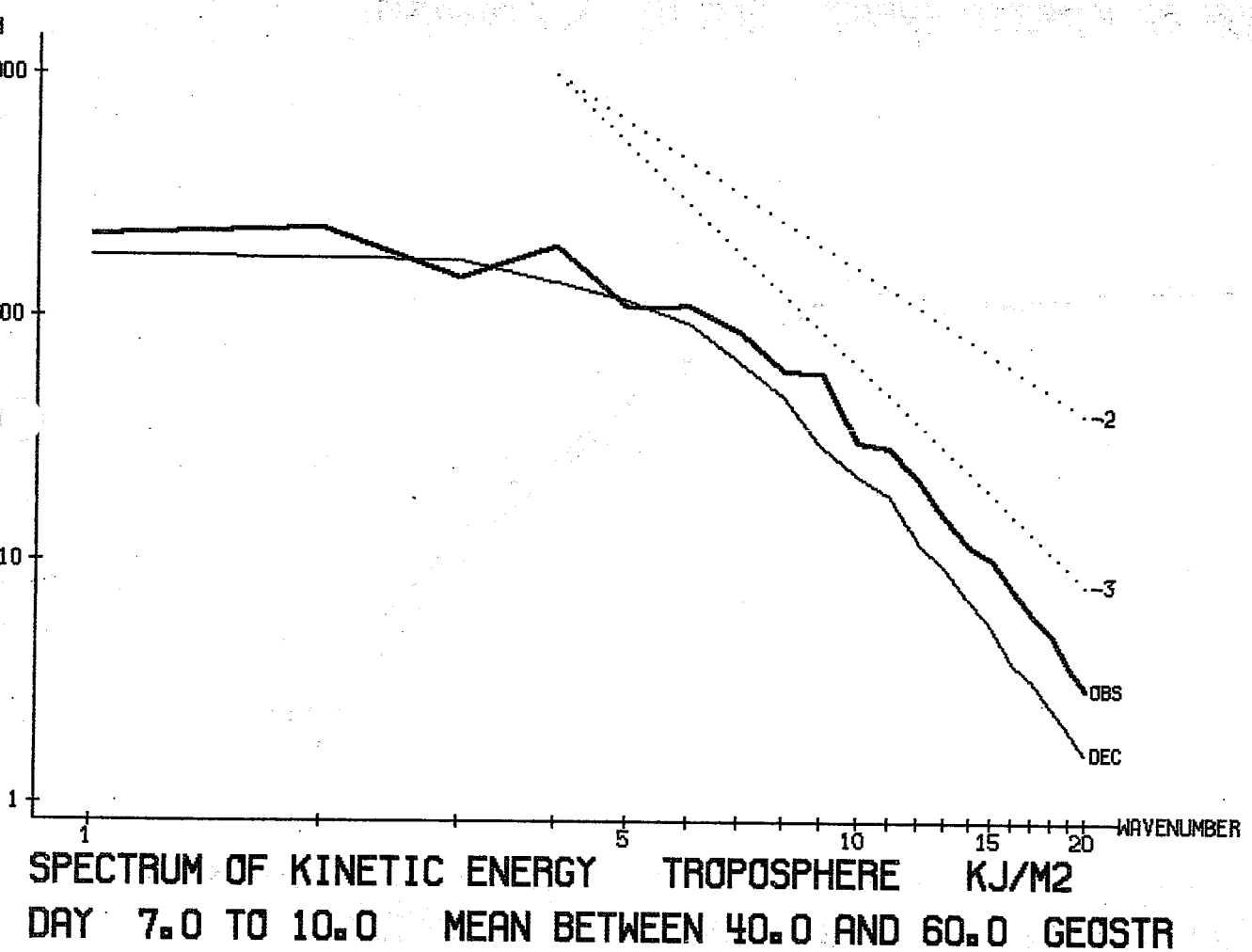
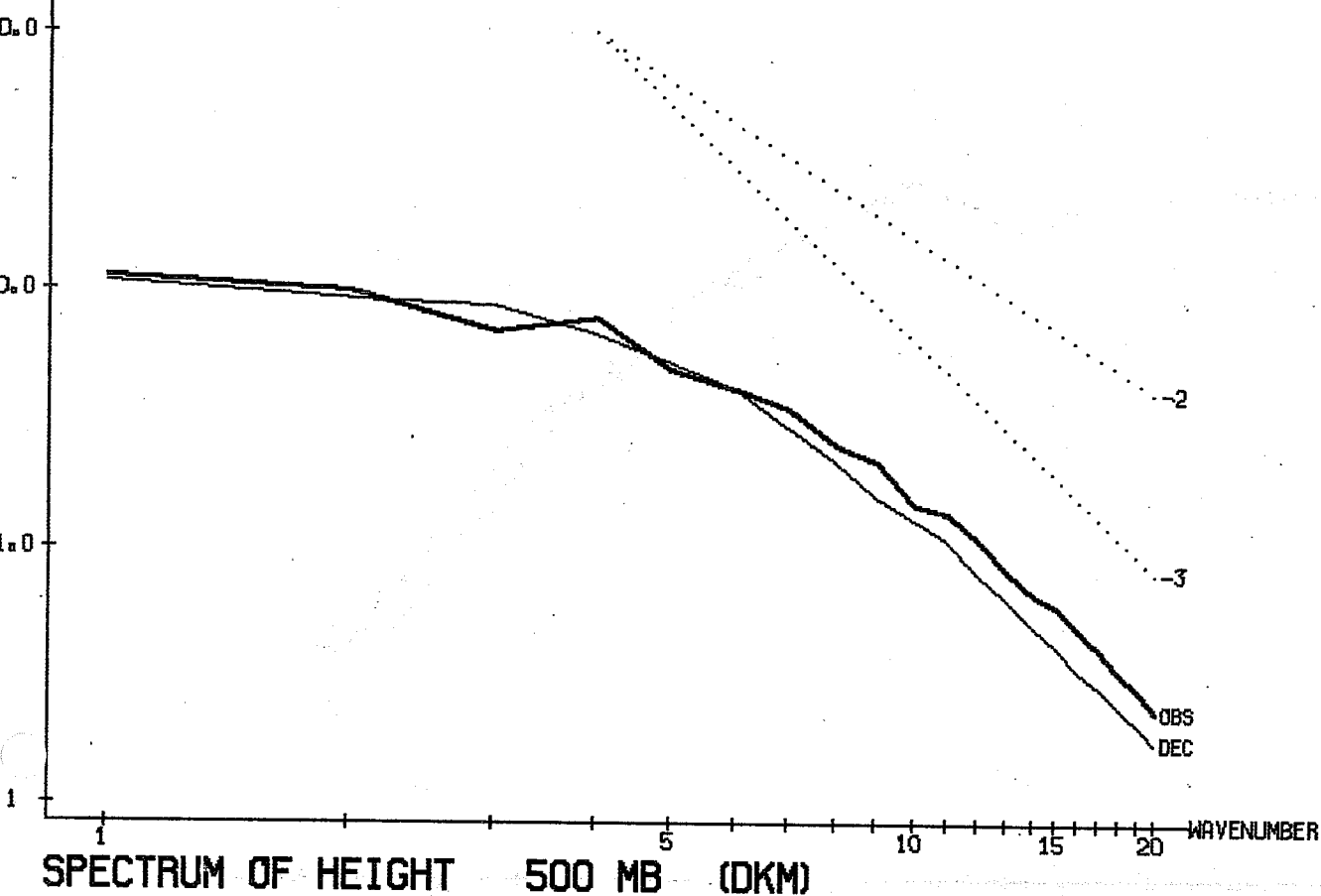


FIG. 5.23

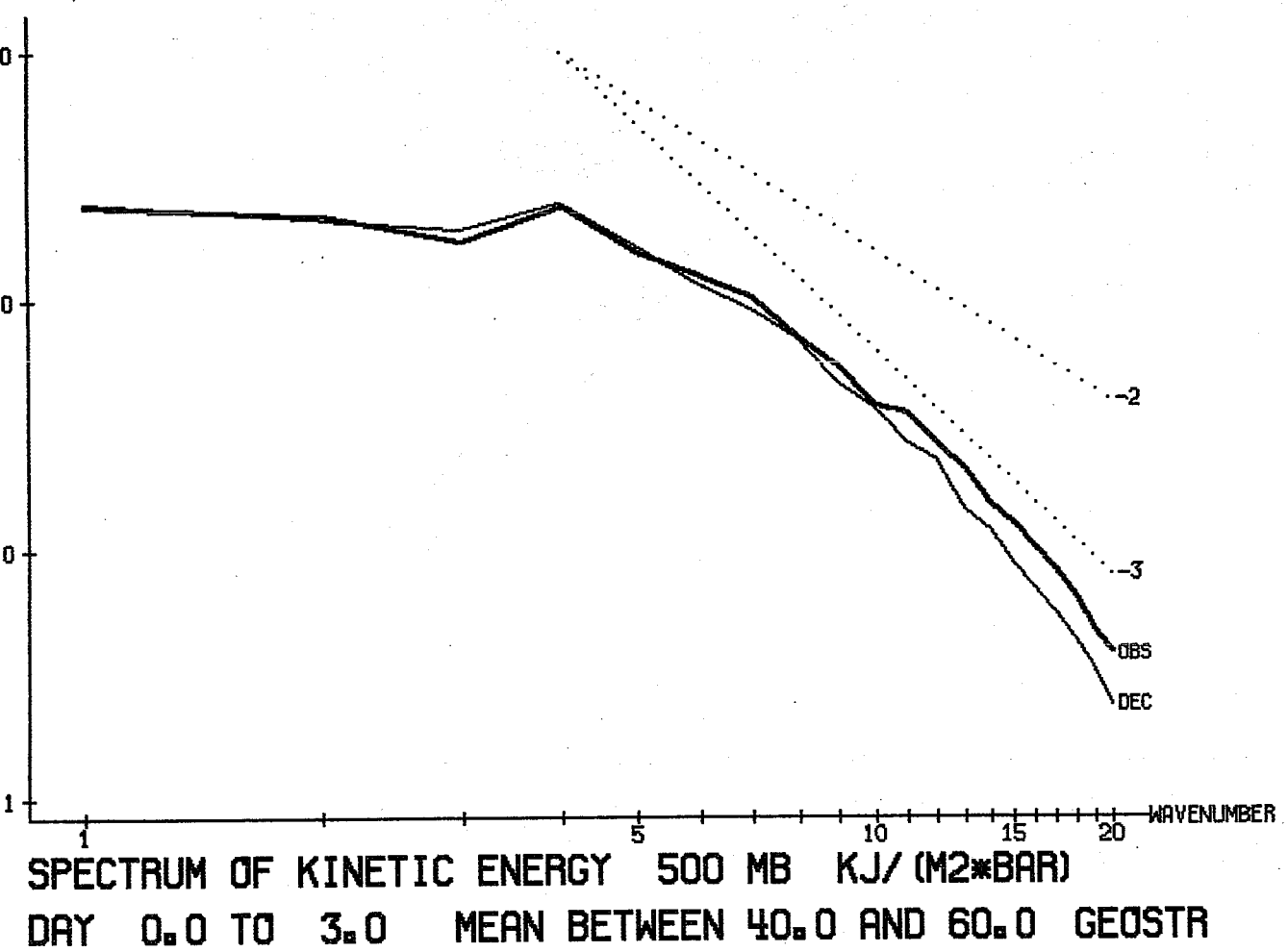
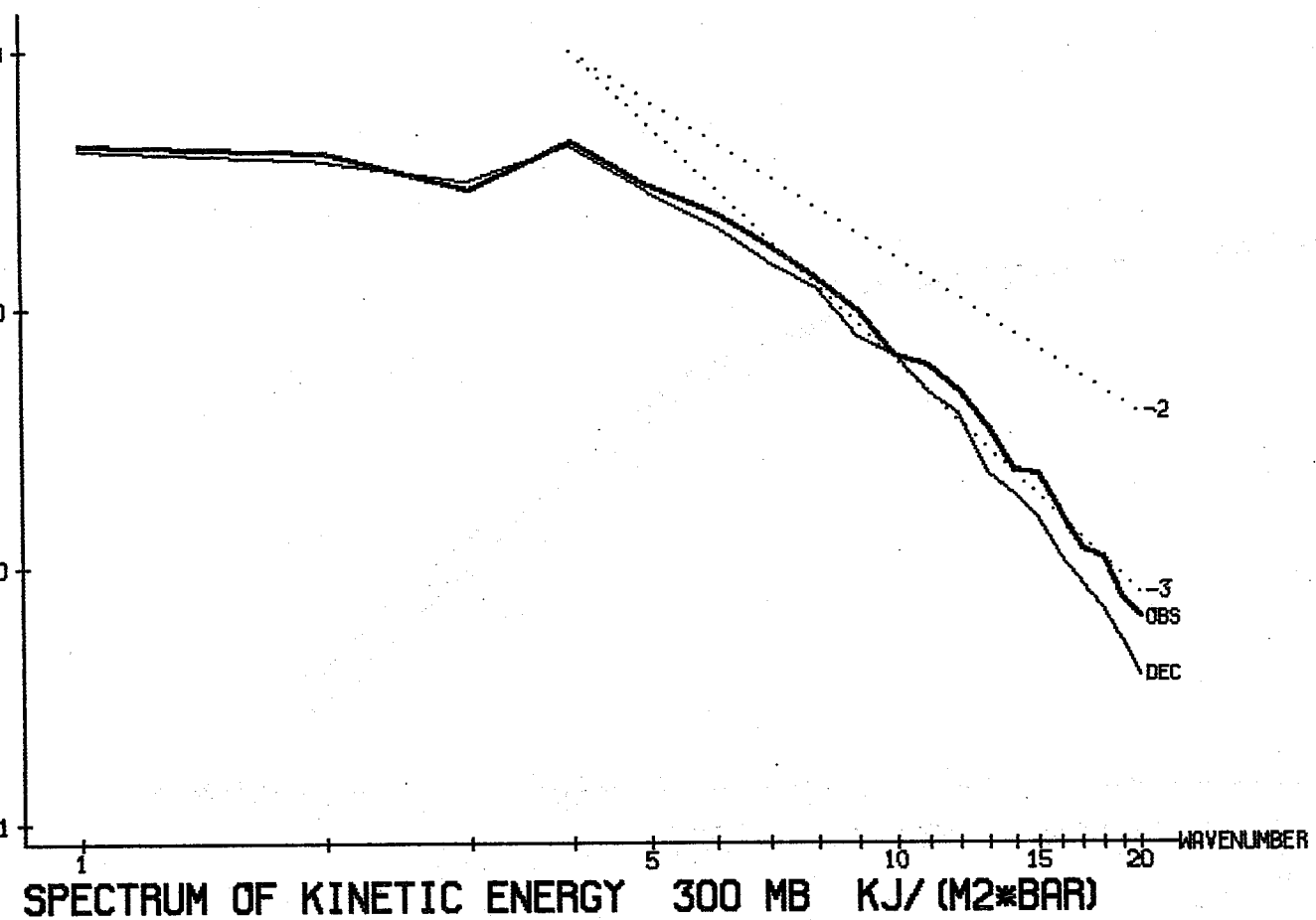


FIG. 5.24

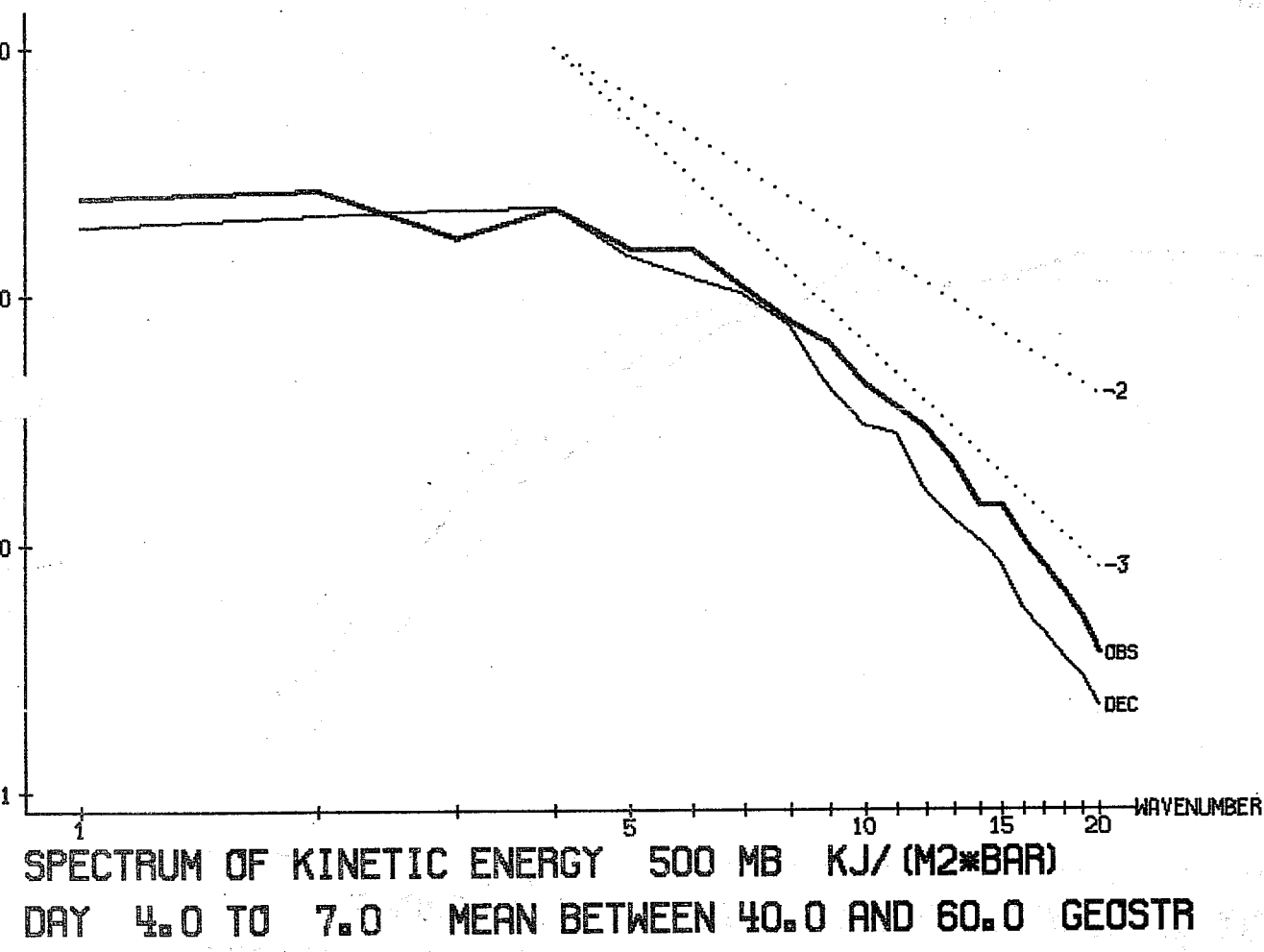
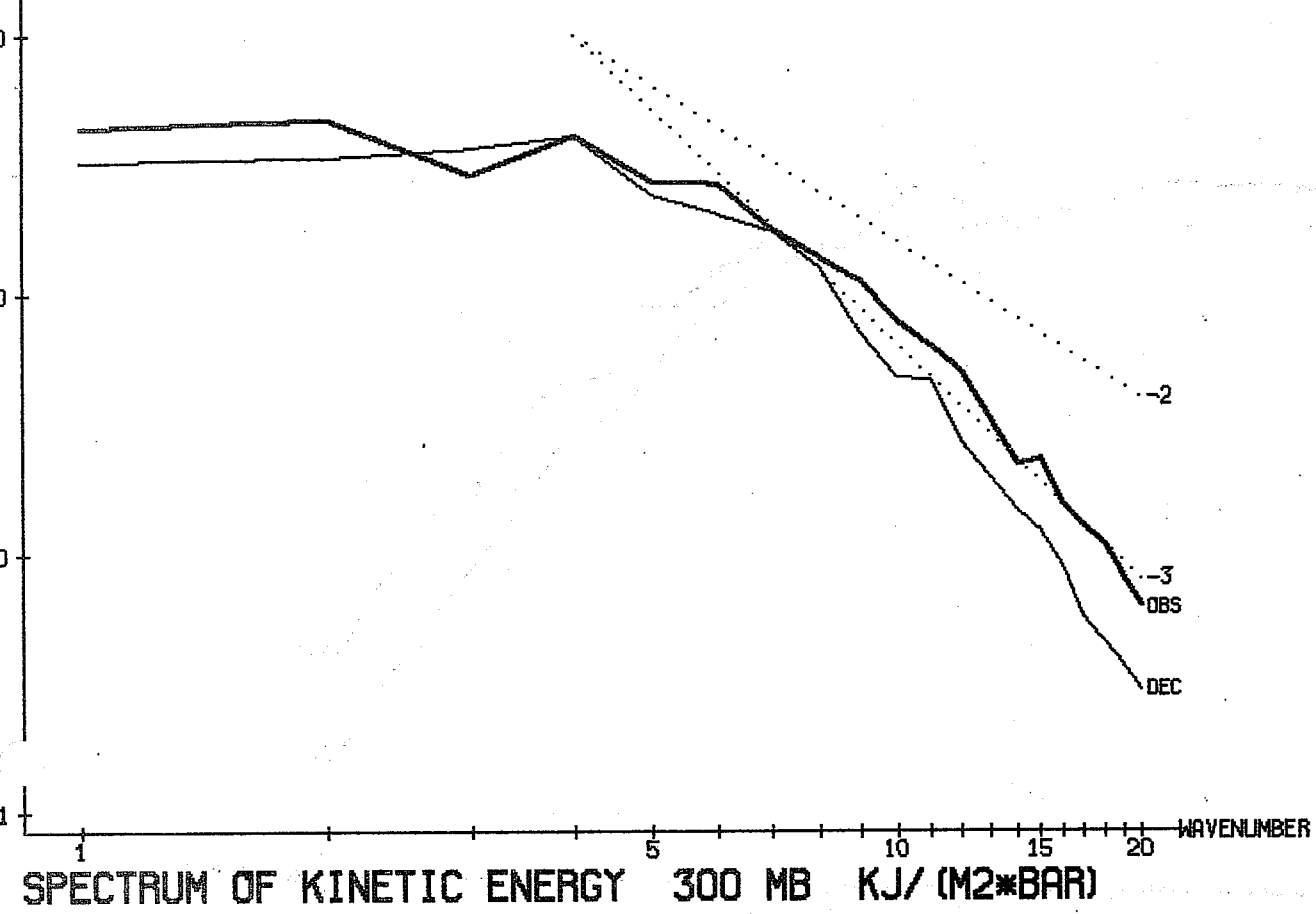


FIG. 5.25

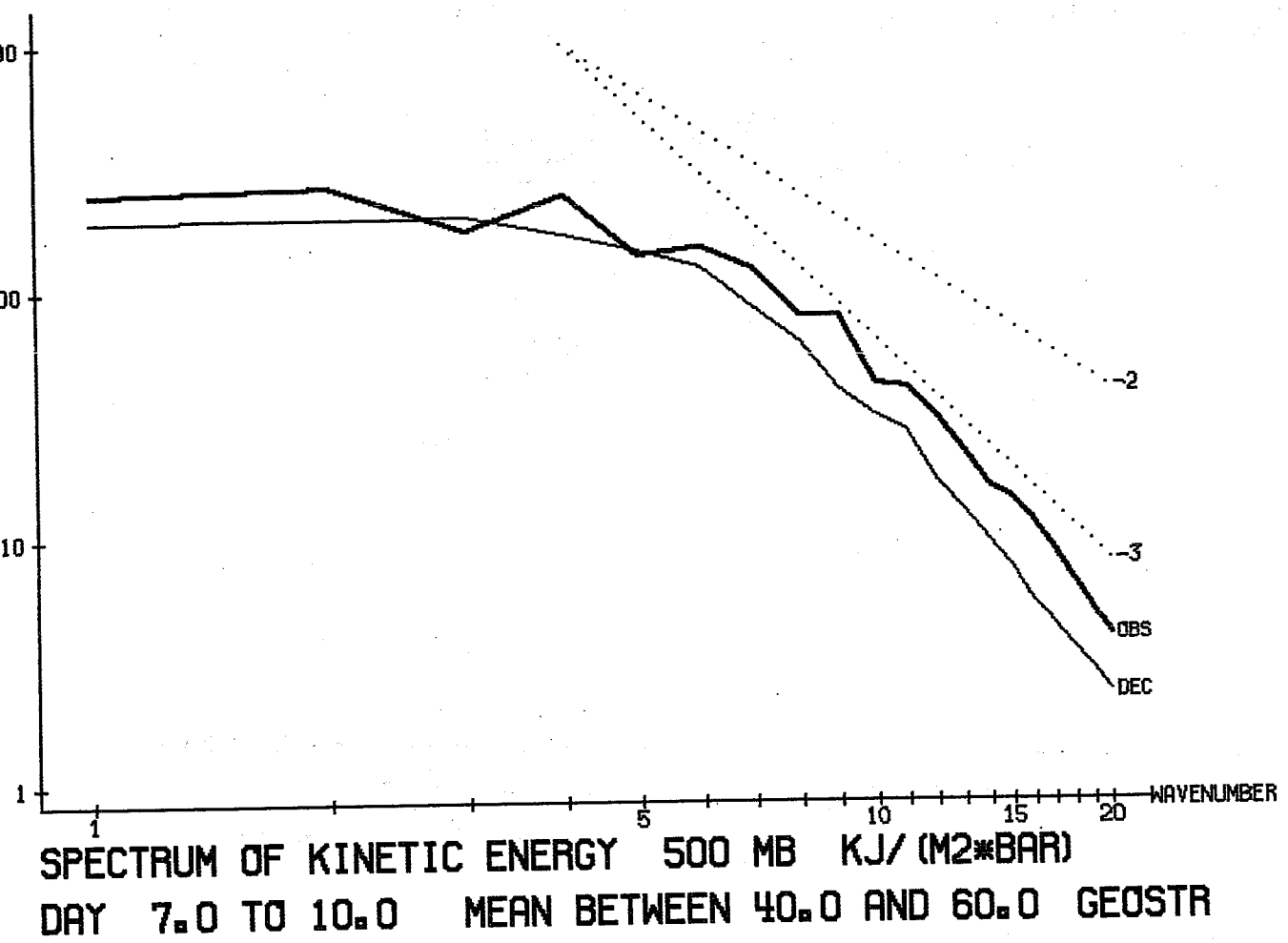
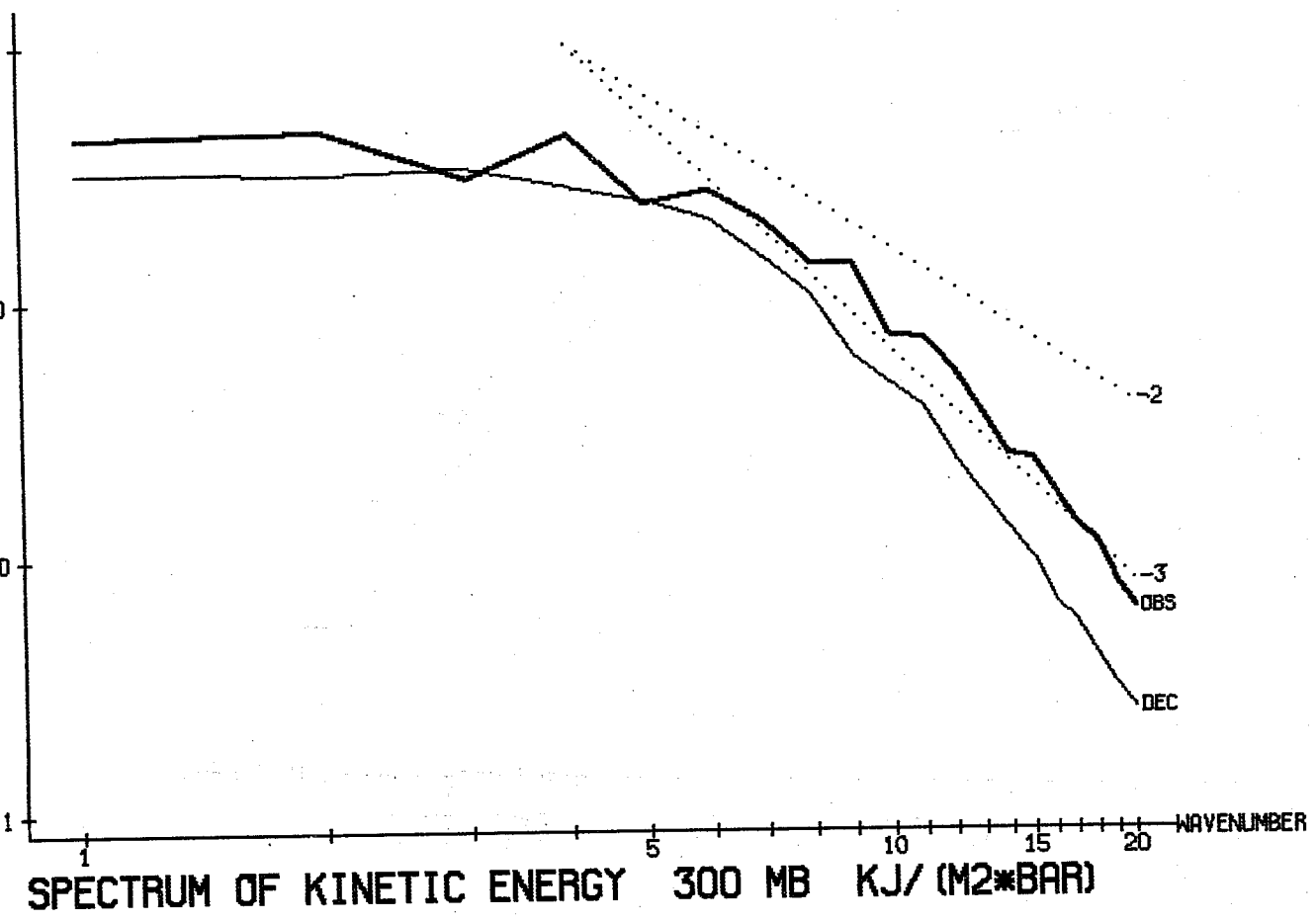


FIG. 5.26

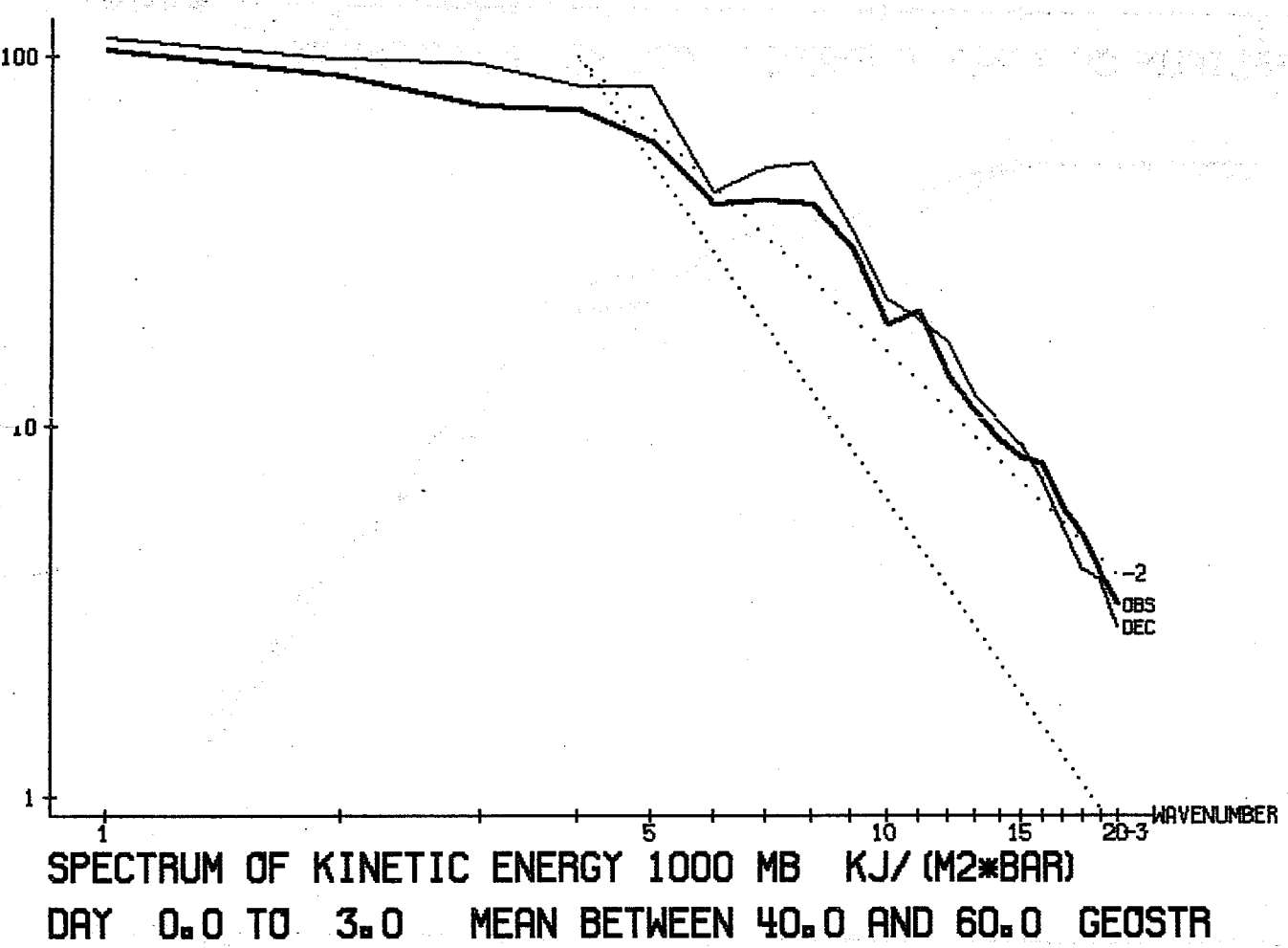
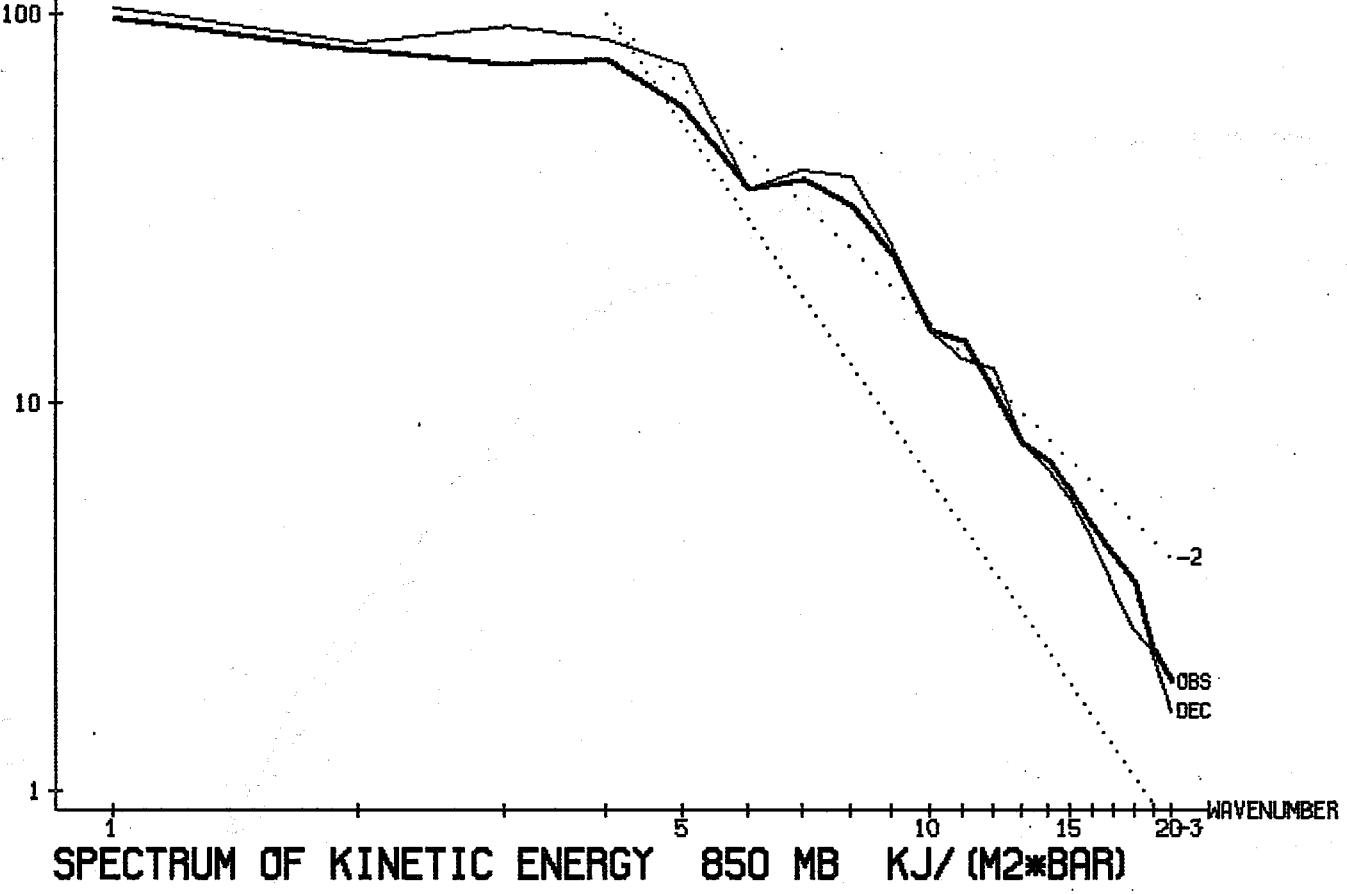


FIG. 5.27

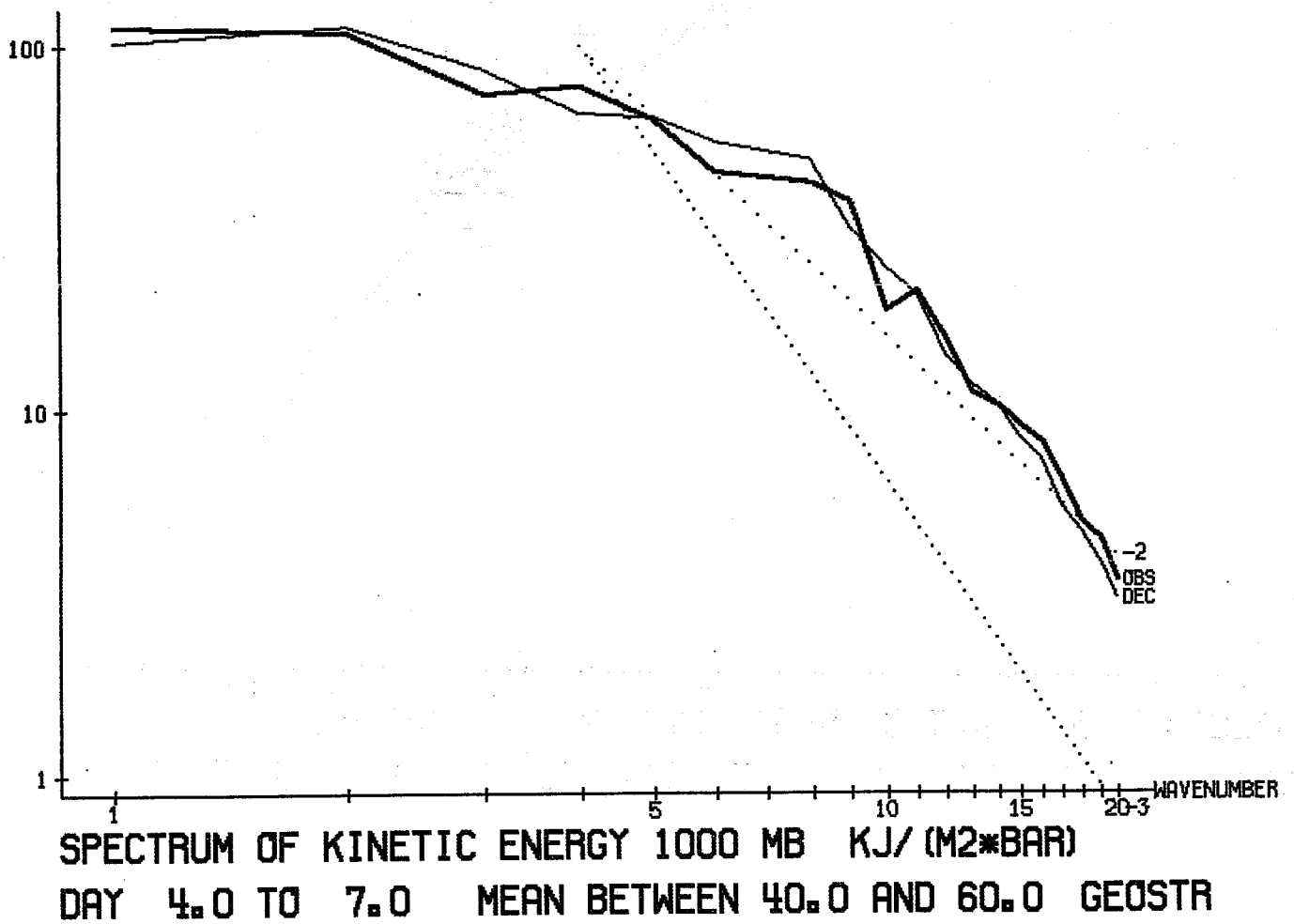
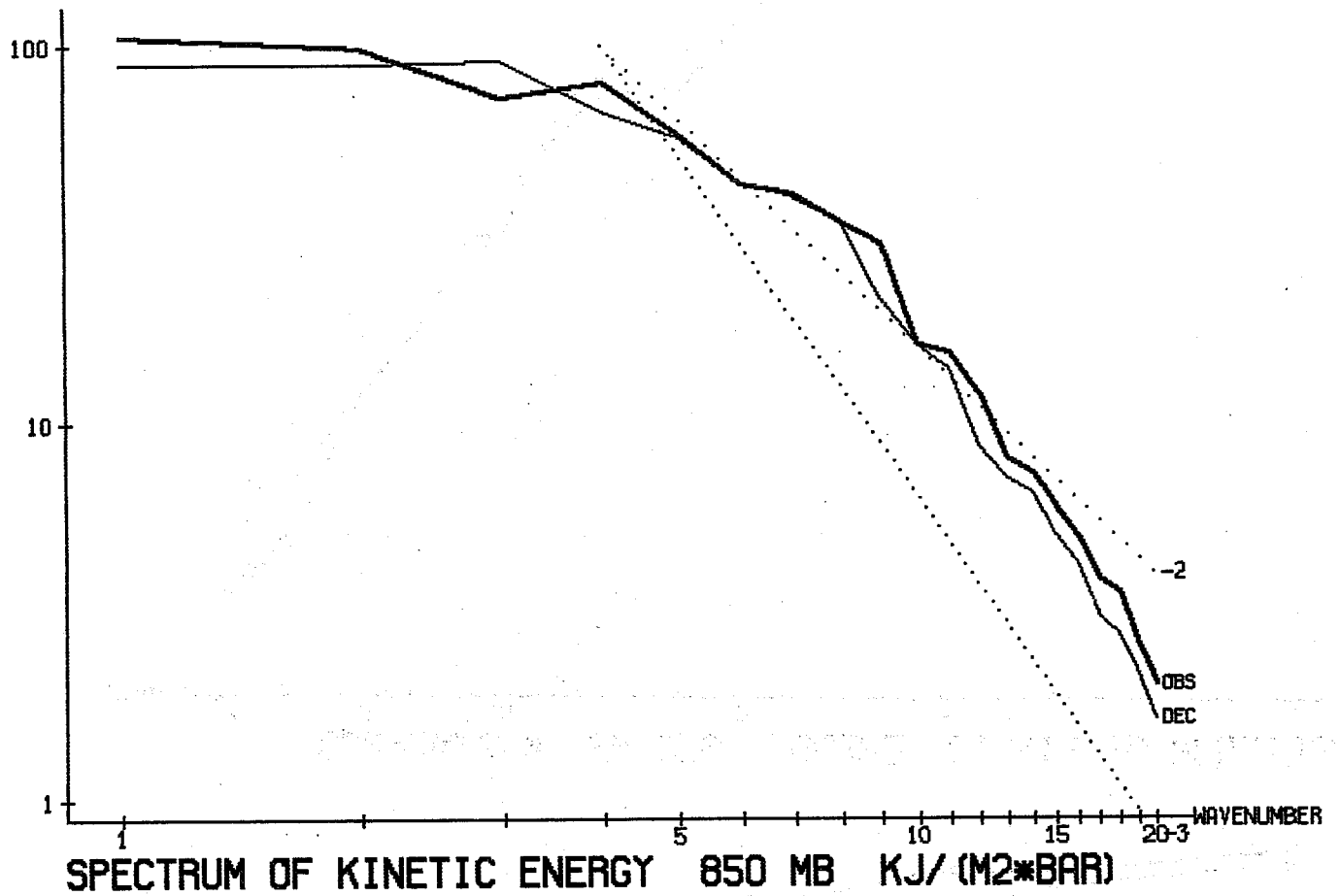


FIG. 5.28

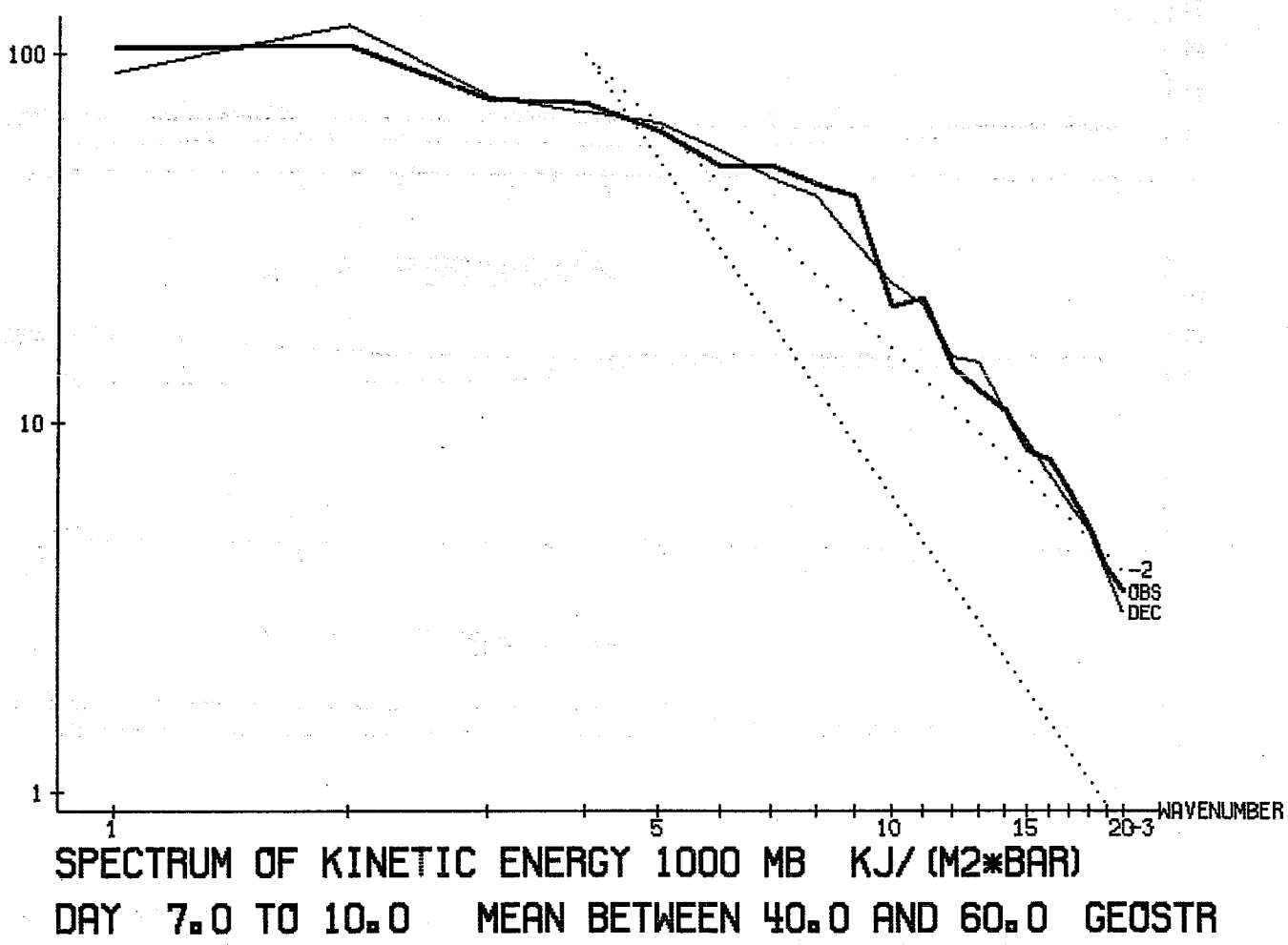
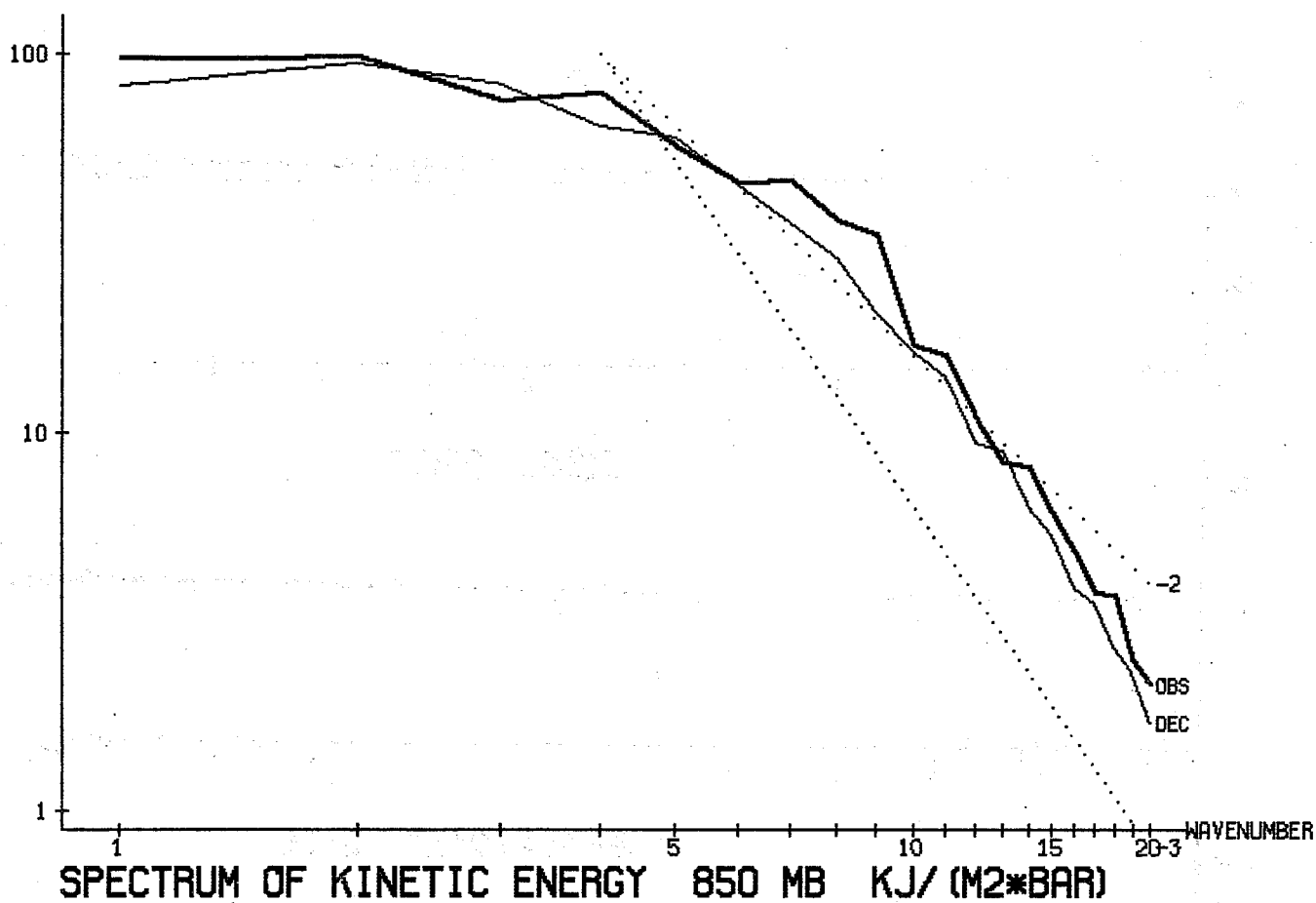
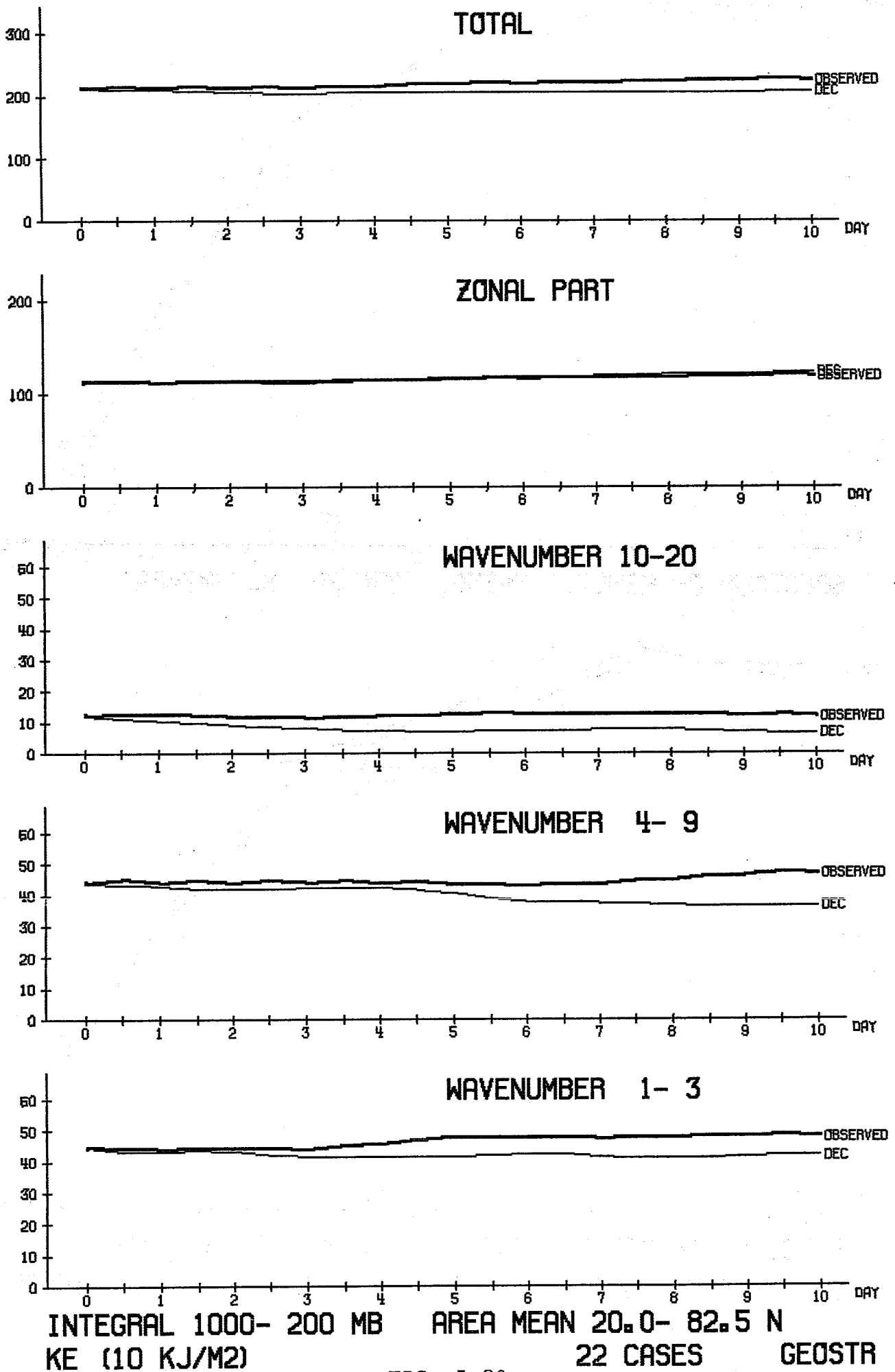
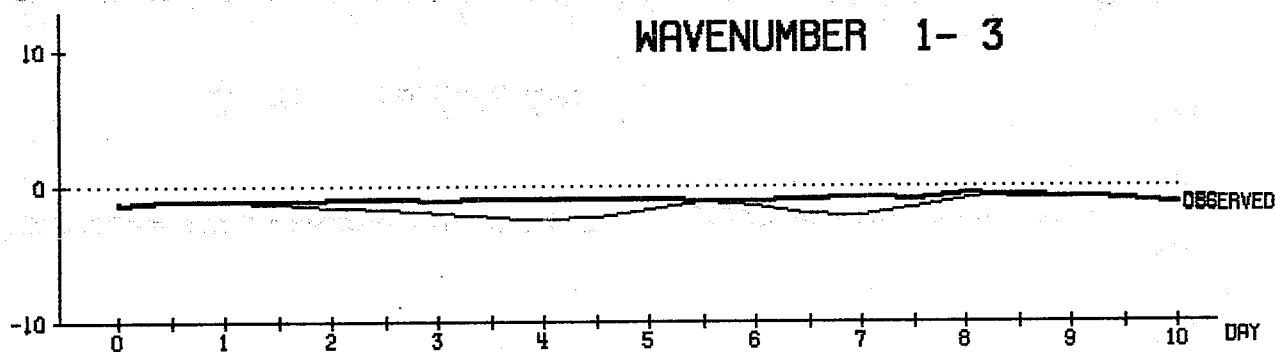
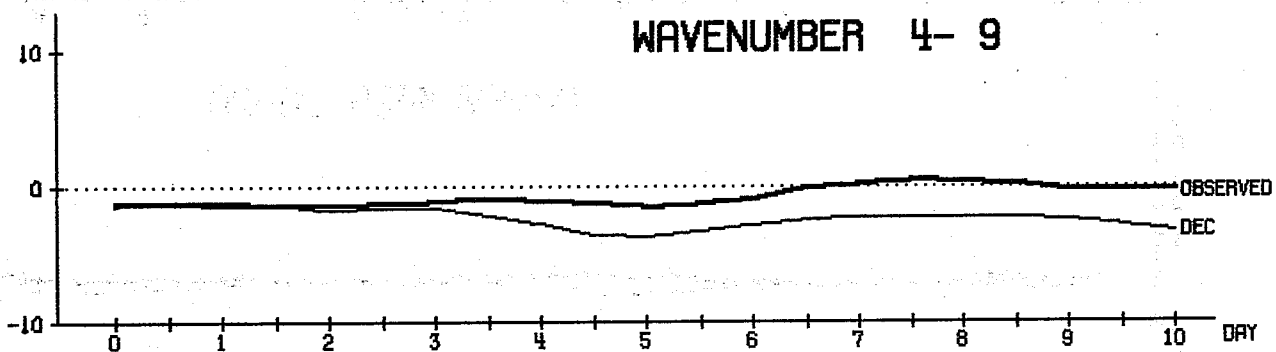
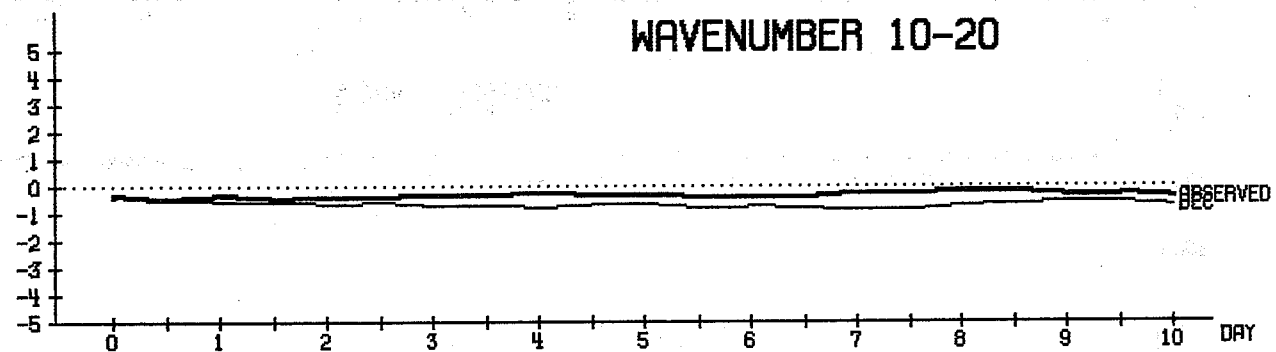


FIG. 5.29



INTEGRAL 1000- 200 MB AREA MEAN 20.0- 82.5 N
 KE (10 KJ/M²) 22 CASES GEOSTR

FIG. 5.30



INTEGRAL 1000- 200 MB AREA MEAN 20.0- 82.5 N
 CK (1/10 WATT/M2) 22 CASES GEOSTR

FIG. 5.31

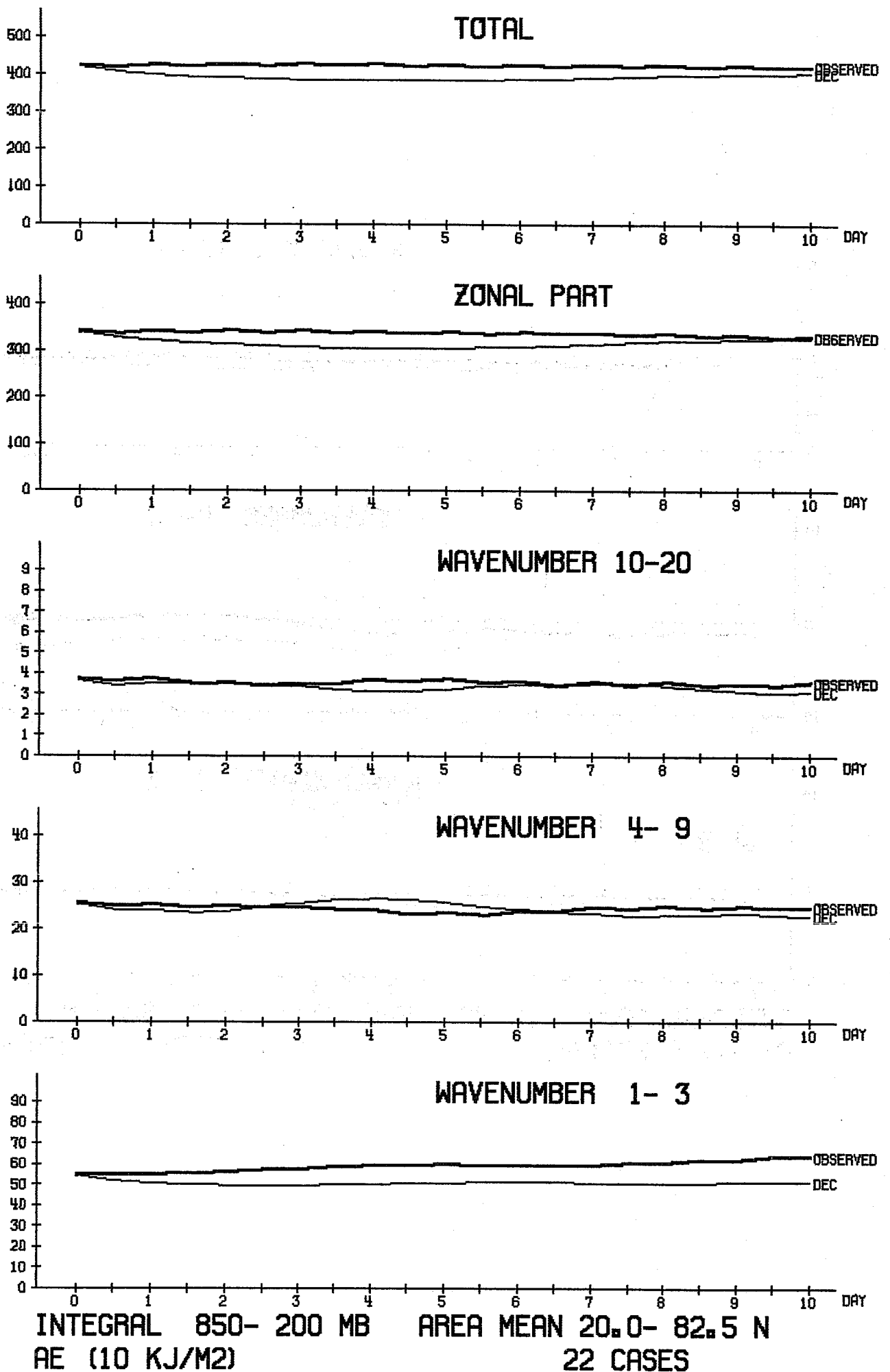
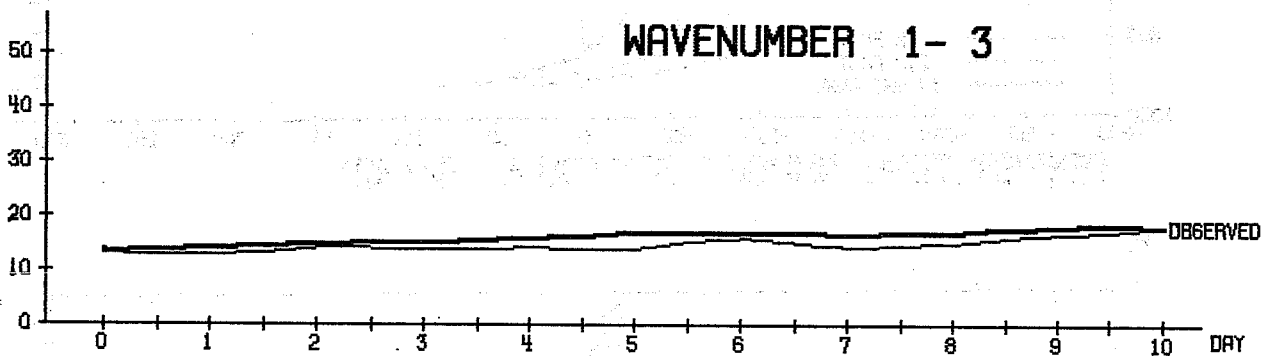
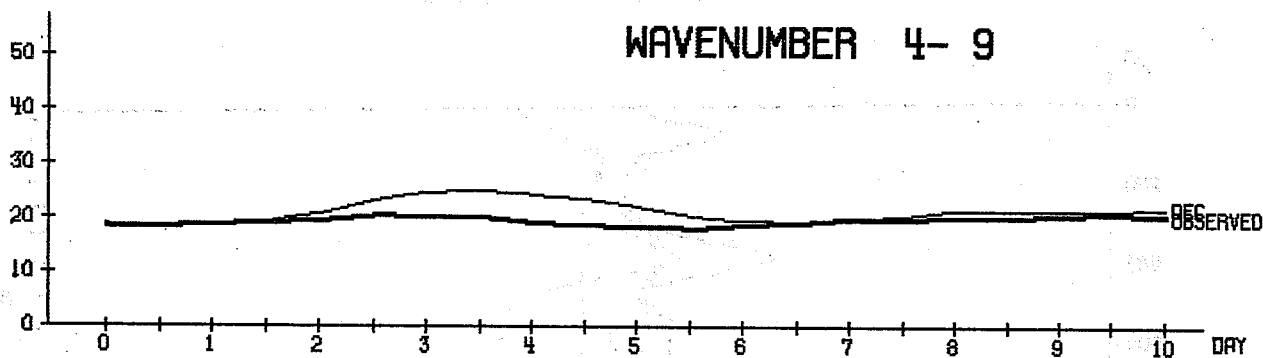
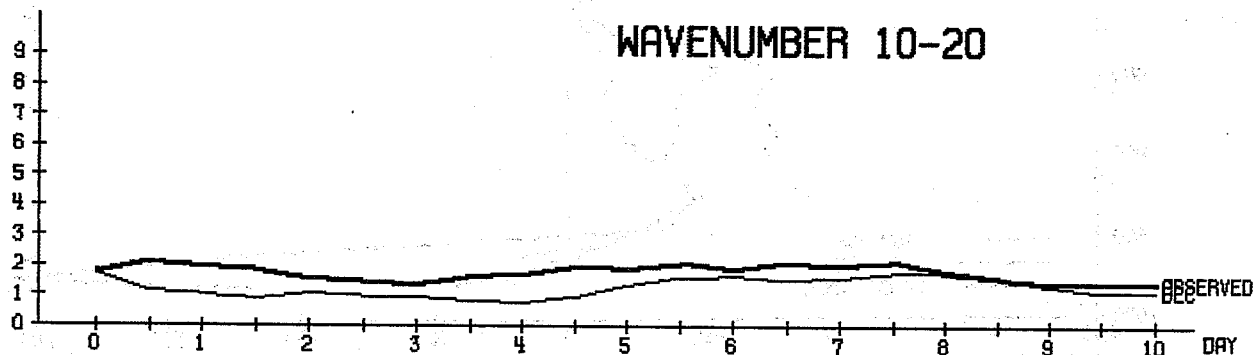
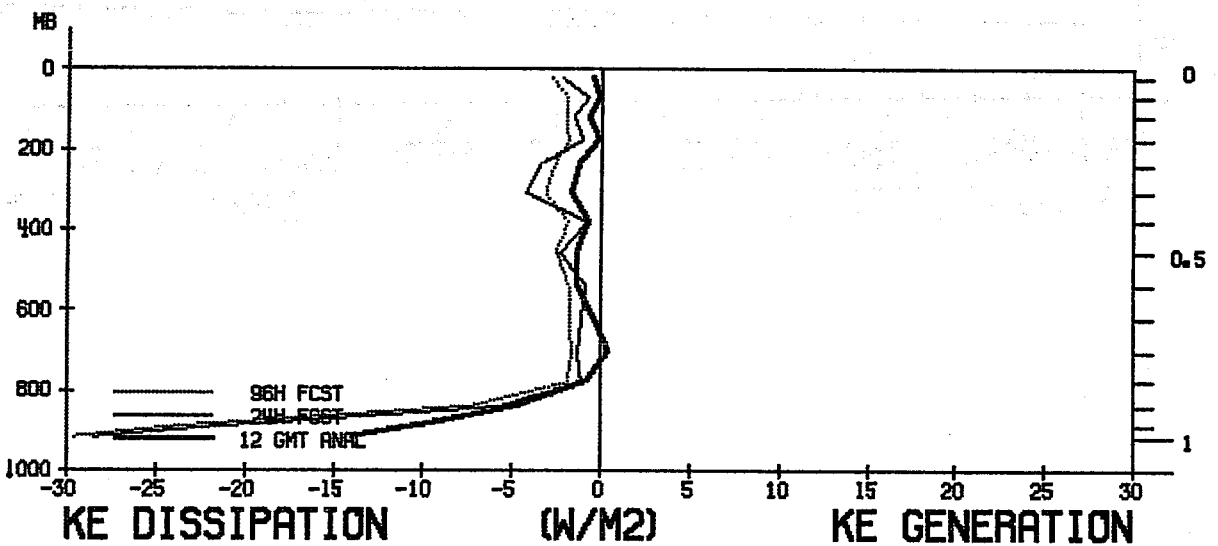
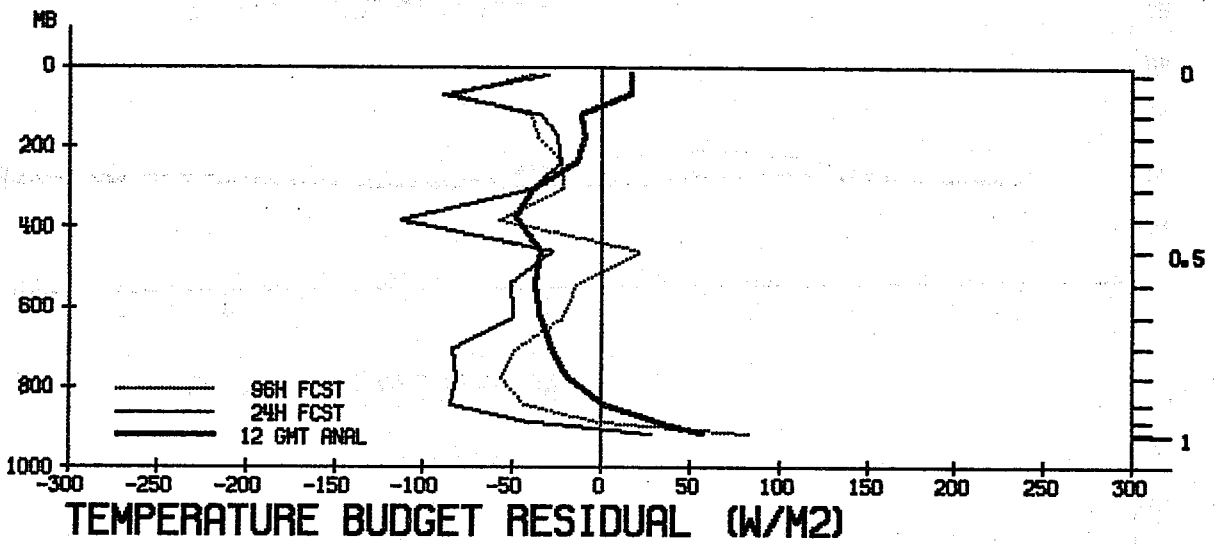
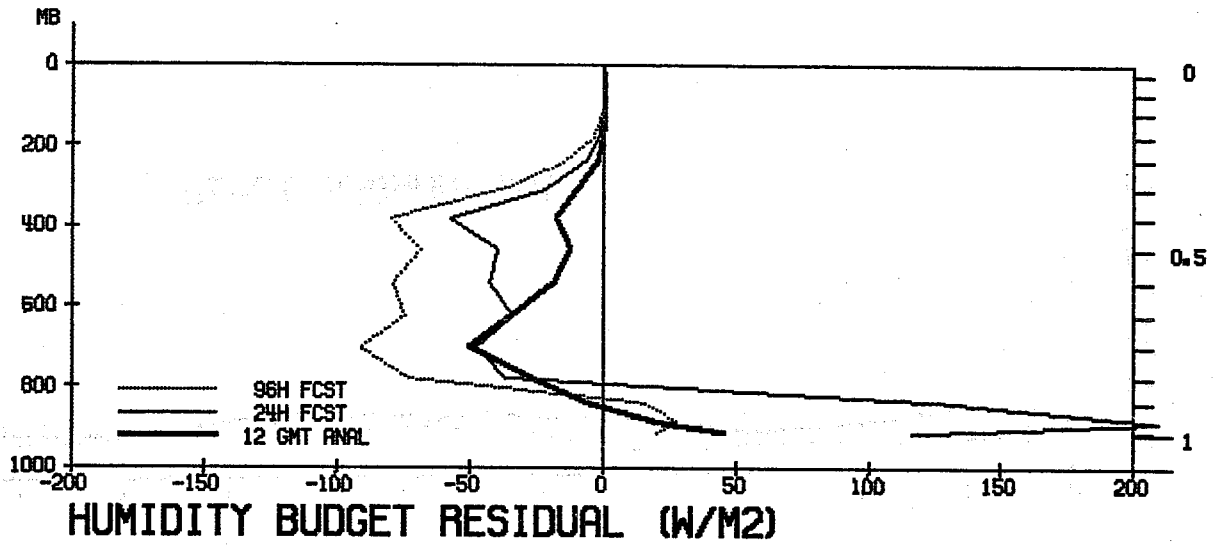


FIG. 5.32



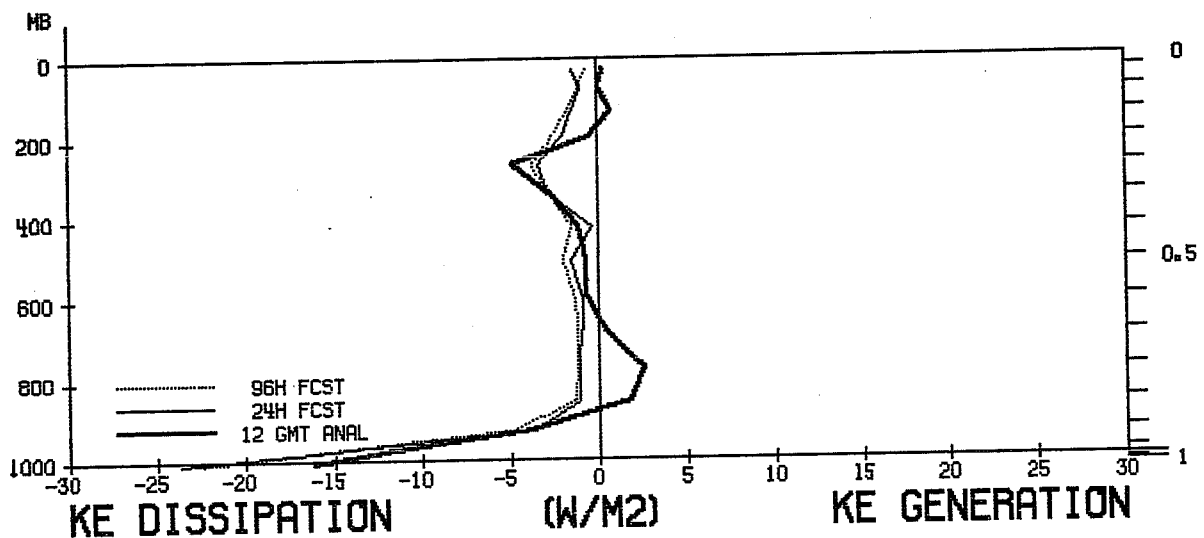
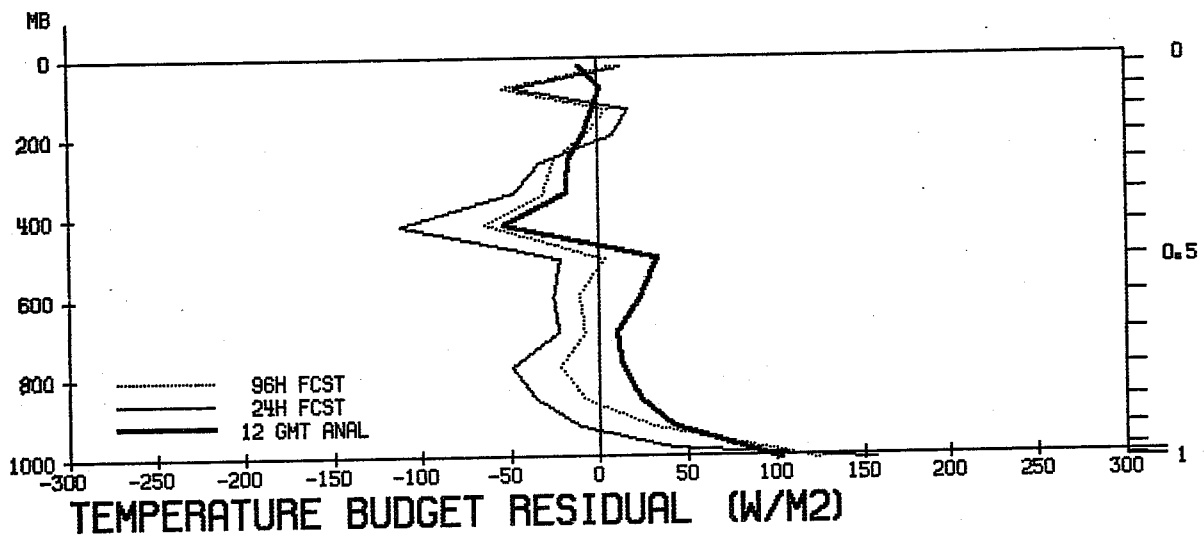
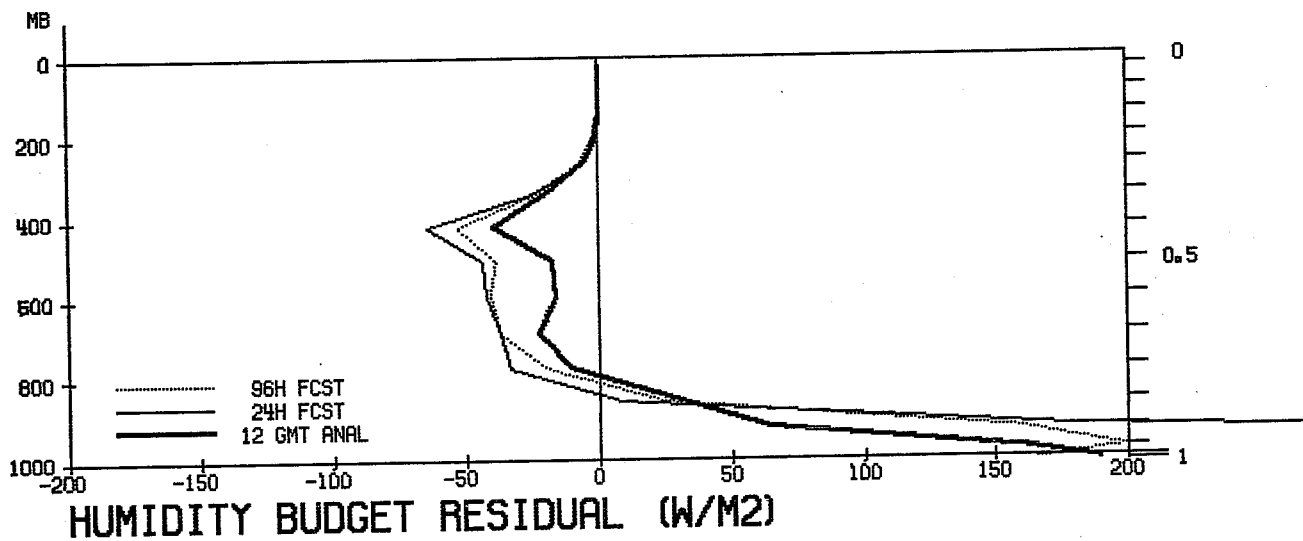
INTEGRAL 850- 200 MB AREA MEAN 20.0- 82.5 N
 CA (1/10 WATT/M2) 22 CASES GEOSTR

FIG. 5.33



DECEMBER 1979 (OPERATIONAL DATA)
ALL LAND

FIG. 5.34



DECEMBER 1979 (OPERATIONAL DATA)
ALL OCEAN AREAS

FIG. 5.35

6. GENERAL REMARKS

In the November report some generalisations were attempted as a seasonal summary. Results of December confirms one of the points made and does not confirm another .

The spectral energy repartition has returned to something similar to October and the error pattern is similar; it is also interesting to notice that the objective scores were better in November. If this is confirmed our model would have better skills in periods when medium waves are relatively more energetic.

The standing wavenumber 3 had a good behaviour in November and this time it was the wavenumber 2 which showed weakened features.